A report from the Advanced Motor Fuels Technology Research Programme

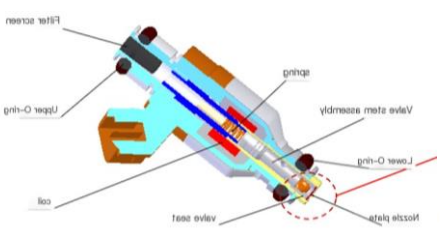

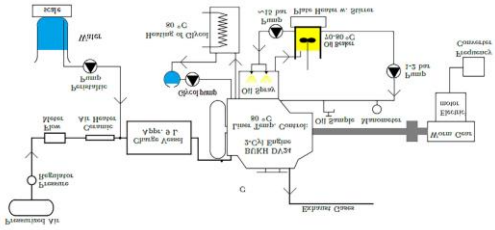

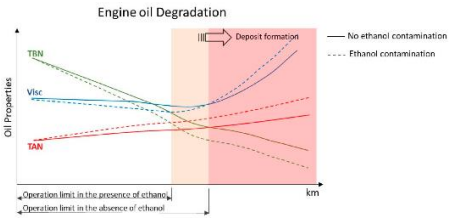

Task 62:

Wear in Engines Using Alternative Fuels

Wear associated with application of methanol in combustion engines

Chinese experiences

Wei Anli,Yang Huizhong,Li Jianhua and Chen Peng
Ministry of Industry and Information Technology, China

Lu Ruijun ,Su Maohui ,Chen Chong and Zhang Zhidong
Geely New Energy Commercial Vehicle Group

Zhu Weibo and Wang Wenjun
Chongqing San'ai Hailing Industrial Co., Ltd

Zou Wuhui ,Hou Qifei and Wang Yong
Zhongyuan Internal Distribution Group Co., Ltd

Sun Jun and Ni Peixiang
Tianrun Industrial Technology Co., Ltd

Liu Hui
Liaoning Sante Petrochemical Co., Ltd

Huang Fenlian
Kunming University of Science and Technology

Li Chengxiao,Deng Fei,Long Meibiao and Wu Xinyi
Nanyue Electric Control (Hengyang) Industrial Technology Co., Ltd

Yuan Yafei and Yu Jing
Wuxi Yajia Deyin Technology Co., Ltd

Zhang Yongming
Wuxi Weishite Automotive Motor Co., Ltd

Wang Nan and Chen Wei
Suzhou Dafei Filter Technology Co., Ltd

Mu Yun
Shanghai Yixiang Power System Co., Ltd

September 2024

Summary / Abstract

This project chooses the application of methanol fuel in internal combustion engines. Based on the characteristics of methanol fuel (low-carbon), it explores and studies the impact of wear on various engine systems, analyzes wear phenomena and possibilities, selects anti wear technology solutions, and predicts the results after implementing effective measures. Sufficient research and demonstration have been conducted.

In terms of selecting the research object for this project, the research group specifically selected the friction pairs of the main components and parts that directly contact methanol fuel. Starting from the analysis of the friction and wear mechanism, the influencing factors of friction and wear were analyzed (including quantitative analysis and weight ratio), revealing the phenomenon of friction and wear, determining the impact of using methanol fuel on friction pair wear, analyzing the reasons, and proposing suggestions.

Due to the research objective of "engine wear using alternative fuels" in this project, it is defined as the study of methanol fuel engine wear during the project initiation and organization process. Therefore, after repeated consultations between the Chinese research group organizers and participants, it is believed that in the next longer development stage, renewable synthetic fuels will be the dominant fuel for the main driving force in the transportation field. For this reason, the research group chose methanol fuel as an alternative fuel and focused on engine wear as the research content. Various parts were selected as the research objects to carry out the above work and reached a consensus.

The Chinese research group of the International Energy Agency's Advanced Automotive Fuel Research Group on "Using Alternative Fuel for Engine Wear" specifically reminds readers that the synthesis of renewable methanol fuel (e-fuel) can be obtained through different technological routes in different regions, countries, and enterprises, but the properties of the fuel are generally the same, especially the carbon content is basically the same. In China, this fuel is collectively referred to as low-carbon (zero carbon) fuel in the transportation sector. Based on this, research team members remind that when referring to the content and results of this report, please pay special attention to the meaning of synthesizing renewable energy to avoid unnecessary misunderstandings.

Content

Preface

The inherent molecular formula CH3OH of methanol fuel determines its low-carbon properties, which poses new challenges for the application of methanol fuel in internal combustion engines, also known as the application of low-carbon clean fuel, in terms of lubrication and wear resistance. This article focuses on the application of low-carbon clean fuels in internal combustion engines, conducting research and evaluation in two dimensions: improving lubrication and resisting wear, and providing constructive preventive (operational/operational) measures from them. In order to ensure consistency with traditional fossil fuel engines in the use of methanol fueled engines.

Chapter 1: Engine Methanol Fuel Supply System

1.1 Introduction

Research background and significance

Methanol fuel has good combustion emissions and is [a] good alternative fuel for engines. As a promising alternative fuel for automobiles, compared to conventional fuels such as gasoline and diesel, methanol as a fuel has the following characteristics:

The molecular formula of methanol (CH_3OH) has a simple structure, low theoretical air-fuel ratio, and contains oxygen elements in the molecule, which is conducive to the full combustion of methanol mixture and reduces harmful emissions in combustion products;

Although the calorific value of methanol is about 50% of that of gasoline and diesel, the thermal efficiency per unit mass is almost the same as that of gasoline and diesel. Methanol combustion has a "self supplied oxygen" effect, and its thermal efficiency and power performance are good;

Good anti knock performance, methanol octane number is higher than conventional fuel, and it has good anti knock performance. Properly increasing the compression ratio of methanol engines can effectively improve the thermal efficiency of the fuel.

Methanol fuel is a colorless and transparent liquid. As a clean alternative fuel, methanol has great advantages in technology and performance. Promoting the application of methanol fuel is one of the important technological routes to achieve carbon peak and carbon neutrality. It is important to optimize the energy structure and reduce the high dependence of human society on oil, making it a better alternative fuel for gasoline and diesel at present. The methanol fuel supply system, as the core component of the engine, determines the quality and lifespan of the engine, which is of great significance for further promoting the promotion and application of methanol fuel engines.

The combustion effect of methanol is equivalent to that of gasoline and diesel, and methanol fueled engines have better fuel thermal efficiency under the same conditions. However, when the engine uses methanol as a single fuel, there are also many drawbacks, and the impact on the components of the methanol supply system is mainly manifested as follows:

Corrosiveness: Methanol generally contains acidic substances such as formic acid during the production process, and the water absorption of methanol itself makes it contain a small amount of water during storage. At the same time, oxidation by air or bacterial fermentation can also produce a small amount of organic acids such as formic acid, which can cause corrosion to metal components in the methanol supply system.

Swelling: Some components in the methanol supply system of the engine are composed of plastic or rubber composite materials. Methanol is a polar organic solvent that has a strong swelling effect on some conventional rubber parts, leading

to an increase in volume and material hardness, resulting in material brittleness or softening; Directly affecting the service life of components in the methanol supply system will become a key issue restricting the development of methanol fuel.
These problems can be summarized as corrosion and wear of the moving pair in the methanol supply system caused by methanol fuel. Therefore, studying the corrosion and wear laws of methanol fuel on the moving pair of methanol supply system under different environmental conditions, and proposing protective measures, is of great significance for the promotion of methanol fuel.

The main research content of this project is:

Wear can be divided into four basic types: abrasive wear, adhesive wear, fatigue wear, and corrosive wear [3]. The methanol fuel supply system is the core component of the engine. The clearance between the pump core of the methanol supply pump, the steel ball and valve seat of the methanol injector, and other moving pairs is small. It needs to ensure both sliding and sealing, and supply fuel to the combustion chamber in a timely and quantitative manner. Its lubrication protection completely depends on the fuel provided. Compared to traditional diesel and gasoline, methanol fuel has lower viscosity and stronger corrosiveness, which can lead to excessive wear of precision components in the injection system, decreased fitting accuracy, decreased injector flow rate, and injector dripping, resulting in a decrease in the reliability of the injection system, insufficient engine power, and a series of problems such as engine shaking. The specific research content includes the following points:
Research on the Performance of Methanol Filter System
Research on the Corrosion Performance of Methanol Fuel on Various Components of Methanol Supply Pump
Research on the corrosion resistance and wear performance of the moving pair of methanol injector.

1.2. Composition and working principle of methanol fuel supply system

As shown in Figure 1.1. The methanol injection system studied consists of a methanol tank, methanol filter, methanol pump, methanol rail, methanol injector, sensor, and electronic control unit ECU. The methanol injection system studied belongs to a low-pressure injection system in the intake duct, which is installed on the intake manifold.
Working principle: Methanol fuel is stored in the methanol fuel tank, and the methanol pump delivers the methanol fuel to the methanol rail at a certain pressure. The main function of the methanol rail is to store methanol fuel and weaken the pressure fluctuations generated by the methanol pump and the methanol injector during fuel injection. The methanol injector is connected to the alcohol rail, and under the drive of the ECU, it injects methanol fuel into the intake pipe in a timed and quantitative manner, mixes with air, and enters the combustion chamber. The performance of

methanol injectors directly affects the generation and combustion of combustible mixtures in the cylinder, which in turn affects the environmental performance, fuel economy, power performance, reliability, and other aspects of the engine

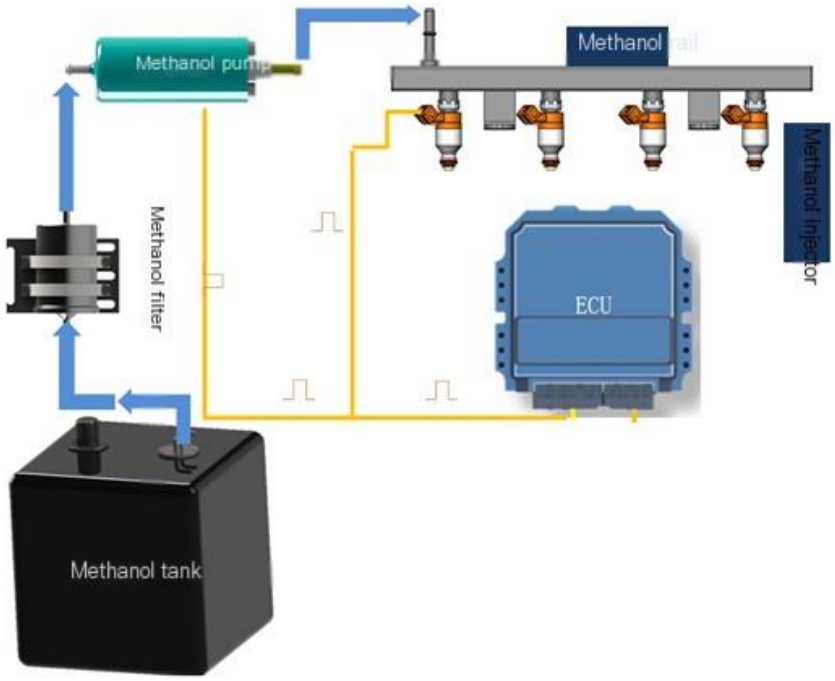

Figure 1. 1. Composition diagram of methanol fuel supply system

1.3. Performance study of methanol filters

The main task of this project is to analyze the factors that affect the filtration efficiency of filters, and then study the reliable operation of fuel cleanliness in hydraulic and fuel injection systems. Finally, the methanol fuel filtration system that ensures the reliable operation of methanol supply systems and methanol engines is studied to avoid the failure of high-precision motion pairs due to wear and tear of particulate pollutants in the fuel and ensure the effectiveness of fuel injection.

1.4. Classification of fuel cleanliness levels

In order to define and classify the cleanliness of fuel oils, the ISO International Organization for Standardization provides pollution standards. The pollution of hydraulic oil is represented by the pollution level, which refers to the content of solid particle pollutants in the working medium per unit volume, that is, the concentration of solid particles contained in the working medium.
As shown in Figure 1.2, the pollution level code reported by the ISO 4406 oil cleanliness level concept using an automatic particle counter consists of three codes,

which represent the particle size and distribution as follows: **the** first code represents particle size ≥ 4 per milliliter of oil μ The number of particles in m (c); The second code represents the number of particles with a particle size of ≥ 6pm (c) per milliliter of oil; The third code represents the number of particles with a particle size of ≥ 14pm (c) per milliliter of oil, for example, fuel oil cleanliness level 24/23/19 is represented as ≥ 4 μ The number of particles above m (c) is between 8000 and 160000 (including 160000), ≥ 6 μ The number of particles above m (c) is between 40000 and 80000 (including 80000), and greater than 14 μ The number of particles above m (c) is between 2500 and 5000 (including 5000).

每毫升颗粒数		
比...更	最多（含）	比例编号
2 500 000		>28
1 300 000	2 500 000	28
640 000	1 300 000	27
320 000	640 000	26
160 000	320 000	25
80 000	160 000	24
40 000	80 000	23
20 000	40 000	22
10 000	20 000	21
5 000	10 000	20
2 500	5 000	19
1 300	2 500	18
640	1 300	17
320	640	16
160	320	15
80	160	14
40	80	13
20	40	12
10	20	11
5	10	10
2.5	5	9
1.3	2.5	8
0.64	1.3	7
0.32	0.64	6

Figure 1.2 ISO 4406 Classification Code

1.5. Analyze the factors that affect the filtration efficiency of filters

Filtering efficiency is one of the most widely accepted criteria for evaluating filter performance. The ISO organization has proposed the standardized performance testing specification ISO 19438-2003 [4], and the verification results indicate that these tests are repeatable. These standards aim to evaluate filters under standard environmental conditions, but these tests do not represent the actual conditions in the filter fuel system. A study by the Charlotte School of Motorsport Engineering at the University of North Carolina [5] shows that under actual conditions, there are four factors that have a significant impact on the filtration efficiency of filters, namely temperature, flow rate, fuel pump, and vibration.

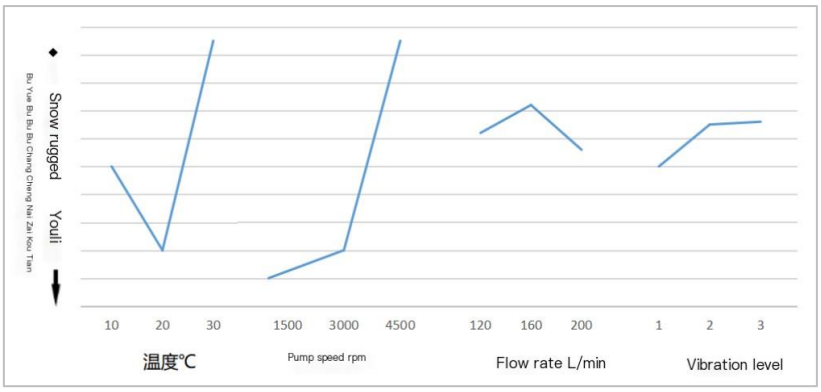

Figure 1.3 Factors affecting filtration efficiency

From Figure 1.3, it can be seen that 1. The temperature parameter will increase with the increase of temperature under certain low temperature conditions, but as the temperature continues to rise, the efficiency will actually decrease; 2. The maximum speed of the oil pump has the greatest impact on the efficiency of the filter; 3. The actual impact of flow on the filter is minimal; 4. Vibration has a significant adverse effect on efficiency, and the impact does not significantly increase when a specific vibration amplitude level is reached.

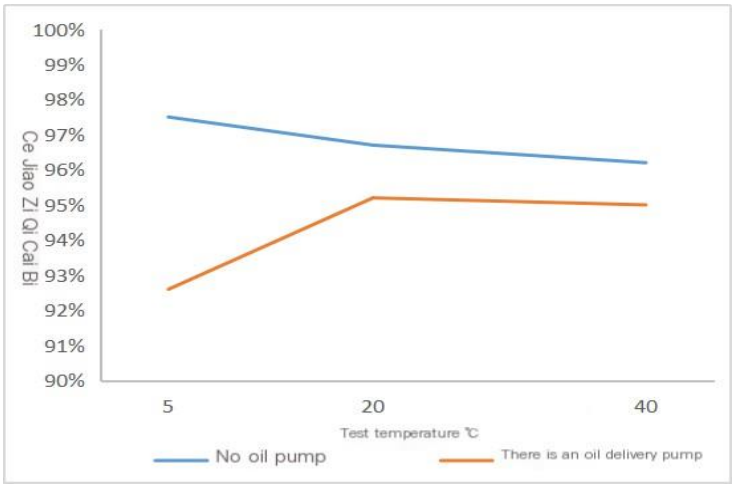

Figure 1.4: The mutual influence between fuel temperature and pump speed

As shown in Figure 1.4, there is a mutual dependence between the temperature of the fuel and the methanol fuel pump under actual operating conditions. The filtration

efficiency with and without oil pumps shows a significant trend of change. The results of the experimental report indicate that in the case of high viscosity fluids, when the filter is exposed to vibration conditions, the filtration efficiency is significantly reduced compared to low viscosity fluids. At the same time, it was also observed that the fuel pump has a significant impact on the filtration efficiency of the filter.

1.6. Research on the Reliability of Fuel Cleanliness in Hydraulic and Fuel Injection Systems

Compared to the standard filter testing method of ISO 19438, in the actual working conditions of vehicles, the fuel in the tank is relatively closed and there is no continuous addition of external pollutants. The fuel in the tank will return to the tank again with the circulation of the oil pump, and the content of pollutants will gradually decrease as shown in Figure 1.5.

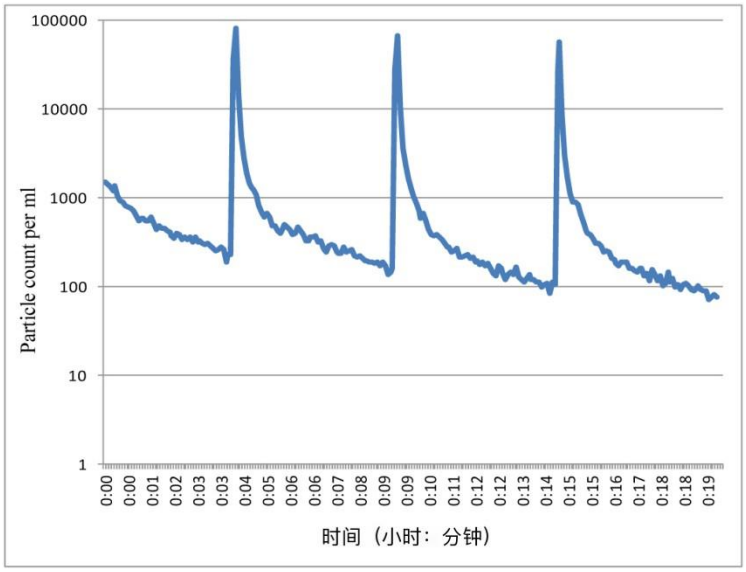

Figure 1.5 Changes in pollutant content in the fuel tank of a real vehicle over time

In order to conduct research on the strengthening and wear resistance of fuel systems, it is necessary to establish an independent fuel supply system to ensure stable pollution levels are obtained during the testing process. The testing process is shown in Figure 1.6.

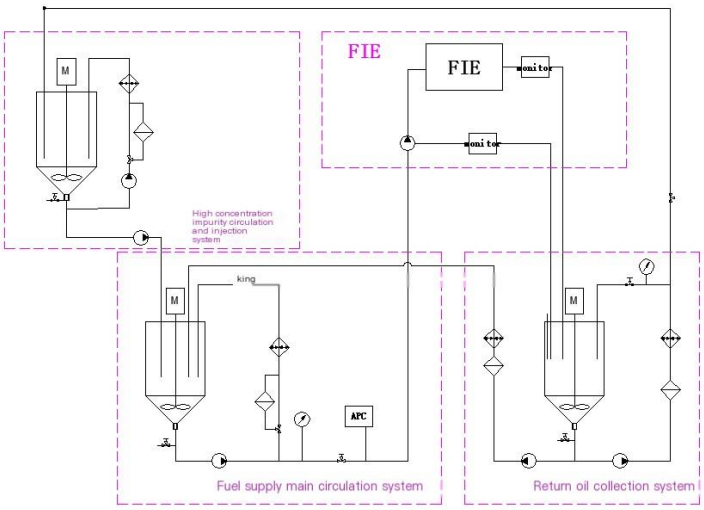

Figure 1.6 Schematic diagram of a stable fuel pollution supply system

The use of a constant pollution concentration testing device can effectively ensure that the fuel supply system can continuously provide a stable concentration of test fuel. To ensure consistency of test results.

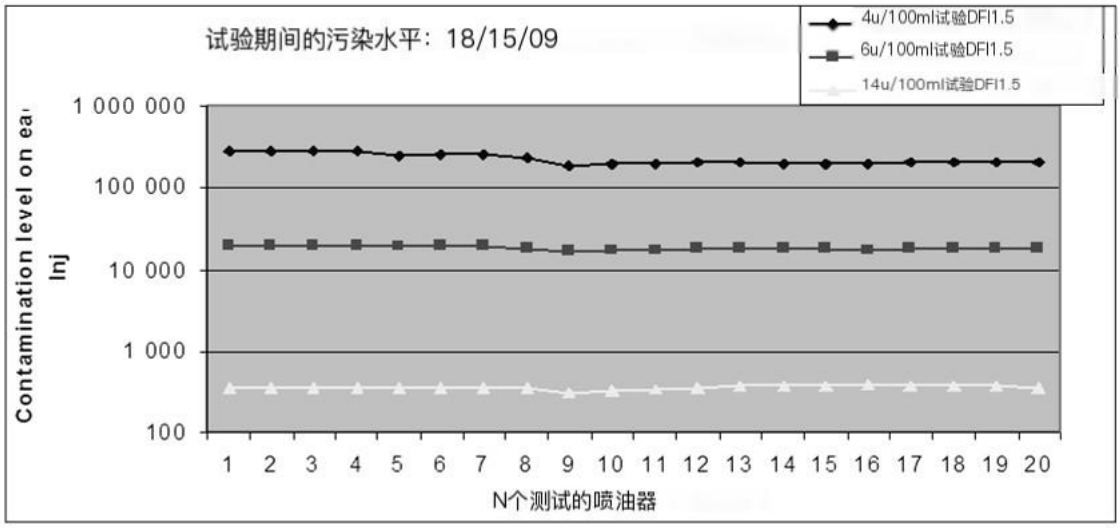

Figure 1.7: Fuel pollutant concentration at the outlet of a stable fuel pollution supply system

As shown in Figure 1.7, ISO 12103-1-A1 dust [8] was used during the testing process, and the pollutant concentration was stably controlled at 18/15/09 level [9]. At the

beginning of accelerated testing, it is necessary to determine a jet duty cycle parameter to determine the testing effect of speed, jet pressure, etc., in order to construct a life distribution between jet pressure and testing life.

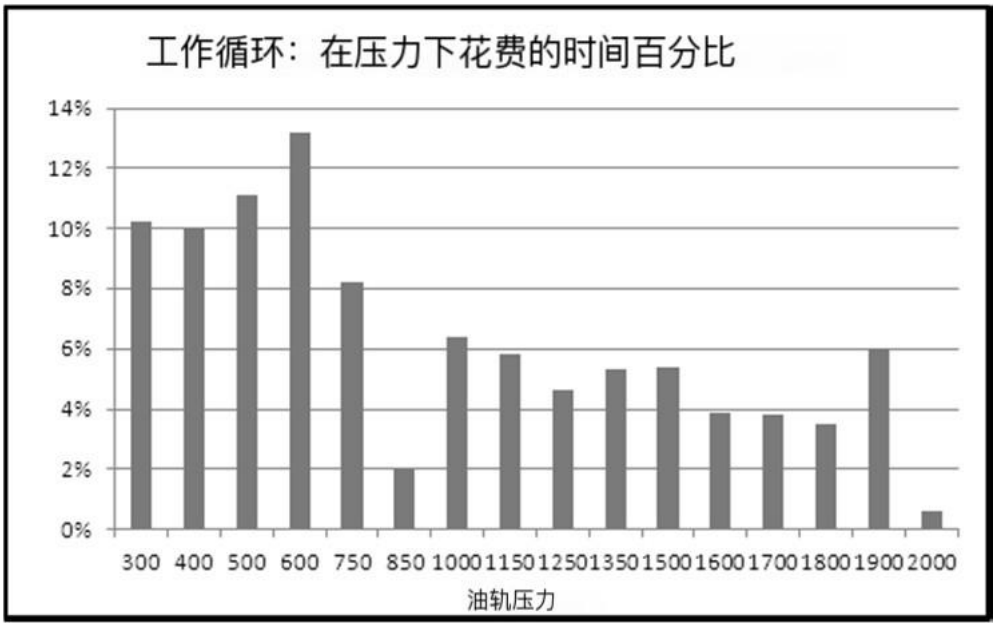

Figure 1.8 Duty Cycle

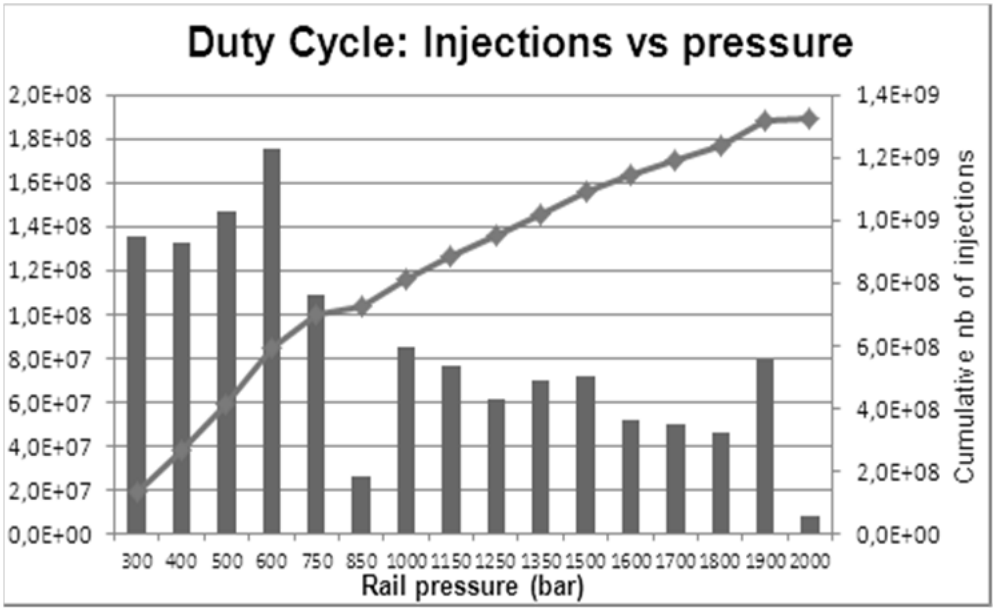

Figure 1.9 Spray VS Pressure

Figure 1.8/9 shows the test parameters of a certain 2.0 engine with a reference average speed of 40 km/h and an average fuel consumption of 6 L/min.

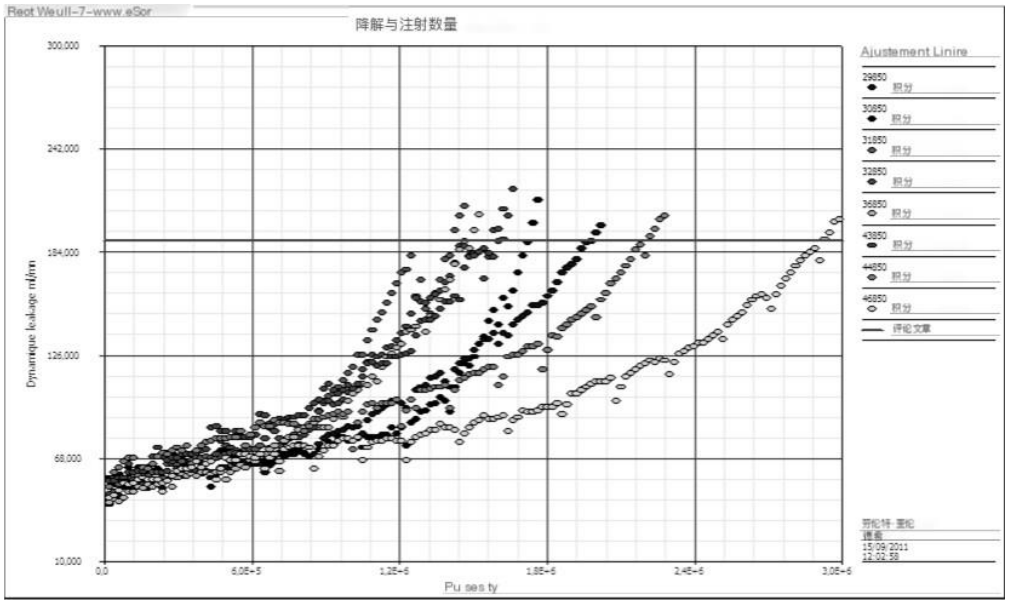

Figure 1. 10 Wear monitoring curve during testing period

During the entire system strengthening wear testing process, continuously monitor the return oil leakage of the fuel supply system injector. When the leakage of the injector reaches its extreme value, the wear limit of the injector is determined. As shown in Figure 1.10.

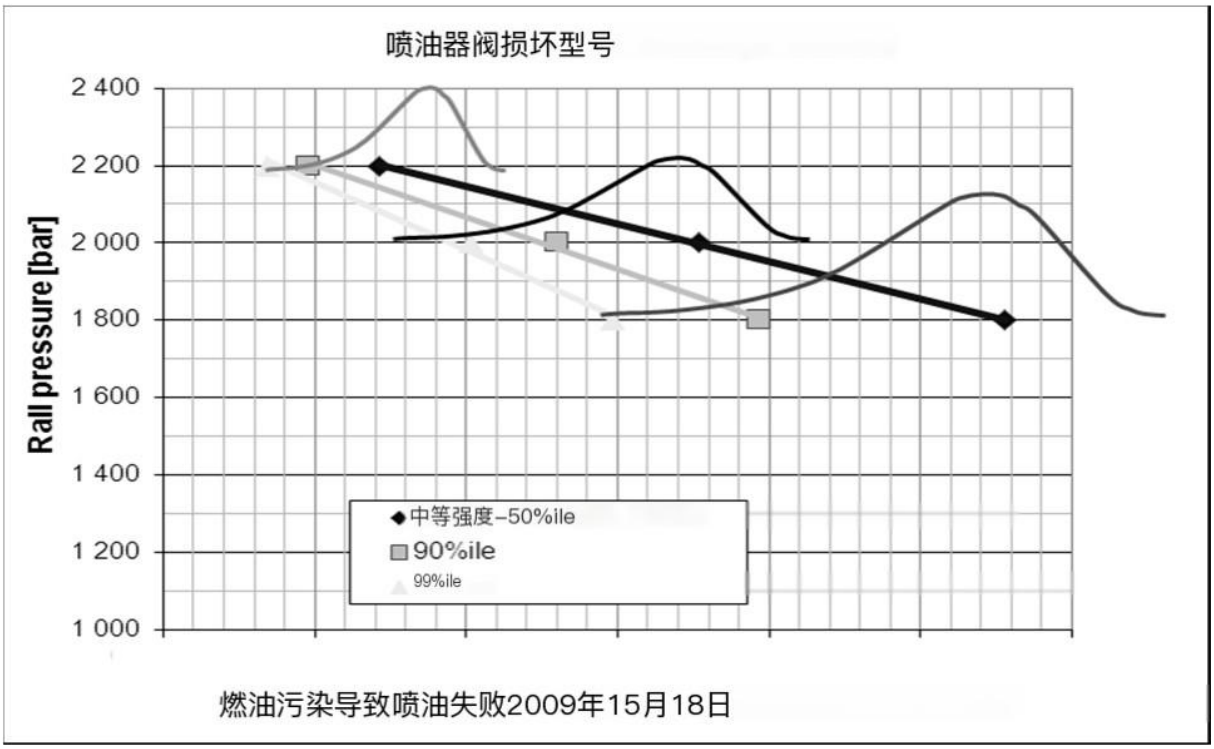

Figure 1.10 Fuel supply system intensity curve

As shown in Figures 1.11 and 1.12, for each pressure level, failure monitoring is used, and the fault time collected in each stage is used to construct the fault distribution in Weibull. Constructing a lifespan system through SN curve Weibull plot of mobile phone parameters

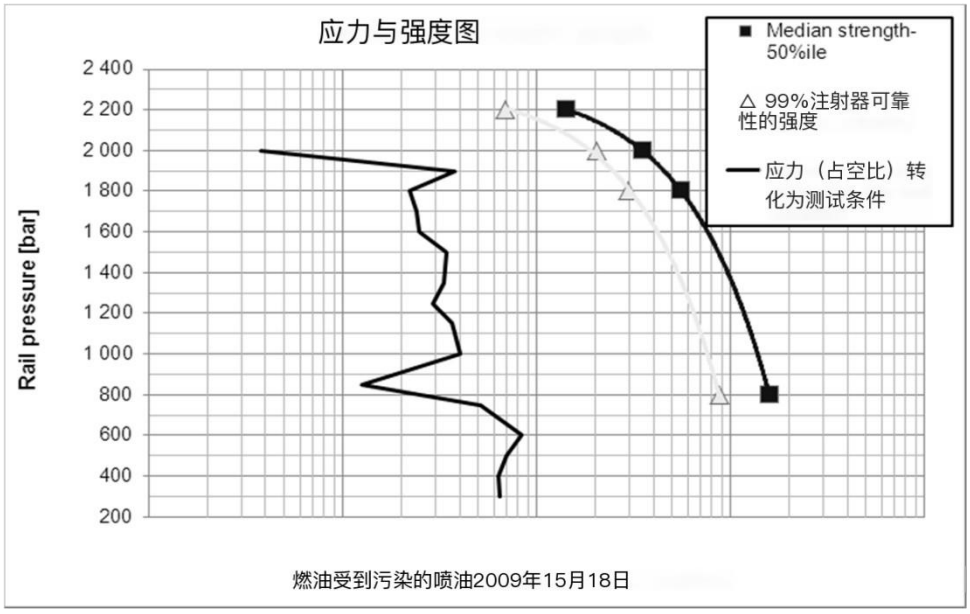

Figure 1.11 Fuel supply system intensity curve

The fuel injector of contaminated fuel must be converted to the final test conditions of the filter using the average ratio of the test pollution level to the pump inlet.
The minimum filter performance required by the system FIE is to ensure a minimum injector reliability of 99% for a given fuel quality market This provides the filtration efficiency of the fuel filter, and finally, it is necessary to β Apply a correction factor to ensure that the engine's fuel system is always at a safe level of cleanliness

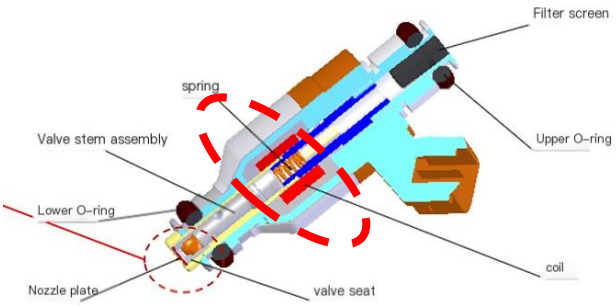

Figure 1.12 Typical methanol fuel system injector

Figure 1.14 shows a typical methanol fuel injector, with the parts of the injector that are most susceptible to pollution particles shown in the dashed box in the figure.

1.7. Research on the reliability of methanol filters

Design scheme of methanol filter and definition of classification efficiency.

Based on the research on engine fuel systems both domestically and internationally, the application of common fuel filtration systems in vehicles is shown in Figure 1.15/16.

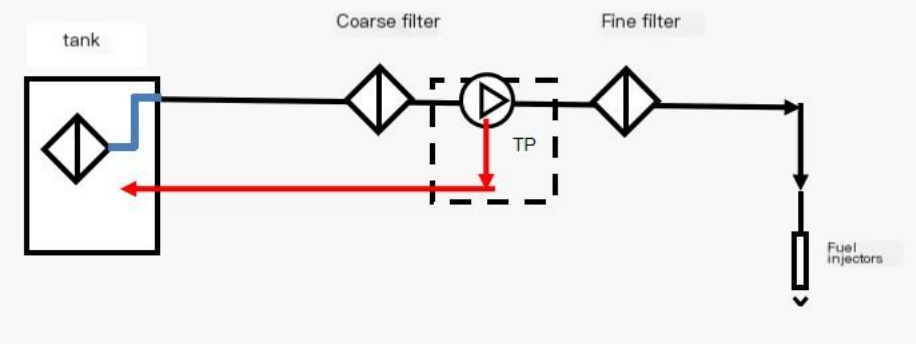

Figure 1.13 Typical methanol fuel filtration system - two-stage filtration

Figure 1.14. Application of two-stage filtering on a certain vehicle model

As shown in Table 1.1, the Chinese standard T/CAAMTB 128-2023 provides guidance on the filtration classification efficiency requirements for methanol fuel filtration systems.

Table 1.1 Requirements for filtration classification efficiency of methanol fuel filtration system

Filter size	Coarse filtration efficiency	Precision filtration efficiency
⩾ 4 μ M (c)	⩾ 40%	⩾ 95%
⩾ 6 μ M (c)	⩾ 50%	⩾ 97%
⩾ 14 μ M (c)	⩾ 90%	⩾ 99%

Research on the Material Resistance of Methanol Filter Components to Methanol Corrosion

Methanol has a small molecular weight and a simple molecular structure. Compared to traditional gasoline, methanol is more likely to penetrate non-metallic components such as rubber and cause swelling, accelerating material aging [10,11]. Rubber components and resin two-component adhesives, as important components of common fuel filter seals and connections, need to be fully verified for durability and reliability.

(1) Research and application of methanol resistance in rubber parts

We selected common automotive rubber sealing materials - nitrile rubber (NBR), chlorohydrin rubber (CHC), polyurethane rubber (PU), and fluororubber (FPM). Through soaking method research and comparison, we determined which test rubber material has the highest solubility, and accurately identified the swelling mechanism of rubber material in methanol gasoline mixed fuel. From a chemical perspective, we solved the swelling property of rubber material in methanol and methanol gasoline mixed fuel [12], as shown in Table 1.2.

Table 1.2 Changes in mass and volume of rubber materials tested in different test liquids

Rubber material	M100 methanol fuel		M85 methanol gasoline		M10 methanol gasoline		Pure gasoline	
	△ M	△ V	△ M	△ V	△ M	△ V	△ M	△ V
NBR-18 nitrile rubber	-0.5	two point one	eleven point one	twenty point three	fifty point three	seventy-four point three	thirty-four point seven	fifty-four point three
NBR-26 nitrile rubber	two point two	five point four	eleven point one	twenty point four	thirty-eight point one	sixty point nine	twenty-eight point four	forty-six point one
NBR-40 nitrile rubber	three point four	eight point three	eleven point one	twenty point four	twenty-eight point three	forty-five point two	twelve point five	twenty point six
CHC chlorophenol rubber	ten point nine	twenty-one point two	thirteen point one	twenty-five point one	thirteen point four	twenty-seven point one	seven point two	fourteen point three
PU polyurethane rubber	thirteen point eight	twenty-three point six	fourteen point eight	twenty-six point five	eighteen point two	twenty-nine point three	four point three	seven point five

FPM-246 fluororubber	fourteen point three	thirty-three point five	twelve point seven	thirty point four	two point four	six point four	zero point six	one point two

From the above table, it can be seen that the volume change rate and mass change rate of different rubber materials in the methanol gasoline mixture fuel test are different. FPM-246 (fluororubber) has a larger swelling degree as the methanol content increases, while CHC (chlorohydrin rubber) and PU (polyurethane rubber) have a much greater swelling degree in the methanol gasoline mixture fuel than in pure methanol and pure gasoline.

1) In M100 methanol fuel, the swelling degree of NBR decreases as the content of acrylonitrile increases (the reduction effect is not significant).

2) In M85 methanol gasoline, the acrylonitrile content of NBR has no effect on the swelling degree of NBR in methanol gasoline blend fuel, and all show the same swelling value.

3) In M10 methanol gasoline and pure gasoline, the acrylonitrile content of NBR has a significant impact on the swelling degree of NBR in methanol gasoline blended fuel. As the acrylonitrile content of NBR increases, the swelling degree of NBR in methanol gasoline blended fuel also increases.

(2) Research and application of resin adhesive for methanol resistance

Two component epoxy resin adhesive is often used in traditional automotive filters to play a bonding and sealing role. However, studies have shown that after the resin is soaked in methanol, methanol can penetrate into the epoxy resin, causing partial hydrolysis of the epoxy resin and producing amine substances. Part of the amine substances exist in the resin, some dissolve out of the resin and enter the methanol solution, contaminating methanol [13].

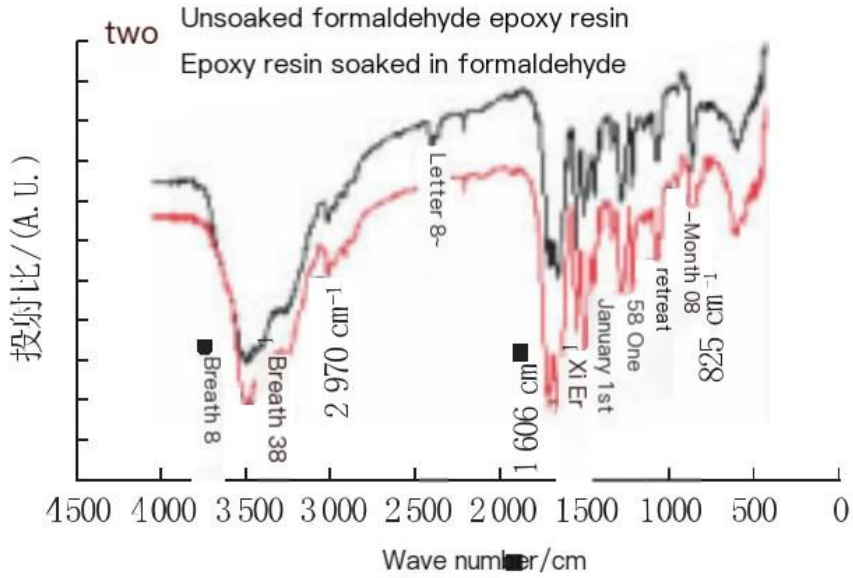

Figure 1.15 FTIR spectroscopic analysis of epoxy resin before and after methanol immersion

（a）浸泡3天　　（b）浸泡5天

Figure 1.16 Color comparison of methanol samples with potassium permanganate added after different soaking times

For the epoxy resin soaked in methanol solution for 7 days, the infrared absorption

spectrum shows an increase in transmittance at 1460cm-11606cm-1 and 3347cm-1, indicating that the stretching vibration of N-H, benzene ring skeleton, and methyl C-H bonds in the soaked epoxy resin is accelerated; At 2354 cm-1, the vibration of the C-N bond weakens. This is because methanol can penetrate into epoxy resin, causing partial hydrolysis of the epoxy resin and producing amine substances. Part of the amine substances exist in the resin, and some dissolve out of the resin and enter the methanol solution, which leads to a shorter time required for potassium permanganate decolorization in the methanol solution during potassium permanganate testing. To further confirm that amines can react quickly with potassium permanganate, trace amounts of organic amines were added to methanol. It was found that less than 0.05mL of amines added to 50mL of methanol solution could instantly cause potassium permanganate to fade, while pure methanol solution took more than 100min to cause potassium permanganate to fade. Therefore, the amine in the epoxy resin curing agent can be dissolved in methanol. Due to the dissolution of amine in the curing agent, the molecular chain of the epoxy resin may be shortened, further causing the epoxy resin to dissolve [13].

Summary:
1) The maximum speed of the fuel supply pump should be reduced while ensuring sufficient flow.
2) On the premise of ensuring stable installation of the fuel filter, the vibration of the filter position should be minimized as much as possible.
3) If conditions permit, try to select a filter with a larger filtration area to reduce the relative flow rate.
4) Efficient filters should be selected to ensure protection of the fuel supply system.
5) Reducing the working pressure of the engine as much as possible while meeting the requirements of combustion emissions can effectively improve the service life of the fuel supply system.
6) Seals in methanol fuel systems should be made of modified nitrile rubber with significant anti swelling effects as much as possible.
Epoxy resin sealing adhesive materials should be avoided in methanol fuel systems.

1.8. Research on the corrosion performance of methanol fuel on various components of methanol supply system

1.8.1 Current research status of methanol pumps

The main task of this project is to study the brushless methanol pump assembly technology suitable for the operating conditions of methanol engines through performance testing of methanol pumps and verification of actual engine operating conditions. Especially, the corrosion degree of various components of methanol pumps by different proportions of methanol fuel was studied, and suitable materials were selected to improve the practicality and reliability of methanol pumps in practical

applications.
Methanol is corrosive to metals and has swelling properties on rubber and plastic parts. Methanol is corrosive to metal materials such as tin, copper, aluminum, magnesium, and zinc. In the engine fuel supply system, it corrodes lead tin alloys, aluminum zinc magnesium alloys, brass, and other metals to form hydroxides. Methanol containing water can also cause corrosion and rusting of steel pipes or thin steel plates. Corrosion products can easily cause blockage of fuel filters and nozzles, while entering the combustion chamber will affect the normal operation of the engine and accelerate the oxidation and deterioration of lubricating oil. At the same time, formic acid, nitric acid, and other substances in methanol combustion products can react with iron at lower temperatures to form iron salts and peel off from the surface of the parts. The new exposed iron surface will further corrode.
Methanol can cause swelling in general rubber and plastic parts, and the swelling problem must be solved in methanol vehicles.
Compared with traditional gasoline and diesel vehicles, the major change in methanol fuel vehicles is the methanol fuel supply pump assembly. Compared with traditional gasoline and diesel supply pumps, the main changes in methanol fuel supply pumps are as follows:
Due to the low calorific value and evaporation pressure of methanol fuel, the same fuel pump bracket assembly may present difficulties in cold starting or insufficient fuel supply at high speeds on the entire vehicle. At the same time, theoretically, the consumption of methanol fuel is about twice that of gasoline fuel, which puts higher demands on the fuel supply capacity of the fuel pump.
Due to the strong polarity of methanol fuel, methanol molecules will directly combine with metal molecules, resulting in strong dry corrosion on metal parts. This mainly leads to oxidation and corrosion of parts with a high proportion of copper, aluminum, or silver in the fuel pump bracket assembly. Especially, corrosion of copper commutators, exposed copper wires, and copper silver brushes in the pump core can cause power attenuation and flow reduction of the pump core motor. In severe cases, it can lead to motor failure, causing the fuel supply pump to lose its fuel supply capacity and causing the vehicle to break down. In addition, if there is a connection design for electrical components with welding technology, it will cause the welding material to melt and pollute the precision of moving parts that require high signal quality.
Methanol fuel has strong chemical permeability, so it has a strong swelling effect on some conventional rubber parts, and in severe cases, rubber parts may dissolve. Some rubber materials commonly used in the design of automotive sealing parts lose their original elasticity due to long-term soaking and expansion in methanol fuel, ultimately leading to sealing failure and fuel leakage. For some anti vibration pad parts, due to severe volume expansion, excessive deformation may occur and escape from the installation groove, leading to serious failure. The swelling rates of rubber parts with different materials and designs vary greatly under different ratios of gasoline and methanol fuel. For rubber or plastic parts with high dimensional change

rate requirements in fuel pump bracket assemblies, especially sealing rubber parts, design improvements can be made in material selection, and anti swelling design is also required.

In response to the above issues, the corrosion resistance of the methanol engine fuel supply pump has been improved as follows:

For the key moving parts of the pump core, design improvements will be made by replacing the copper steering gear with a carbon steering gear in the pump core, which plays a role in corrosion resistance and wear resistance; Copper wires must undergo chrome plating treatment indicating corrosion resistance; Change the aluminum inlet and outlet oil plates to high-strength methanol resistant plastic inlet and outlet oil plates; For non-ferrous metal bearings on the inlet and outlet oil plates, carbon bearings have been improved to enhance wear resistance and corrosion resistance.

As shown in Figure 1.19, another new solution is to replace traditional brushed motors with brushless motors. The motor eliminates the commutator and brush structure, completely avoiding the corrosion problem of the commutator and brush.

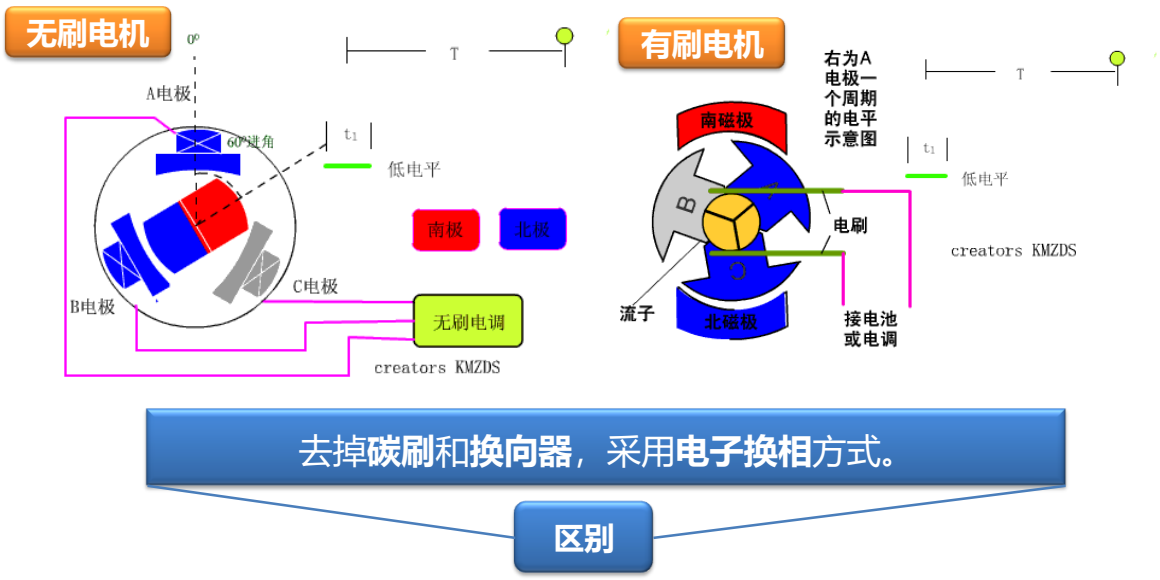

Figure 1.17 Brushless and Brushless Motors

For corrosion-sensitive liquid level sensors, there are currently two ways to avoid methanol corrosion in the design direction: one is a sealed design, which seals the guide belt, spring plate, and contact in the box. However, this design has high cost, and the dry wear of the guide belt and contact can cause design problems such as low component life, high cost, and unstable signal quality of the sensor; Another approach is to use anti-corrosion measures to design and remove copper corrosion. The specific solution is to optimize the material formula on the resistance conduction band. The conduction band circuit is designed with parallel double contacts, the

spring plate is treated with chrome plating, and the gold-plated metal contacts are designed with gold composite contacts. All exposed copper wires are removed from the circuit to improve oxidation resistance and corrosion resistance.
For the wiring harness plug part in the fuel supply pump assembly, a sealed design should be used as much as possible to avoid exposed welding inserts and isolate direct contact with methanol fuel; To avoid contamination of the guide belt of the liquid level sensor and the inlet and outlet oil plates and commutator of the pump core after the welding material melts.
For larger plastic components such as flanges and oil storage tanks on the fuel supply pump assembly, due to the widespread use of POM or polyoxymethylene with glass fiber, polyoxymethylene has good solubility, oil resistance, weak acid and alkali resistance, and can still meet design requirements in M85 and M100 methanol fuels.

1.8.2. Effect of Fuel with Different Methanol Concentrations on Metal Materials of Methanol Pump

Based on the characteristics of methanol medium, the component materials of methanol fuel supply pump were selected and a series of immersion tests were conducted, as shown in Figure 1.20. Different metal materials were immersed in different concentrations of methanol medium to study the corrosive effect of fuel with different methanol concentrations on the metal materials of methanol pump.

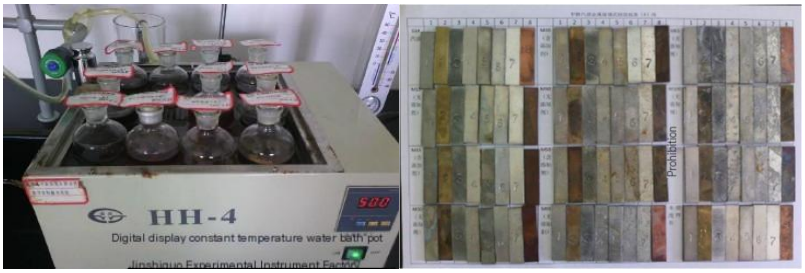

Figure 1.18 Different metal materials soaked in different concentrations of methanol

Methanol is corrosive to metal materials such as tin, lead, aluminum, copper, and magnesium, which can cause corrosion of metal components such as lead tin alloys, aluminum zinc magnesium alloys, and brass in the fuel supply system, leading to premature failure. The experimental results are shown in Figure 1.21.

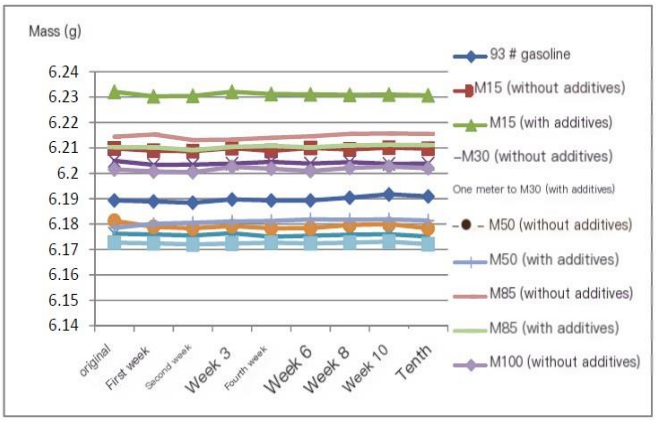

Figure 1.19 Analysis of the Effect of Different Methanol Concentrations on Different Metal Materials

1.8.3. Effects of Fuel with Different Methanol Concentrations on Methanol Pump Rubber Materials

Methanol has a swelling effect on conventional rubber components, and in severe cases, it can cause them to melt, leading to premature sealing failure. Therefore, as shown in Figure 1.22, the macroscopic changes of different rubber materials were verified by soaking them in different ratios of methanol solution for different times, in order to find suitable methanol resistant rubber materials.

Figure 1.20 Immersion of different rubber materials in solutions with different methanol concentrations

As shown in Figure 1.23, silicone rubber, nitrile rubber, and EPDM rubber have the smallest swelling in M100 methanol solution, while fluororubber has the largest swelling in M100 methanol solution.

	93 # gasoline	M15 methanol oil	M30 methanol oil	M50 methanol gasoline	M85 methanol gasoline	M100	methanol
Nitrile rubber	1.24	7.82	8.79	9.19	*1.52*	*-1.55*	*-1.62*
Fluororubber	4.51	12.40	14.61	16.39	18.09	17.33	15.19
silicon rubber	52.67	45.28	37.32	24.11	4.27	0.02	-0.05
EPDM rubber	42.53	30.21	23.31	*15.99*	*2.20*	*-2.96*	*-3.05*

Note: The data in the table represents the rate of change in the outer diameter of the rubber ring after swelling (%).

Dark green (-4%~+5%) with slight swelling deformation; Green (+5%~+10%) has smaller swelling deformation; Yellow (+10%~+20%) has significant swelling deformation; Brown yellow (+20%~+35%) has significant swelling deformation; Red (+35%~+60%) has severe swelling deformation; The italicized part makes the material harder.

1.2

Figure 1.21 Analysis of the Effect of Different Methanol Concentrations on Different Rubber Materials

1.8.4. Effects of fuels with different methanol concentrations on plastic materials for methanol pumps

The swelling effect of methanol fuel on plastic materials can affect their performance, such as sealing, lubrication, mechanical properties, etc. As shown in Figure 1.24, the macroscopic changes of plastic materials were observed by immersing different plastics in methanol solutions of different proportions for different times. Search for suitable methanol resistant plastic materials.

Figure 1.22 Analysis of the Effect of Different Methanol Concentrations on Different Plastic Materials

As shown in Figure 1.25, it was found through immersion tests that there is a significant difference in the swelling properties of plastic materials between gasoline and methanol.

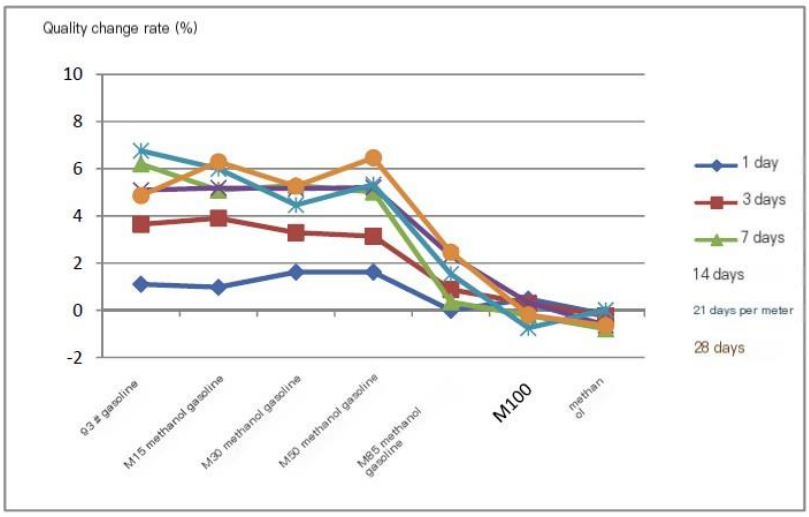

Figure 1.23 Analysis of the Effect of Different Methanol Concentrations on Different Plastic Materials

1.8.5. Research on Reliability Performance of Methanol Pump

During the use of methanol pumps, methanol is prone to corrosion and wear on its key moving parts, especially when energized. If there is a slight current leakage in the conductor, it will exacerbate the corrosion of methanol on the components. The main core components include rotor, stator, coil, shaft, impeller, etc., and reliability research is needed on the core moving parts of the methanol pump.

Conduct long-term performance testing on the methanol pump, analyze the overall performance and corrosion and wear of components. The testing conditions are as follows:

The same batch of methanol pumps were placed in a sealed container and subjected to immersion tests. They were immersed in M100 vehicle methanol fuel (filled with methanol solution inside) under conditions of 40 ℃± 2 ℃, and operated with electricity (rated voltage) for 4000 hours. The main performance of the methanol pump was retested in M100 vehicle methanol fuel solution, and a certain proportion of water was added to the methanol solution to simulate the actual working process of the methanol pump. The methanol solution will absorb water, which will intensify the corrosion of components.

After long-term testing, the main failure modes of methanol pumps directly related to the use of methanol fuel are two aspects. On the one hand, the methanol pump rotor is stuck, resulting in the failure of the methanol pump function. On the other hand, the wear and tear of the impeller leads to an increase in internal leakage of the methanol pump and a decrease in oil supply capacity. In Figure 1.26, a and b show the rusting of the methanol pump rotor and stator, resulting in rotor jamming and methanol pump failure. In Figure 6, c is due to wear on the impeller end face, which leads to a

decrease in the oil pump's supply capacity and causes the oil pump to fail.

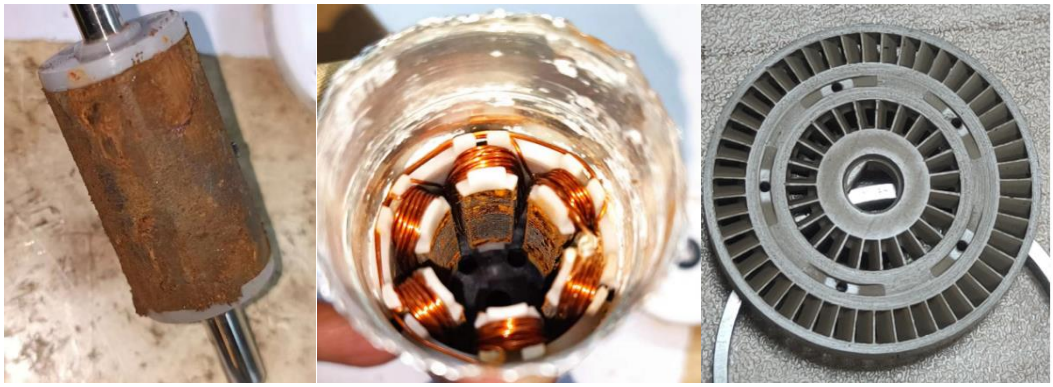

(a) (b) (c)

Figure 1.24 Corrosion and wear parts of methanol pump moving parts

In response to the corrosion and wear of the key components mentioned above, it is necessary to carry out anti-corrosion and wear-resistant treatment on these components. The main plan is as follows:
The solution to the rusting and jamming fault of the rotor and stator is to isolate the contact between the surface of the rotor and stator and methanol fuel, and to isolate the corrosion of methanol fuel on the surface of the stator through the use of encapsulation technology. At the same time, the rotor is wrapped in a stainless steel sleeve to solve the problem of rust and jamming on the surface of the rotor. In addition, during the operation of the methanol pump, the current continues to flow through the stator coil, further improving the insulation of the stator through encapsulation to prevent micro current leakage problems.
For the problem of fuel supply capacity degradation caused by impeller wear in methanol pumps. Due to the non lubricity of methanol fuel itself, and the corrosiveness of methanol fuel exacerbates the wear of the impeller end face, it has a greater impact on methanol pumps with lower speeds. The solution is as follows: replace the impeller material and use materials with better corrosion resistance and self-lubricating performance, such as PEEK. In addition, increase the rated operating speed of the methanol oil pump to reduce the impact of impeller end face wear on the oil supply capacity of the oil pump assembly.

1.8.6. Summary:
Methanol is corrosive to metal materials such as tin, lead, aluminum, copper, and magnesium, which can cause corrosion of metal components such as lead tin alloys, aluminum zinc magnesium alloys, and brass in the fuel supply system, leading to premature failure.

Seals in methanol fuel systems should be made of modified nitrile rubber with significant anti swelling effects as much as possible.
Epoxy resin sealing adhesive materials should be avoided in methanol fuel systems. Methanol fuel has strong corrosion and wear on key moving parts of the methanol pump, especially in the energized state. If there is a slight current leakage in the conductor, it will exacerbate the corrosion of methanol on the parts. By adopting a plastic coating process on the stator surface, the corrosion of methanol fuel on its surface is isolated. At the same time, the rotor is wrapped in stainless steel sleeve to solve the problem of rust and jamming on the surface of the rotor

Chapter 2. Research on corrosion resistance and wear performance of the moving parts of methanol injector

2.1. Current research status of methanol injectors

The corrosion resistance and wear resistance of methanol injector materials determine the reliability of the injector's operation. The reliability of methanol injectors in the early stage of the market was poor. After running for a period of time, various moving parts had varying degrees of corrosion and wear, leading to varying degrees of attenuation or dripping leakage of fuel injector flow, resulting in engine shaking, misfire, and other phenomena. In response to the corrosive and low viscosity characteristics of methanol medium, it is necessary to study the corrosion resistance and wear resistance of the surfaces of various components of methanol injectors.

The motion pair composed of steel balls and valve seats is one of the key motion pairs in methanol injectors. The clearance between the motion pairs is small, and there are often high-frequency impacts between the steel balls and valve seats during operation, ensuring both sliding and sealing performance. Compared to traditional gasoline engine nozzles, it is also necessary to consider their resistance to methanol corrosion. Therefore, both parts need to choose high hardness stainless steel materials, which can improve surface hardness through heat treatment. From previous market research, it was found that due to the presence of certain formic acid in methanol, there is corrosion and wear on the surface of the steel ball and valve seat, which leads to the failure of the injector seal. Therefore, further research is needed on the corrosion resistance of the steel ball and valve seat motion pair materials to methanol and formic acid.

The motion pair composed of the armature and nozzle body is also one of the key motion pairs in methanol injectors, especially the armature parts. This part requires magnetic materials with low coercivity and high magnetic permeability, and soft magnetic materials need to be selected. Compared with traditional gasoline engine nozzles, it is necessary to consider their methanol corrosion resistance and choose stainless steel soft magnetic materials with better corrosion resistance. Due to the high-frequency reciprocating motion of the armature in the nozzle body, its wear resistance needs to be considered, so it needs to have a certain degree of hardness. However, this type of stainless steel soft magnetic material cannot improve its hardness through heat treatment due to its low carbon content, which is a

contradiction in the application field of stainless steel. In the preliminary experimental verification, after working for a period of time, the surface of the armature is prone to wear, resulting in significant changes in the flow rate of the injector. Therefore, further research is needed on the surface strengthening treatment method of the armature to make the surface of the armature corrosion-resistant and wear-resistant.

2.2. Research on methanol corrosion resistance of steel balls and valve seat motion pairs in methanol injectors

The motion pair composed of steel ball and valve seat is one of the key motion pairs in methanol injectors. The clearance between the motion pairs is small, and during the working process, there are often high-frequency impacts between the steel ball and valve seat, ensuring both sliding and sealing performance. Compared to traditional gasoline engine nozzles, it is also necessary to consider their resistance to methanol corrosion. Therefore, both parts need to choose high hardness stainless steel materials, which can improve surface hardness through heat treatment. From previous market research, it was found that due to the presence of certain formic acid in methanol, there is corrosion and wear on the surface of the steel ball and valve seat, which leads to the failure of the injector seal. Therefore, further research is needed on the corrosion resistance of the steel ball and valve seat motion pair materials to methanol and formic acid.

2.2.1.Test plan

Prepare samples of three different types of materials, first polished with 120 # sandpaper, and then polished with 240 # and 400 # metallographic sandpaper until the final surface roughness is about Ra0.1. The polished samples are cleaned in ultrasonic waves and weighed. After observing its surface morphology under an optical microscope, immerse it in a quantitative test solution and maintain it at a certain temperature for a period of time. Observe the color change of the test medium before and after immersion; Take out the metal sheet again, weigh it again, and calculate the corrosion rate of the metal sheet using the weight loss method; After final purification treatment, observe the surface morphology changes after corrosion using an optical microscope, and finally analyze the corrosiveness of various materials.

(1) Test samples

Material 1: Ordinary steel, size specification 55 * 10 * 10mm, quantity 3

Material 2: Martensitic stainless steel; Size specification 55 * 10 * 10mm, quantity 3

Material 3: Martensitic stainless steel+surface coating; Size specification 55 * 10 * 10mm, quantity 3

(2) Test medium

Methanol generally contains acidic substances such as formic acid in the production process, and its water absorption makes it contain a small amount of water during storage. At the same time, oxidation by air or bacterial fermentation can also produce

a small amount of organic acids such as formic acid, which can cause corrosion to metal components in the methanol supply system. Test medium: mass ratio of mixed solution: 70% M100 methanol, 25% formic acid, 5% water;

2.2.2. Test results and analysis

(1) Observe the color change of the test medium before and after soaking
Due to the strong volatility of methanol, as shown in Figure 2.1, the test sample was immersed in the test container and sealed with a thin film bag. A pure methanol corrosion test was conducted at room temperature. After soaking for 25 days, the color change of the test medium before and after soaking was observed. As shown in Figure 2.2, after the test specimen is immersed in the test container, the solution in ordinary carbon steel undergoes chemical corrosion and turns brown, while in martensitic stainless steel, the solution turns light brown. The color of martensitic stainless steel+surface coating remains unchanged.

Figure 2.1 Image before soaking in the test

From left to right are ordinary steel, martensitic stainless steel, martensitic stainless steel+surface coating

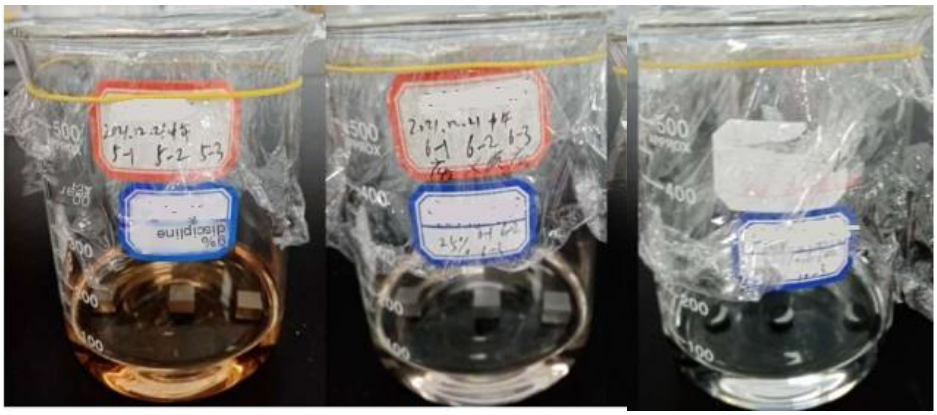

Figure 2.25 Image before soaking in the test

(From left to right are ordinary steel, martensitic stainless steel, martensitic stainless steel+surface coating)

Through immersion tests in a solution mass ratio of 70% M100 methanol, 25% formic acid, and 5% water, it was found that the solution in ordinary carbon steel undergoes chemical corrosion, rust, and turns brown in color, resulting in the worst corrosion resistance; The solution in martensitic stainless steel turns light brown, with a lighter color and better corrosion resistance; The solution color of martensitic stainless steel with surface coating remains unchanged and has the best corrosion resistance.

(2) Corrosion rates of different materials

Corrosion rate, also known as quality loss rate, is a physical quantity used to characterize the changes in quality of materials before and after corrosion. The calculation formula is:

$$X=G/S \quad (1)$$

In the formula:

X - corrosion rate, unit $g/^{m2}$;

G - The weight change of the metal sheet after the experiment, in grams;

S - The total area of the metal surface, in square meters.

As shown in Table 1, the weight of each specification of material is recorded before soaking. After soaking for 25 days, each metal sheet is taken out and weighed again. The corrosion rate of the metal sheet is calculated using the weight loss method.

Table 2.1 Corrosion rates of different materials

Material Name	**Before invasion (g)**	**After invasion (g)**	**Weight reduction Mean (g)**	**Mean surface area (m2)**	**Corrosion rate (g/m2)**
Ordinary carbon steel	seven point three one one one seven point two two seven seven seven point zero six eight seven	seven point three zero five three seven point two one three five seven point zero five nine three	zero point zero zero nine eight	zero point zero zero two four	four point zero eight
Martensitic stainless steel	eight point five three nine eight eight point five one two eight eight point six zero three eight	eight point five three five eight eight point five zero nine two eight point six zero zero six	zero point zero zero three six	zero point zero zero two four	one point five zero
Martensitic stainless steel+surface coating	eight point seven eight two two eight point seven eight one six	eight point seven eight two zero eight point seven eight one five	zero point zero zero zero two	zero point zero zero two four	zero point zero eight

	eight point seven seven nine five	eight point seven seven nine two			

As shown in Table 2.1, by using the corrosion rate method for evaluation, it was found that ordinary carbon steel has a corrosion rate of 4.08g/m2, and its corrosion resistance is the worst; Martensitic stainless steel has a corrosion rate of 1.5g/m2 and good corrosion resistance; Martensitic stainless steel+surface coating corrosion rate 0.08g/m2, with the best corrosion resistance

(3) Observing the changes in appearance of different materials before and after testing

Before and after the experiment, observe the appearance changes of different materials through an optical microscope, and soak them in a solution for 25 days. As shown in Figure 2.3, the surface corrosion of ordinary carbon steel is severe and the effect is the worst; As shown in Figure 2.4, the surface corrosion of martensitic stainless steel is slight and the effect is good; As shown in Figure 2.5, martensitic stainless steel+surface coated metal sheet has the best effect with no significant corrosion on the surface.

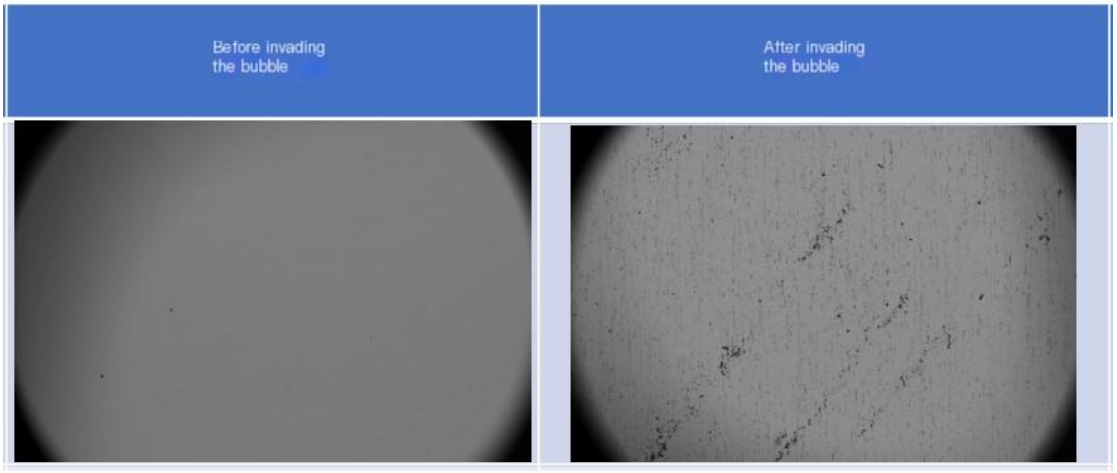

Figure 2.3 Appearance of ordinary carbon steel before and after immersion

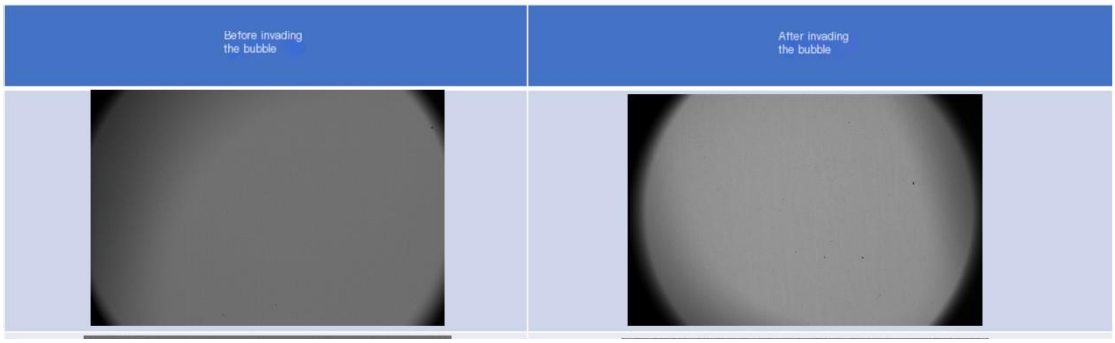

Figure 2.4 Appearance of Martensitic Stainless Steel Before and After Immersion

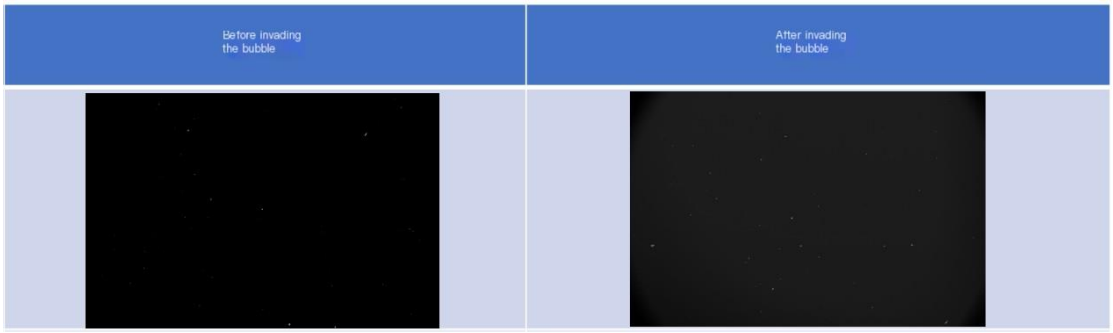

Figure 2.5 Appearance of Martensitic Stainless Steel+Surface Coating Before and After Immersion

By using an optical microscope to observe the appearance of each metal sheet, it was found that the appearance of ordinary carbon steel metal sheets is severely corroded and has the worst corrosion resistance; The appearance of martensitic stainless steel metal sheets is slightly corroded and has good corrosion resistance; Martensitic stainless steel+surface coated metal sheet has no obvious corrosion on the surface, and has the best corrosion resistance

2.2.3 Experimental Conclusion

Through immersion tests in a solution mass ratio of 70% M100 methanol, 25% formic acid, and 5% water, the following conclusions were drawn:;
Ordinary carbon steel has the worst resistance to methanol corrosion
Martensitic stainless steel materials have slight corrosion and good corrosion resistance.
Horse body stainless steel material+surface coating has the best corrosion

resistance

2.3 Study on Friction and Wear Performance of the Moving Pair of Methanol Ejector

The motion pair composed of the armature and nozzle body is also one of the key motion pairs in methanol injectors, especially the armature parts, which are made of stainless steel soft magnetic materials. Due to the high-frequency reciprocating motion of the armature in the nozzle body, its wear resistance needs to be considered, so it needs to have a certain degree of hardness. However, this stainless steel soft magnetic material has a low carbon content and cannot be treated by heat treatment. The surface coating (diamond-like carbon) can improve its hardness and reduce the friction coefficient. Using a multifunctional friction and wear testing machine, the friction coefficients of the motion pair surface composed of the armature and nozzle body were compared under surface coating and non surface coating conditions for different schemes.

2.3.1 Test plan

As shown in Table 2.2: The first experimental plan is to use the uncoated surface of the armature (ferritic stainless steel) and the uncoated surface of the nozzle body material (ferritic stainless steel) as friction and wear matching materials; Option 2 is to use the surface coating of the armature (ferritic stainless steel) and the non surface coating of the nozzle material (ferritic stainless steel) as friction and wear matching materials; The surface coating of the three-dimensional armature (ferritic stainless steel) and the surface coating of the nozzle material (ferritic stainless steel) are used as friction and wear matching materials. Firstly, a multifunctional friction and wear testing machine is used to compare the friction coefficients of the three schemes.

Table 2.2 Surface Coating Scheme of Test Samples

Experimental plan	Armature iron	Nozzle body	Table Coarse
Plan One	Surface uncoated	Surface uncoated	Ra0.2
Option 2	Surface coating	Surface uncoated	Ra0.2
Plan Three	Surface coating	Surface coating	Ra0.2

(1) Test samples
As shown in Table 4, Scheme 1: Two sample surfaces are coated, with the upper friction pair being a ferritic stainless steel shaft (surface coating) and the lower friction pair being a ferritic stainless steel disc (surface coating).
Option 2: One sample has a surface coating, while the other sample does not have a surface coating. The upper friction pair is a ferrite stainless steel shaft (surface coating), and the lower friction pair is a ferrite stainless steel disc.
Option 3: The surfaces of the two sample blocks are not coated, with the upper friction pair being a ferritic stainless steel shaft and the lower friction pair being a ferritic stainless steel disc.
(2) Test medium
M100 methanol solution
(3) Test steps
a. Install the ferrite stainless steel plate on the friction and wear testing machine, install the ferrite stainless steel pin on the fixture, and add M100 methanol solution to the plate.
b. Open the friction and wear testing machine, enter its operating interface, and input various experimental parameters. Including: test force F (3N), frequency f (3Hz), test time t (60min), then perform zero adjustment, click the operation interface and move the button to start the test.
c. After the experiment, save the friction coefficient data.

2.3.2 Test results and analysis
As shown in Figure 2.6, from the data, the friction coefficient of the two parts without coating is 0.136, and the friction coefficient of both parts with coating on the surface is 0.04. After adding coating on the surface, the friction coefficient significantly decreases; The friction coefficient of one of the two parts with a surface coating (armature surface coating) is 0.05. Compared with the non coating scheme of the two parts, the friction coefficient of this scheme is also significantly reduced. Compared with the coating scheme of both parts, the friction coefficient is close.

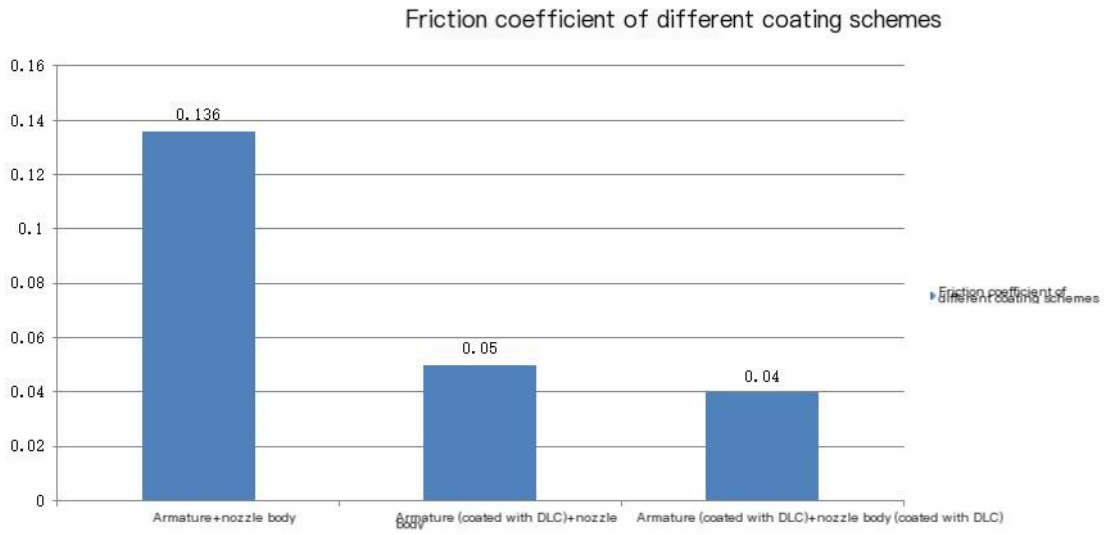

Figure 2.6 Comparison of friction coefficients between different coating schemes

2.3.3 Experimental Conclusion

Under the same testing conditions, by comparing the friction systems of different coating schemes on the armature and nozzle body motion pair, the following conclusions were drawn:

Both surfaces of the parts are coated, which significantly reduces the friction coefficient compared to the two parts without coating

The friction coefficient of one surface coating (armature surface coating) of two parts is significantly reduced compared to the friction coefficient of two parts without coating;

The friction coefficient of one surface coating (armature surface coating) of two parts is close compared to the scheme of coating both parts.

2.4 Research on reliability performance of methanol injectors

During the preliminary verification process, the corrosion resistance and wear resistance of the methanol injector material determine the reliability of the injector's operation. The reliability of methanol injectors in the early market was poor. After running for a period of time, various moving parts had varying degrees of corrosion and wear, resulting in varying degrees of attenuation or leakage of methanol injector flow rate. The motion pair composed of steel ball and valve seat, as well as the motion pair composed of armature and nozzle body, are key motion pairs in methanol injectors. Different coating schemes are formulated for the surfaces of each motion pair, and then 200 million reliability spray tests are conducted on the methanol injector assembly. The flow rate changes before and after the tests are measured and analyzed, and a suitable surface treatment scheme is ultimately selected.

2.4.1 Test plan

After initial research, it was found that the surface coating of one of the moving parts is equivalent to that of the zero moving parts. Through a dedicated reliability test bench, as shown in Table 2.3, 200 million spray tests were conducted on products with and without surface coatings. The performance changes before and after the tests were measured and compared to study the impact of surface coatings on the reliability of the injector assembly for each moving pair.

Table 2.3 Surface coating schemes for each motion pair

Experimental plan	Armature iron	Nozzle body	steel ball	valve seat	quantity
Plan One	Surface uncoated	Surface uncoated	Surface uncoated	Surface uncoated	eight

Option 2	Surface coating	Surface uncoated	Surface uncoated	Surface uncoated	eight
Plan Three	Surface uncoated	Surface uncoated	Surface coating	Surface uncoated	eight
Plan Four	Surface coating	Surface uncoated	Surface coating	Surface uncoated	eight

(1) Test samples
There are 4 different coating scheme samples, with 8 pieces for each scheme.
(2) Test conditions
A. Experimental equipment: Using a dedicated reliability testing bench
B. Working pressure: 4 bar ± 0.1 bar;
C. Working medium: M100 methanol solution;
D. Working frequency: 200Hz;
E. Working pulse width: 2.5ms;
F. Working environment: Room temperature
(3) Test steps
a. Before the experiment, test the flow rate of the methanol injector assembly for each scheme and record the data.
b. Install the methanol injector assemblies of each scheme onto a dedicated reliability test bench, check the equipment parameters, and start the switch after meeting the requirements.
c. Run for 288 hours (200 million injections) to retest the flow rate of the methanol injector assembly, record relevant data, and analyze the changes in flow rate before and after the experiment.

2.4.2 Test results and analysis

As shown in Figure 2.7, none of the motion pairs in Scheme 1 were coated, and the average flow rate decreased by 21.46% after the experiment, with a maximum decrease of 28.32%; On the basis of scheme one, scheme two only adds surface coating on the armature, with an average flow rate attenuation of 6.53% and a maximum attenuation of 9.42%, which improves the effect compared to scheme one; On the basis of scheme one, scheme three only adds surface coating on the armature, with an average flow rate attenuation of 9.4% and a maximum attenuation of 10.36%. The effect is improved compared to scheme one and close to scheme two; On the basis of scheme one, scheme four adds surface coatings on two parts, namely the armature and steel ball, with an average flow rate attenuation of 2.61%

and a maximum attenuation of 3.67%. The performance is relatively good and the effect is the best.

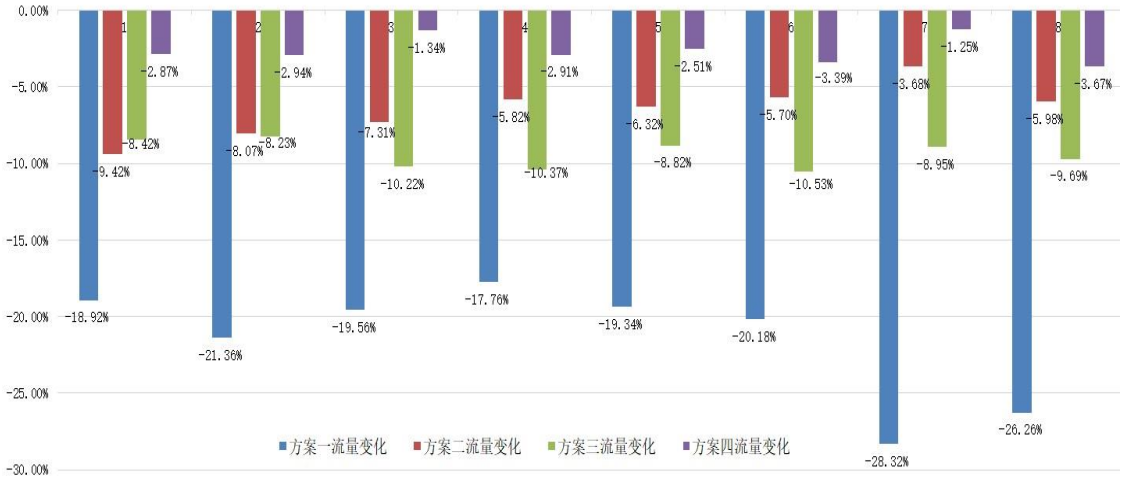

Figure 2.7 Methanol injector assembly with different coating schemes

2.4.3 Experimental Conclusion

None of the motion pairs in Plan One were coated, and the flow attenuation of the 8 methanol injectors was the greatest and the effect was the worst after 200 million injection tests;

On the basis of Scheme 1, Scheme 2 only adds surface coating on the armature. After 200 million injection tests, the flow attenuation of 8 methanol injectors has slowed down, and the effect has been improved compared to Scheme 1;

On the basis of Scheme 1, Scheme 3 only adds surface coating on the armature. After 200 million injection tests, the flow attenuation of 8 methanol injectors has slowed down, and the effect has been improved compared to Scheme 1, which is close to Scheme 2;

On the basis of scheme one, scheme four adds surface coatings on two parts, namely the armature and steel ball. The flow rate changes of each methanol injector before and after the test are within ± 5%, and the effect is the best.

2.5 References

Zelenka P, Kapus P, Mikulic L A. Development and optimization of fuel fueled compression ignition engines for passenger cars and light duty trucks [J] SAE transactions, 1991: 425-433

Zhang Kunyi. Research on the Development Status and Trends of Methanol Vehicles [J]. Automotive Testing Report, 2023, (18): 146-148

Tang Chunfeng, Qu Xuanhui, Duan Baihua Internal combustion engine piston ring materials and their surface treatment Internal combustion engine accessories, 2010, 6 (2): 3-4

ISO 19438-2003 Diesel fuel and petroleum filters for internal combustion engines

Filtration efficiency using particle counting and continuous retention capacity
Sumit Khadilkar and Ahmed Soliman UNC Charlotte Motorsports Engineering A Representative Testing Methodology for System Influence on Automotive Fuel Filtration
Jin Tao, Du Lipeng, Hao Xinyou Fluid Pollution and Purification Metrological Detection Technology Chemical Industry Press 2016
Du Lipeng, Research and Practice on Pollution Tolerance of Hydraulic Components, Machine Tool and Hydraulic, January 2020, Volume 48, Issue 1
ISO 12103-1 Road vehicles Test due for filter evaluation Part 1: Arizona test due
ISO 4406 Hydraulic fluid power Fluids Method for coding the level of contamination by solid particles
Wang Ganlin, Wu Zhijun, Hu Zongjie, et al. Study on the swelling properties of methanol gasoline on rubber materials [J]. Automotive Engineering, 2010,32 (7): 643-647
Mu Shifang, Shang Rujing, Song Can, Zhou Xiumiao, Wei Lingchao, Jiang Yuanli, Research on the Anti Swelling Performance of Rubber Materials in Methanol Gasoline, Natural Gas Chemical · C1 Chemistry and Chemical, Volume 41, 2016
Yang Haifeng, Zhang Ping, Li Jin, Research on Swelling Degree of PVC Modified NBR in Methanol Gasoline Blended Fuel, Science Forum 1009-914X (2013) 08-283-01
Feng Lajun, Liu Xiao, Shen Wenning, Lei Ali, et al., Study on the Influence of Anticorrosive Epoxy Coatings for Methanol Storage Tanks on Methanol Quality, Volume 37, Issue 9, September 2014

Chapter 3. Engine Valve Train

3.1. Background

Methanol is a renewable and sustainable alternative fuel for engines, with advantages such as abundant raw material sources, mature production processes, and safe storage and transportation. It has good application prospects; Heavy duty methanol engines have experienced rapid development in recent years, but due to their fast combustion speed and the characteristics of methanol fuel being prone to corrosion and not easily evaporating, they have brought new challenges to the engine, especially the problem of exhaust valve erosion. The valve cone and valve seat ring are one of the friction pairs in engines that work under extremely harsh conditions. They bear extremely high mechanical and thermal loads during operation, and are also corroded by corrosive gases, resulting in extremely poor lubrication. The exhaust valve is very prone to faults such as cone wear and disc burning, which affect the reliability of the engine. At the same time, the valve guide is a reliable sealing structure to ensure the reliability of the valve and valve seat ring, and also an important structure to ensure the sealing of the valve guide oil seal. It plays an important role in ensuring that the engine does not burn oil and operates reliably.

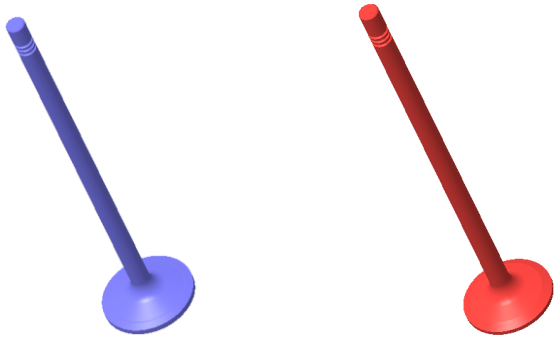

3.2.1 Structure and Materials of Valve

According to the requirements of working temperature and corrosion resistance, different matrix materials are selected, from martensite, austenite to high nickel alloy. The corrosion resistance and high temperature resistance of the materials are sequentially improved. In order to improve the wear resistance of the conical surface, exhaust valves are usually welded with alloy materials with better wear resistance and corrosion resistance, such as 3733-10, STL 1 #, etc. The commonly used matrix materials and compositions are shown in the table below.

Table 3.1 Material Chemical Composition

Classification e catalog	Name e Name	Chemical composition – (%)											
		C	Si	Mn	S	P	Ni	Cr	Mo	W	Nb	N	Fe	Other
Martensite Martensite material	45CrSi93	0.40~0.50	2.70~3.30	≤0.80	≤0.030	≤0.030	≤0.60	8.00~10.00	—	—	—	—	Yu e Base	—
austenite Austenite material	21-4N (X53CrMnNiN219)	0.48~0.58	≤0.25	8.00~10.00	≤0.030	≤0.050	3.25~4.50	20.00~22.00	—	—	—	0.35~0.50	more than Base	—
	21-4NWNb (X50CrMnNiNbN219)	0.45~0.55	≤0.45	8.00~10.00	≤0.030	≤0.050	3.50~5.50	20.00~22.00	—	0.80~1.50	1.80~2.50	0.40~0.60	more than Base	C+N≥0.90
High-temperature alloy Super alloy	Ni30 (NCF 3015)	≤0.08	≤0.50	≤0.50	≤0.015	≤0.015	29.50~33.50	13.50~15.50	0.40~1.00	—	0.40~0.90	—	Yu e Base	Al:1.60~2.20 Ti:2.30~2.90 B:≤0.01
	Inconel 751 (GH4751)	0.03~0.10	≤0.50	≤0.50	≤0.015	≤0.015	more than Base	14.00~17.00	≤0.50	—	0.70~1.20	one	≤3.00	Al:1.00~1.80 Ti:1.80~2.70 Co:≤2.00 B:≤0.008
	Ni80 A (Nimonic 80A)	0.04~0.10	≤1.00	≤1.00	≤0.015	≤0.020	more than Base	18.00~21.00	—	—	—	—	≤3.0	Al:1.00~1.80 Ti:1.80~2.70 B:≤0.008 Co≤2.0

3.2.2 Failure modes of valves

A heavy-duty M100 methanol engine adopts an integral cylinder head and 4-valve structure, with 2 intake and 2 exhaust valves in each cylinder head. The intake and exhaust channels are both twisted in series, with a single overhead camshaft structure. The methanol adopts an intake port injection type. During the reliability bench test of the entire machine, exhaust valve erosion failure faults occurred multiple times, resulting in no pressure in the working cylinder of the engine and the inability to conduct reliability tests. The time when the

exhaust valve undergoes erosion is approximately a certain period of time during the reliability test, as shown in the figure for the eroded exhaust valve. At present, the failure mode of the valves in the K11M methanol engine is all "exhaust valve disc erosion".

Photo of exhaust valve erosion

2.3 Failure mechanism analysis of valves (including ablation and wear, etc.)

The erosion of the valve disc is caused by the inadequate sealing between the valve cone and the seat ring, forming a leakage channel. The exhaust valve disc is eroded by high-temperature and high-pressure gas, forming a notch. Deposits adhering to the sealing surface, abnormal wear of the valve cone surface and seat ring friction pair, etc., can affect the sealing, leading to valve disc erosion.

2.3.1 Micro inspection of exhaust valves

At the same time, the surface treatment of the exhaust valve cone surface was tested. The non ablative area of the disc cone surface was slightly worn, with a surface nitride layer of 0.024mm (technical requirement ≥ 0.01mm). The microstructure was austenite+precipitated phase, and no abnormalities were found (see Figure 3.2). The hardness of the disc cone surface was HRC: 42 (technical requirement ≥ 35HRC).

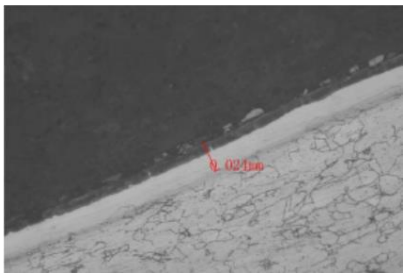

Figure 3.2 Non ablative zone of exhaust valve (etched state, 400X)

2.3.2 Macro inspection of exhaust valves

Within the 90 ° range of the disc cone surface on both sides of the exhaust valve ablation notch, there are multiple small ablation notches; At the same time, the non ablative cone surface of the exhaust valve has slight overall wear and there are many mechanical pits, as shown in Figures 3.3 to 3.4.

Figure 3.3 Morphology near the ablation area of the exhaust valve

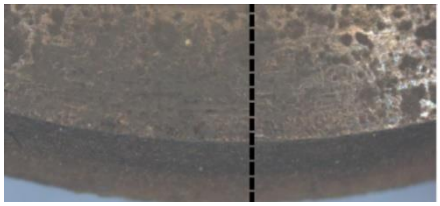

Figure 3.4 Morphology of non ablative area on the conical surface of the exhaust valve

The detection analysis shows that mechanical pits are formed by deposits adhering to the valve cone surface and seat ring sealing surface, which are compressed by the deposits when the valve is seated.

2.3.3 Exhaust valve wear

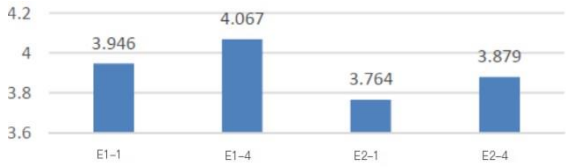

Figure 3.5 Broadband of contact between exhaust valve and seat ring

From the measurement results, it can be seen that the sealing strip width of the exhaust valve and exhaust valve seat ring is between 3.7 and 4.1. Within the design requirements, the wear of the exhaust valve is between 0.004 and 0.017, indicating relatively small wear.

2.3.4 Exhaust valve temperature field test

In order to verify whether the exhaust valves exceed the design temperature of the substrate material, temperature field tests were conducted on 12 exhaust valves of 6 cylinders of the engine, with the engine load at 105% of the original engine. The temperature

field results of the exhaust valve test are shown in Figure 3.6.

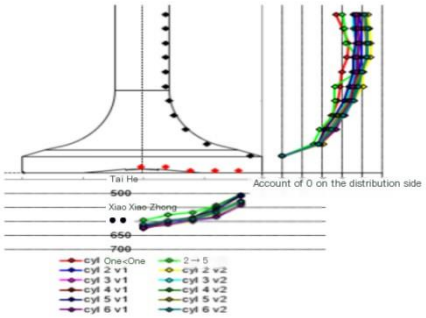

Figure 3.6 Exhaust valve temperature field test results

From the experimental results in the figure, it can be seen that the temperature at the bottom of the exhaust valve is between 505 ℃ and 628 ℃, and the temperature at the back and stem of the exhaust valve is between 500 ℃ and 720 ℃, both lower than the design temperature of 820 ℃, which is within the safe range.

2.4 Valve lifting measures

Based on the previous analysis of the reasons, the material of the exhaust valve itself meets the requirements. The wear of the engine exhaust valve is relatively small, and the erosion is mainly caused by a large amount of sediment adhering to the sealing surface, forming a leakage channel. The improvement measures mainly focus on optimizing the exhaust valve structure, reducing sediment adhesion on the sealing surface by matching the size of the exhaust valve/seat ring, and optimizing methanol evaporation.

2.4.1 Optimization of exhaust valve and seat ring structure

From the previous analysis, it can be seen that there is severe carbon accumulation and pitting around the conical surface of the engine exhaust valve disc, and the wear of the exhaust valve is relatively small. Therefore, it is necessary to reduce the exhaust valve cone angle appropriately. The exhaust valve cone angle is reduced from 130 ° to 120 ° (Figure 3.7) to improve the contact stress between the exhaust valve cone surface and the seat ring matching working surface, enhance the ability to clean carbon impurities. At the same time,

the reduction of the exhaust valve cone angle improves the self alignment and self rotation of the exhaust valve, and impurities are not easily accumulated on the exhaust valve cone surface.

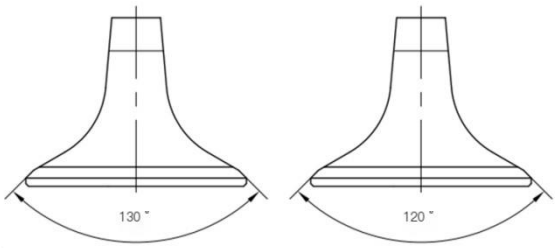

Figure 3.7 Cone angle scheme for exhaust valve disc

2.4.2 Matching dimensions of exhaust valve/seat ring

At present, the width of the sealing strip on the conical surface of the exhaust valve/seat ring is about 4mm. According to the wear situation, the width of the sealing strip should be appropriately reduced, controlled at around 3.2mm, to increase the stress on the contact surface and reduce the risk of impurity accumulation on the conical surface.

3. Research on 3-valve seat rings

3.1 Structure and Material of Seat Ring.

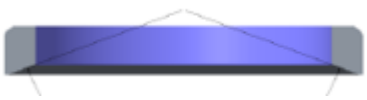

name	Chemical composition%													density g/cm³	hardness
	C	Si	Mn	P	S	Cu	Cr	Mo	Ni	V	Co	W	other		
Intake valve seat ring	0.7-1.3	0.3-1.0	-	-	0.1-0.5	-	1.0-4.0	5.0-10.0	-	-	17.0-21.0	-	10 years ago lower	7.2-7.8	HRC 27-42
Exhaust valve seat ring	0.7-1.3	0.3-1.0	-	-	-	-	3.0-6.0	6.0-9.0	-	-	17.0-21.0	1.5-3.0	20 years ago lower	7.2-7.8	HRC 35-50

3.2 Failure modes of seat rings

(including the wear and tear of intake valve seat rings and exhaust valve seat rings in the reliability of methanol engines)

After the reliability test, four exhaust valves and four exhaust valve seat rings of the first and second cylinders were taken for wear and fitting inspection, as shown in Figures 3.8 to 3.10.

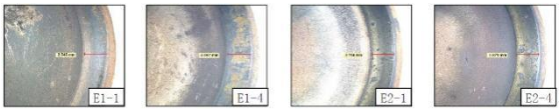

Figure 3.8. Contact morphology and contact bandwidth of exhaust valve cone surface

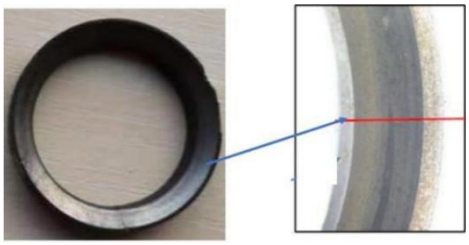

Figure 3.9. Morphology and contact broadband of exhaust valve seat ring

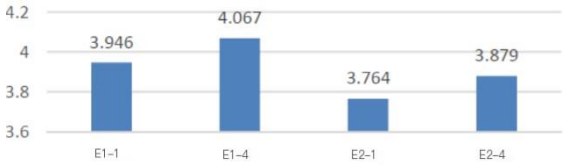

3.10. Morphology and contact broadband of exhaust valve seat ring

The width of the sealing strip for the exhaust valve and exhaust valve seat ring is between 3.7 and 4.1, and within the design requirements, the wear of the exhaust valve is between 0.004 and 0.017, which is relatively small.

3.3 Failure mechanism analysis of seat ring (wear mechanism)

Due to methanol being a clean fuel, there is no carbon smoke during engine combustion, which does not provide lubrication for the operation of valves and seat rings; At the same time, the strong corrosiveness of methanol causes direct flushing of the valve seat ring by the methanol injected into the airway, resulting in surface corrosion of the valve seat ring; The combustion temperature of methanol fueled engines is relatively high compared to diesel engines, and the material's high temperature hardness decay is fast. Based on the above reasons, higher requirements have been put forward for the wear resistance, corrosion resistance, and hardness degradation of valve seat rings in high-temperature environments.

3.4 Improvement measures for seat rings (improvement plan)

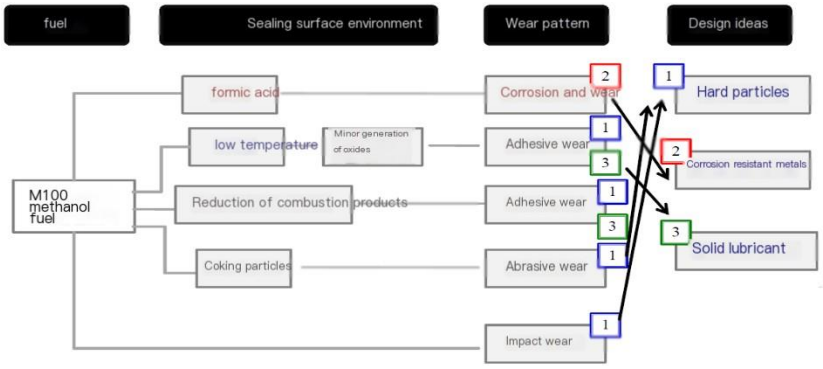

Improvement of strength: The material of the present invention adopts a hard phase particle reinforced material, and the chemical composition of the material is shown in Table 2 (???). A certain amount of alloy elements are added to the sintered matrix alloy. During the sintering or heat treatment process, these elements react to generate a certain hard phase (such as carbides) to strengthen the alloy, playing a role in strengthening the sintered valve seat ring matrix; On the other hand, it will have a solid solution strengthening effect; At the same time, increase the density of the valve seat ring to 7.2 g/cm3 or above, and enhance the crushing strength of the valve seat ring.

Corrosion resistant design: Changing the previous process of copper powder infiltration on the surface of the seat ring, as methanol has a strong corrosive effect on metals such as copper, zinc, magnesium, and aluminum. Methanol can easily damage the sealing cone surface of the seat ring and valve, so Cu element is not used; The main alloying elements Cr, Co, and Mo added to the material of the methanol specific seat ring form hard phase particles such as Cr Co Mo carbides (Figure 4.1), which improves the wear resistance of the seat ring and avoids the corrosion of Cu element by methanol.

Chapter 4. Research on 4-valve guide

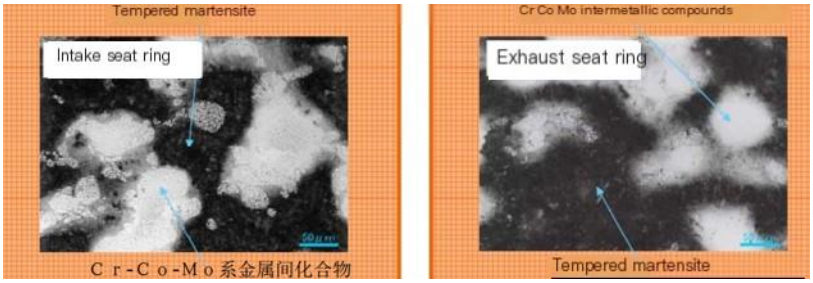

Figure 4.1 Metallographic Structure of the Inlet/Exhaust Seat Ring

4.1 Structure and Materials of Conduits

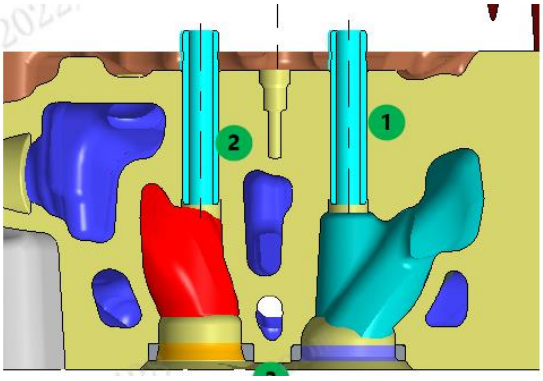

4.2 Failure Mode of Conduit

(including the wear and tear of methanol engine reliability)

1500 hour durability test for methanol engine, bench disassembly, and eccentric wear on the intake side exhaust valve duct.

(Note: The standard inner diameter of the catheter is 9.0-9.015mm.)

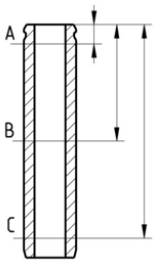

气缸号	1	2	3	4
序列号				
A	9.015	9.013	9.019	9.084
B	9.014	9.013	9.013	9.339
C	9.027	9.041	9.087	10.014
平均的	9.019	9.022	9.040	9.479

4.3 Failure Analysis of Conduits

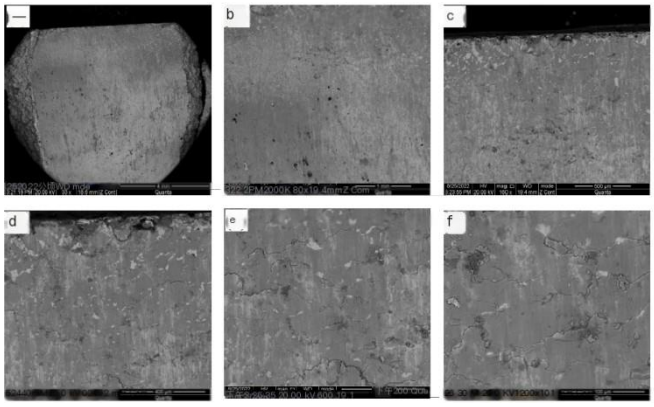

This engine is located in an environment where the temperature of the parts is too high due to detonation, forming a layered structure. When the guide tube repeatedly contacts the valve, the material slips, resulting in adhesive wear.

4.4 Improvement of valve guide

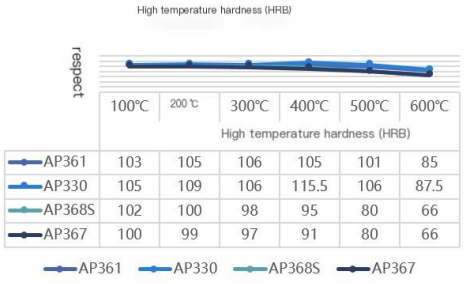

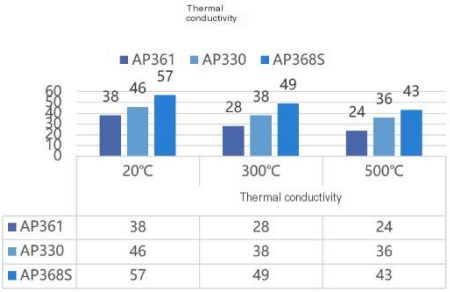

Upgrade the material grade of the conduit to enhance its heat dissipation and wear resistance.

Chapter 5. Research on the Matching of Cylinder Liners, Pistons and Piston Rings in Methanol Engines – Introduction.

5.1.1 Background and significance of the study

Methanol, as a clean fuel, is an important choice for engines to achieve energy conservation and carbon reduction. It is also an important technological route for China to achieve carbon peak and carbon neutrality. Studying methanol engines has extremely high strategic significance. The cylinder liner, piston, and piston ring are the core components of the engine PCU, and their adaptability to methanol fuel determines the quality and lifespan of the engine.

5.1.2 Research Status

At present, a large number of experiments have been conducted on the combustion characteristics and performance of methanol engines, and the main technical problems have been solved. However, research on the corrosion of methanol combustion products on PCU components is still in the research and verification stage. The main improvement methods currently adopted for corrosion problems are optimizing and improving the materials on the working surface of moving parts, as well as matching and upgrading the quality and composition of lubricating oil.

5.1.3 Research Report on this Project

The main task of this project is to study the material technology of PCU components suitable for methanol engine operating conditions, as well as the matching and selection of specialized lubricants, through individual experiments and actual operating conditions verification. The impact of combustion products from methanol engines on lubricating oil, cylinder liners, pistons, and piston rings, as well as the selection of cylinder liner, piston, and piston ring materials.

5.2.1 Effects of methanol combustion products on lubricating oil and friction pairs

The experimental results of Chang'an University in China show that methanol gasoline and its combustion products have a significant negative impact on the anti-wear

performance of engine lubricating oil, with methanol and its combustion product - formic acid having the greatest impact on the anti-wear ability; Methanol gasoline and its combustion products have a significant impact on the coking amount of engine lubricating oil. The higher the methanol content, the greater the coking amount, and the poorer the cleanliness and dispersion; Methanol gasoline and its combustion products have a significant impact on the high temperature dispersion coefficient and low temperature dispersion coefficient of engine lubricating oil, that is, methanol gasoline and its combustion products have a significant impact on the cleanliness and dispersion of engine lubricating oil.

5.2.2 Effects of methanol combustion products on lubricating oil and friction pairs

Xi'an Jiaotong University in China studied the corrosion effects of different methanol, formaldehyde, and formic acid contents in lubrication on cast iron. The research results show that the methanol content in lubricating oil has a relatively small impact on cast iron corrosion, while formic acid and formaldehyde have a greater corrosiveness on cast iron, as shown in Figures 5.1 to 5.3. [2]

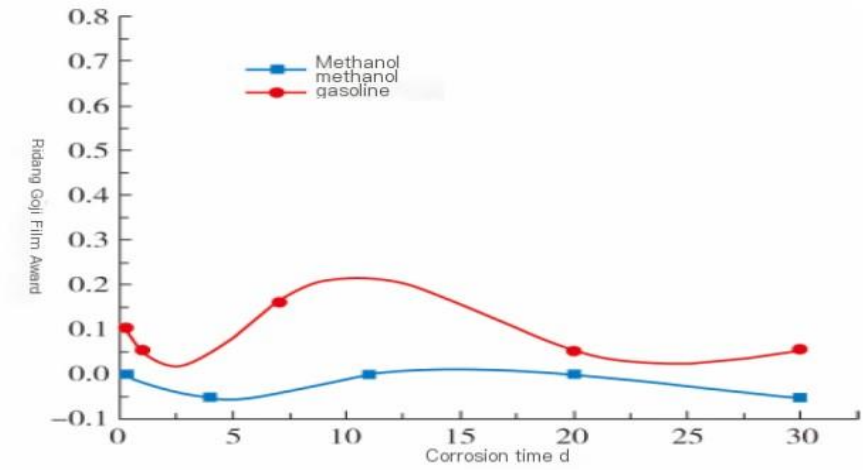

Figure 5.1 Corrosion rate of pure methanol and methanol gasoline on cast iron materials

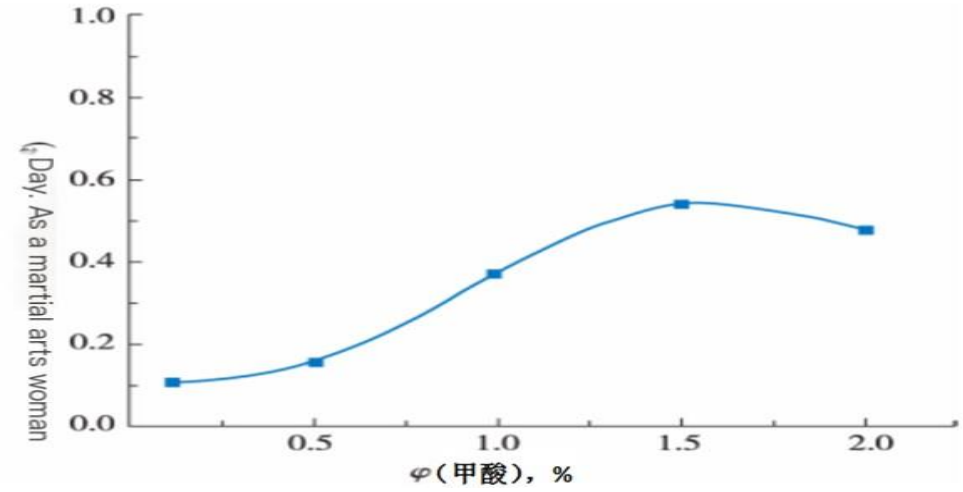

Figure 5.2 Corrosion rate changes with formaldehyde content

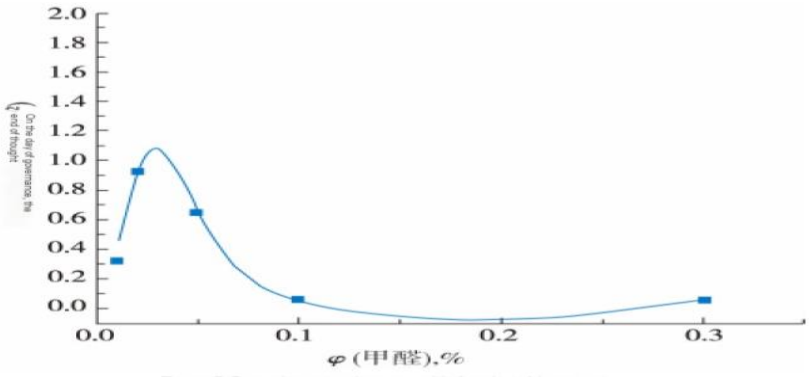

Figure 5.3 Corrosion rate changes with formic acid content

When using methanol fuel in the engine, due to the high evaporation heat of methanol, the engine undergoes poor gasification during startup. A large amount of unburned methanol condenses on the cylinder wall and enters the lubricating oil, causing the lubricating oil to be diluted and washed, resulting in friction and wear.

The oxidation products such as formic acid and formaldehyde generated during the combustion of methanol fuel cause corrosion and wear on the working surface of the piston

ring cylinder liner. According to literature reports, gas chromatography analysis was conducted on the components of M100 used lubricating oil, and the results showed that the used oil samples mainly contained water and methanol. The content of formaldehyde and formic acid was extremely low, and some were evaporated. However, some also reacted with the additives in the lubricating oil, causing the additives to lose their anti-corrosion effect and accelerate the corrosion and wear of the piston and cylinder wall [4].

Research has shown that under the same operating conditions, if the lubricating oil temperature is higher than 70 ℃, the degree of wear is closer to that of using gasoline. If it is below 70 ℃, the wear is higher than that of gasoline internal combustion engines. When the oil temperature drops to 46 ℃, the wear of an internal combustion engine that burns methanol is 10 times greater than that of a gasoline engine.

② The wear of methanol containing water is greater than that of anhydrous methanol, and if it contains 11% water, it is almost three times greater

③ When the cooling water temperature is low, wear increases. When the cooling water temperature is within the range of 50-70 ℃, the iron content in the lubricating oil is much lower than when the cooling water temperature is low.

Compared with traditional fuel engines, methanol engines for short distance transportation, frequent starts, and large load changes in urban areas during low temperature seasons have more severe wear on the upper part of the cylinder liner and piston ring travel area during cold start, cold operation, or warm-up, and the wear is most intense within a few minutes of starting.

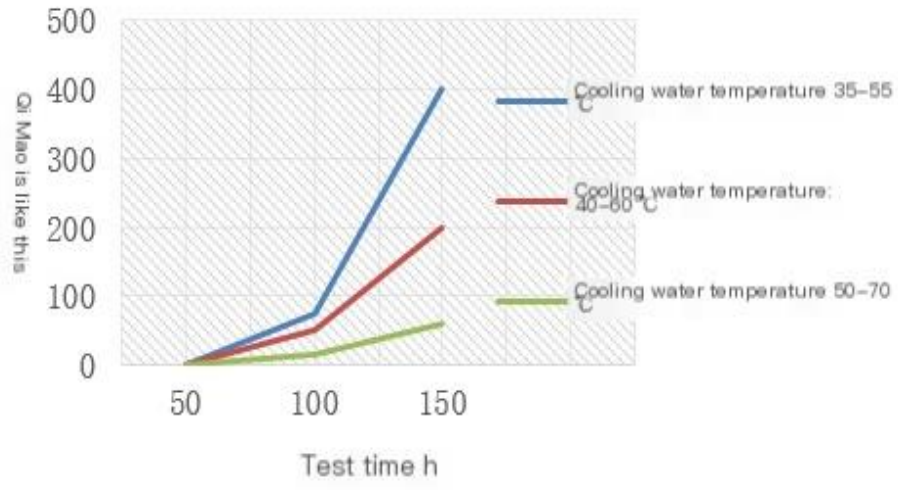

Figure 5.4 Effect of cooling water on iron content in lubricating oil

5.2.3 Matching working conditions of piston rings and pistons

The piston is one of the worst working parts in an engine. It undergoes complex second-order movements of reciprocating and swinging during the engine's operation, withstanding high temperature and pressure from the gas, and the lubrication state between the piston and the cylinder liner changes sharply.

During the working process, the piston ring is subjected to various forces and twisting moments such as gas compression pressure, motion inertia force, self elasticity, friction force, piston side thrust, etc., resulting in axial motion, radial motion, and rotational twisting motion, and withstanding the erosion of gas.

The working environment of pistons and piston rings is harsh and their movements are complex. They form a set of friction pairs with the cylinder liner, including piston ring cylinder liner, piston cylinder liner, piston ring groove piston ring side. The failure of each set of friction pairs will cause a decrease in the overall performance of the machine.

The substances such as formic acid, formaldehyde, and water produced by methanol combustion can disrupt the lubrication state of the three friction pair interfaces and cause

electrochemical corrosion on the friction pair surfaces. Methanol mixed with lubricating oil forms an emulsion with water at low temperatures, causing the lubricating oil to fail and resulting in greater wear of the friction interface, reducing the working life of moving parts.

5.3. Research and testing on corrosion of methanol engine lubricating oil and PCU components

5.3.1 Improvement effect test of methanol specific lubricating oil

The Geely brand M100 methanol vehicle from China Pingliang Zhongli New Energy Methanol Taxi Co., Ltd. underwent road driving tests (test data is shown in Table 5.1). From the test data, it can be seen that the viscosity of the oil has decreased to varying degrees after the vehicle runs for about 7000 km, but the viscosity reduction rate does not exceed 5%. At the same time, the oxidation degree of the oil is relatively shallow, indicating that the oil in use still has good surface film-forming ability and can effectively protect the friction surface.

Table 5.1 Changes in oil viscosity during vehicle operation of 7000 km

project		Mileage km	Kinematic viscosity (100 ℃)/(mm^2. S)	Viscosity change rate%
New oil	Special oil	0	ten point six three	
	Reference oil	0	ten point seven	
Gan 82361	Special oil	seven thousand five	ten point three two	-2.9

		hundred and fifty-one		
	Reference oil	seven thousand and fifty-six	ten point two six	-4.1
Gan A83177	Special oil	seven thousand three hundred and thirty-two	ten point four eight	-1.4
	Reference oil	seven thousand and twenty-one	ten point four five	-2.33
Gan A83054	Special oil	six thousand nine hundred and eighty	ten point four six	-2.26
	Reference	six thousand	ten point three eight	-2.34

	oil	eight hundred and twenty		
Gan A83464	Special oil	seven thousand three hundred and ten	ten point four eight	-1.4
	Reference oil	six thousand nine hundred and eighty-eight	ten point three six	-3.18
Gan A83153	Special oil	six thousand nine hundred and eighty-six	ten point three eight	-2.35
	Reference oil	six thousand seven hundred	ten point four six	-2.24

	and sixty-seven	
SL gasoline engine oil change standard		± 20

The acid and alkali value test results of M100 methanol automotive lubricating oil are shown in Figures 5.5 and 5.6. From Figure 5.5, it can be seen that the acid value of the special oil and the reference oil increased to different degrees during the test cycle. The maximum acid value and increase value of the special lubricating oil were only 1.3 mgKOH/g and 0.406 mgKOH/g, while the reference oil was 1.724 mgKOH/g and 0.924 mgKOH/g, both of which did not exceed the acid value specified by the lubricating oil change index, that is, the maximum increase was not greater than 2.0 mgKOH/g. It indicates that the two types of oil have good acid neutralization ability, and the performance of specialized oil is more prominent, with better antioxidant performance than the reference oil. From Figure 5.5, it can be seen that the change in the alkaline value of the reference oil is significantly greater than that of the specialized oil product, indicating that the alkaline value of the reference oil is consumed quickly and its retention is poor; Specialized lubricating oils have high alkali value and alkali value retention. 【5】

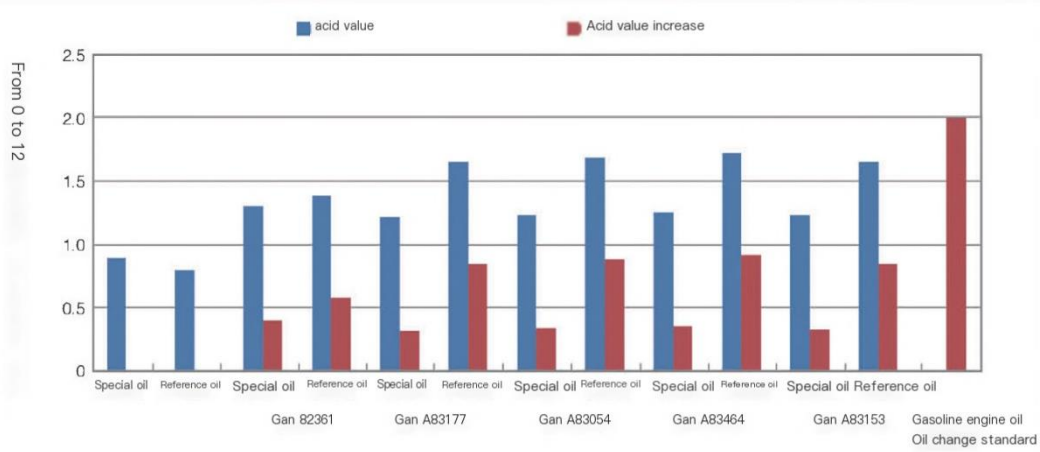

Figure 5.5 Changes in Acid Value of Oil Products

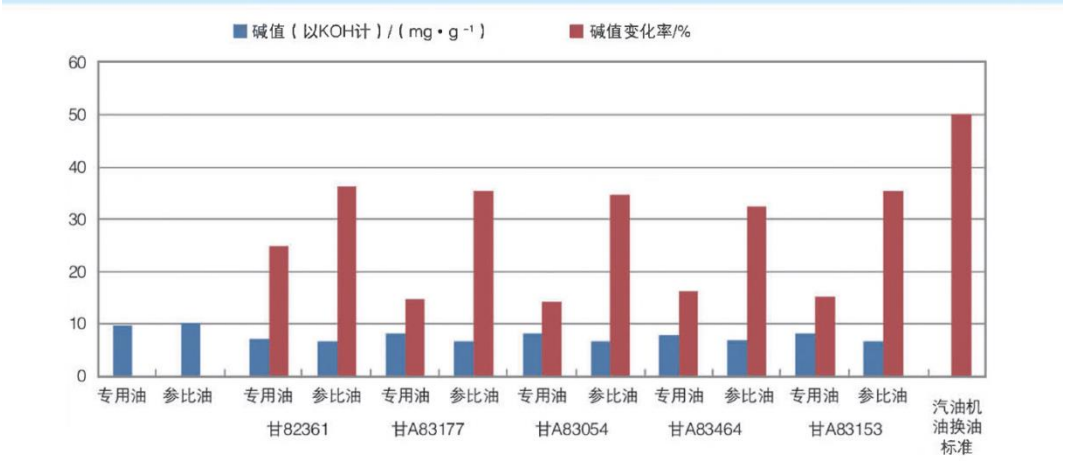

Figure 5.6 Changes in Alkali Value of Oil Products

The variation of residual element content in M100 methanol automotive lubricating oil is shown in Figure 5.7. Compared with the reference oil, the content of iron and aluminum in the special oil is basically the same, while the content of copper, lead and other elements in the oil is lower, especially the copper content is significantly lower than the reference oil, indicating that the special oil has better wear resistance, especially for copper containing parts such as engine crankshafts and bearing shells.

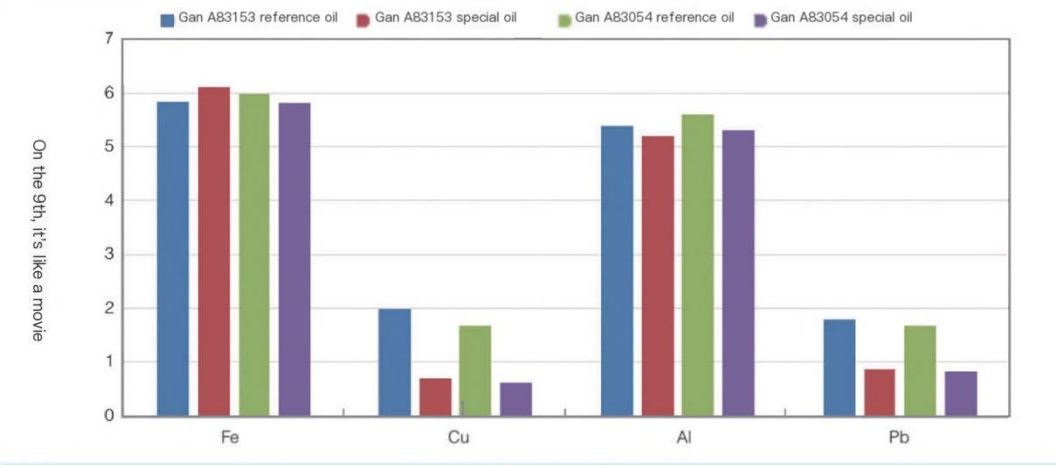

Figure 5.7 Changes in elemental content of in-service oil

products

Geely Automobile conducted tests on heavy-duty methanol engine specific lubricating oil, and the results showed that the kinematic viscosity and total alkali value of methanol specific lubricating oil changed significantly with the operation of the engine during the heavy-duty engine test, and the content of various metal elements changed significantly. The test results are shown in Figures 5.8, 5.9, and 5.10 (engine lubricating oil is changed every 300 hours) [6].

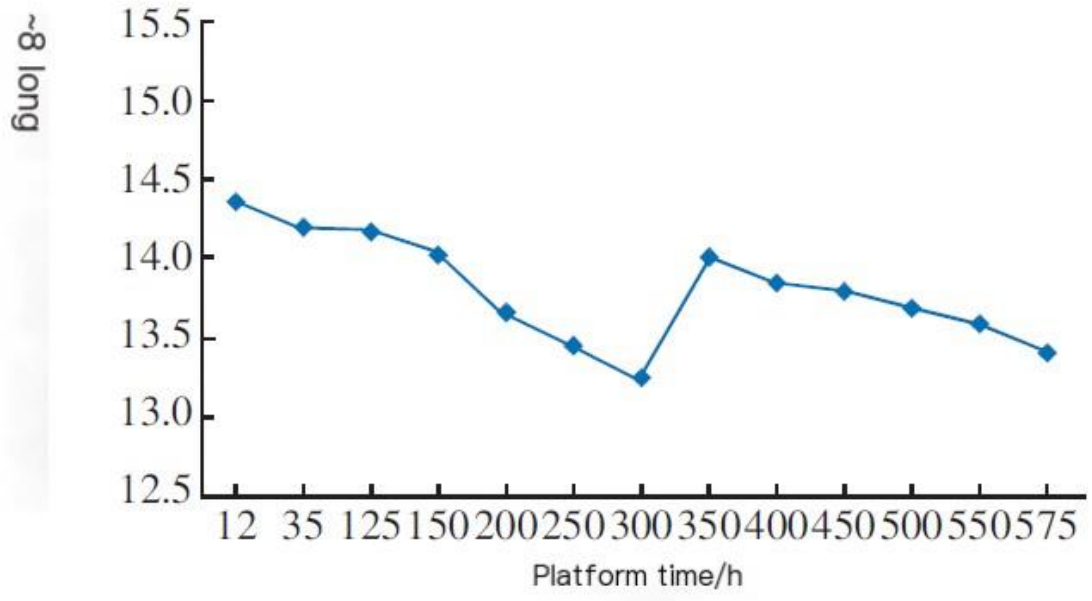

Figure 5.8 Changes in oil viscosity over test time

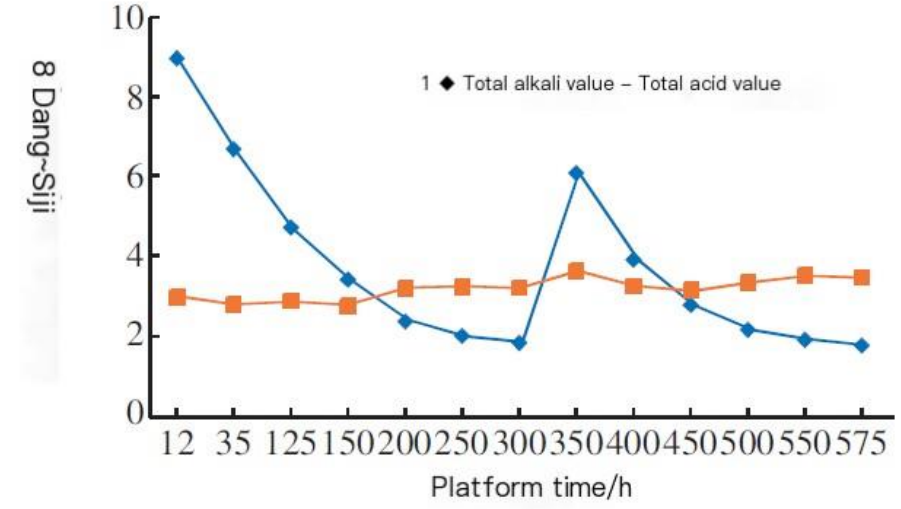

Figure 5.9 Changes in total alkaline value of oil products over test time

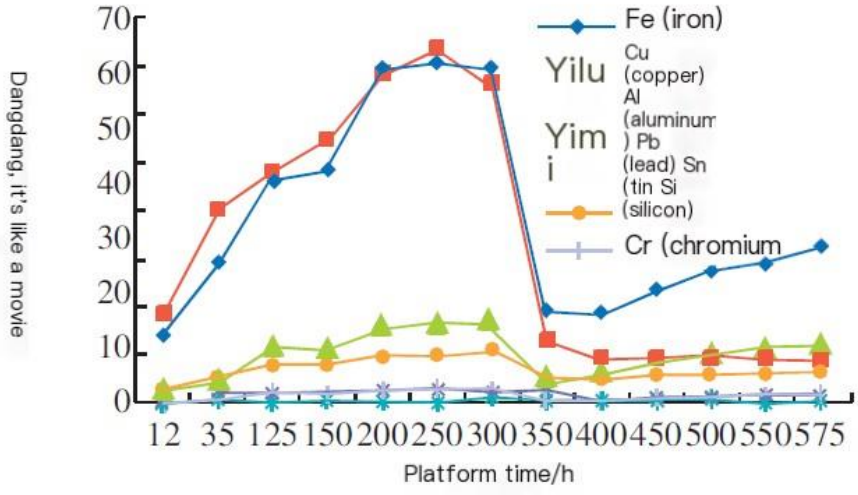

Figure 5.10 Changes in Oil Elements over Test Time

5.3.2. Corrosion resistance test of cylinder liner, piston, and piston ring materials for methanol engines

5.3.2.1 Material and Test Conditions of Test Pieces

Cylinder liner: Quenched ductile iron, corrosion-resistant gray cast iron, high chromium cast iron (due to the poor corrosion resistance of ordinary gray cast iron cylinder liners such as boron alloy cast iron, phosphorus alloy cast iron, molybdenum nickel copper, and bainite gray cast iron, they were not considered in the material test. This material test mainly tested ductile iron, corrosion-resistant gray cast iron, and high chromium cast iron with better corrosion resistance than gray cast iron).

Pistons: ZL109, 38MnV66;

Piston rings: DLC ring, PVD ring (CrN/Cr2N), GDC.

Corrosion solution ratio 1: 0.5% formaldehyde, 0.01% formic acid, and the remaining lubricating oil is 10W30; Corrosion solution ratio 2: formaldehyde 1.5%, formic acid 0.02%, and the remaining lubricating oil 10W30; Corrosion solution ratio 3: formaldehyde 2.5%, formic acid 0 1%, the remaining is lubricating oil 10W30.

Test block: The size of the cylinder liner and piston test block is 25mm x 15mm x 5mm; The piston ring is an integral piston ring made of different materials with a diameter of 110mm (because the rings of different materials have different surface roughness and good corrosion resistance, the difference before and after corrosion is not significant through metallographic analysis. Therefore, the whole ring corrosion is used for weight loss comparison, all of which are rectangular rings with the same type and structure, and are considered to have the same surface area).

Test method: JB/T 7901 Metal Materials Laboratory Uniform Corrosion Full Immersion Test Method; GB/T 21621 Test Method for Metal Corrosion of Dangerous Goods

Test temperature: 45 ℃ constant temperature, corrosion time: 180 minutes

5.3.2.2 Test results

According to previous bench test results, ordinary gray cast iron has poorer corrosion resistance than ductile iron. The results of this experiment (Figure 5.11) indicate that high chromium cast iron and alloy corrosion-resistant cast iron are more resistant to formic acid and formaldehyde corrosion than ductile iron and ordinary gray cast iron.

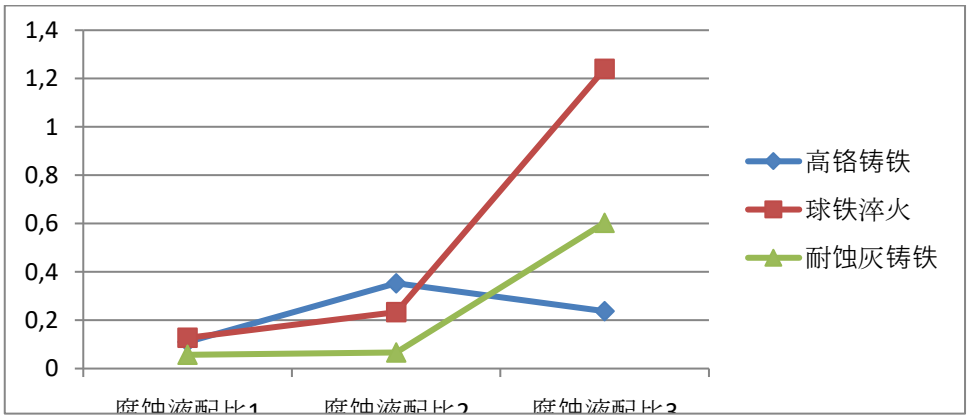

Figure 5.11 Corrosion depth of cylinder liner material in 10W30 lubricating oil containing formaldehyde and formic acid

Table 5.2 Corrosion test results of piston material

Piston material	Corrosion solution ratio 1 (g)	Corrosion solution ratio 2 (g)	Corrosion solution ratio 3 (g)
38MnVS6Ti steel	Weight loss 1.4mg	Weight loss of 1.5 mg	Weight loss 6.1 mg
ZL109 aluminum	Weight gain of 2.3 mg	Weight gain of 5.0 mg	Weight gain of 3.7 mg

The piston was subjected to corrosion tests using two commonly used materials. Among

them, aluminum (ZL109) piston had slightly more severe corrosion, and the data results showed weight gain. Analysis suggests that chemical reactions occurred between aluminum, formic acid, and formaldehyde during the test process, forming reactants. Based on experimental data analysis, the weight change rate of aluminum pistons is greater than that of steel pistons, indicating that aluminum pistons have weaker corrosion resistance than steel pistons in methanol engines.

Corrosion test results of piston rings:

Three types of piston rings with the same specifications but different surface coatings showed that under the same test conditions, the weight loss of DLC coated piston rings was the smallest, indicating that DLC coated piston rings have better corrosion resistance in methanol engines. (Data shown in Figure 5.12)

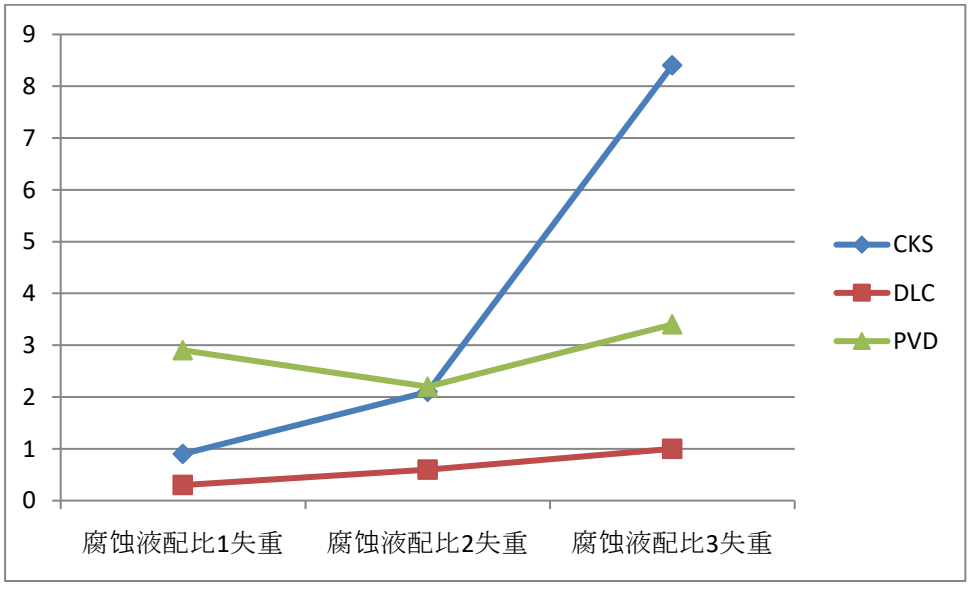

Figure 5.12 Corrosion weight loss of different piston rings in 10W30 lubricating oil containing formaldehyde and formic acid

3.3 Geely Medium Methanol Engine Bench Test

1000h durability test of 11L methanol engine

1000h durability test for 11L (cylinder diameter 123mm) methanol engine. The engine adopts methanol engine specific lubricating oil, corrosion-resistant gray cast iron cylinder liner, 38MnVS6Ti material piston, and DLC coated piston rings (one ring DLC, two ring chrome plating, oil ring DLC). The test data is shown in Table 3.

The test results show that there is significant wear in the upper dead center area of the cylinder liner after the test, and the wear depth in the direction of the auxiliary and main thrust sides exceeds 15 μ m. The wear depth on the push side of cylinder 1 # is the highest, reaching 32.684 μ m. The wear morphology of the inner hole of the cylinder liner is shown in Figures 5.13 and 5.14, and it can be seen that there are obvious signs of wear on the cylinder liner.

Table 5.3 Wear of Inner Bore of Corrosion Resistant Gray Cast Iron Cylinder liner after 1000 Hours of Operation

Wear of cylinder liner after 1000h bench test of 11L methanol engine（μ M)					
number	position	1 (front side)	2 (Auxiliary push side)	3 (rear side)	4 (Main push side)
1#	Top dead center	two point four two four	thirty-two point six eight four	four point four one six	ten point zero four three
2#	Top dead center	one point two nine nine	thirty point zero five six	five point zero two two	eight point three nine eight
3#	Top dead center	three point six three six	twenty-five point one three zero	six point two three four	twenty-three point one eight two

4#	Top dead center	three point two nine zero	seventeen point four zero three	seven point two seven three	eight point four eight five
5#	Top dead center	one point three eight five	twenty-six point three two zero	three point two nine zero	eight point four eight five
6#	Top dead center	two point nine four four	thirty-one point five five eight	nine point six one zero	seven point one zero zero

Figure 5.13 Morphology of cylinder liner inner ho

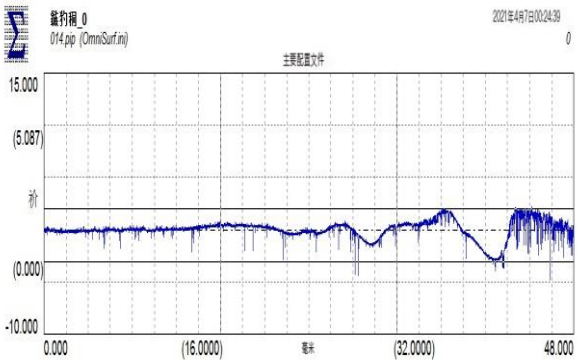

Figure 5.14 Roughness meter at top dead center for detecting the contour of cylinder liner inner surface

3361 hour durability test for 11L methanol engine

From the bench data (as shown in Table 4), it can be seen that there is still corrosion and wear on the inner wall of the corrosion-resistant gray cast iron cylinder liner in medium-sized methanol engines.

Table 5.4 Inner hole wear of corrosion-resistant gray cast iron cylinder liner after 3361 hours of operation

Wear amount of cylinder liner after 3361h durability test of 11L methanol engine （μ M)					
number	position	1 (front side)	2 (Auxiliary push side)	3 (rear side)	4 (Main push side)
1#	Top dead center	five point eight one five	one point three two two	thirty-seven point five three	six point one six seven

				three	
	Bottom dead center	zero point seven zero five	one point zero five seven	zero point seven zero five	zero point seven zero five
2#	Top dead center	nineteen point zero three one	zero point eight three seven	thirty-one point nine eight two	fifty-seven point three five seven
	Bottom dead center	zero point eight eight one	zero point nine six nine	zero point seven zero five	one point two three three
3#	Top dead center	fifteen point three zero eight	one point five eight six	forty-one point six three	ten point five seven three
	Bottom dead center	one point nine three eight	two point four six seven	one point four one	one point four one
4#	Top dead center	eighteen point six eight seven	two point nine zero seven	twenty-two point four six seven	twenty point zero eight eight
	Bottom dead center	one point six seven four	one point five eight six	zero point eight eight one	one point two three three
	Top dead	nineteen	one point	seventy	five point

5#	center	point two nine five	eight five zero	point nine two five	two eight six
	Bottom dead center	one point two three three	one point eight five zero	zero point five two nine	one point zero one three
6#	Top dead center	twelve point one five nine	three point seven zero zero	fifty-five point nine four seven	eight point three seven
	Bottom dead center	one point two three three	one point seven six two	two point one one five	one point two three three

1500 hour durability test of 13L heavy-duty methanol engine

In the 13L methanol engine bench test, the cylinder liner was made of ordinary corrosion-resistant gray cast iron, the piston was made of steel, and the piston ring was made of DLC ring. After 1500 hours of bench test, the piston and piston rings were used normally, and there was obvious corrosion and wear on the cylinder liner. The corrosion and wear results of the cylinder liner are shown in Table 5.5, and the condition of the inner hole is shown in Figure 5.15.

Table 5.5 Wear of Inner Bore of Corrosion Resistant Gray Cast Iron Cylinder liner after 1500 Hours of Operation

Wear of cylinder liner after 1500h bench test of 13L methanol engine（μM)						
number	position	1 (front side)	2 (Auxiliary	3 (rear side)	4 (Main push	Maximum wear

			push side)		side)	amount
1#	Top dead center	eleven point six eight eight	one point two nine nine	fifteen point one five two	one point four zero seven	fifty-seven point five eight nine
	Bottom dead center	one point one nine	one point four zero seven	zero point eight six six	one point two nine nine	
2#	Top dead center	zero point eight six six	twelve point seven seven one	four point five four five	thirty-three point eight nine six	fifty-nine point nine five seven
	Bottom dead center	two point nine two two	one point three six four	eight point five seven one	one point one six nine	
3#	Top dead center	six point four two nine	forty-seven point six	one point nine four	forty point two six	eighty point four seven six

			one nine	eight		
	Bottom dead center	five point one nine five	sixteen point eight eight three	two point zero seven eight	one point two nine nine	
4#	Top dead center	thirteen point five zero six	thirteen point seven six six	forty-four point nine three five	two point three three eight	one hundred and eleven point zero three nine
	Bottom dead center	one point zero three nine	five point one nine five	eleven point nine four eight	two point three three eight	
5#	Top dead center	forty-three point three seven seven	two point three three eight	thirty-four point eight zero five	two point zero seven eight	one hundred
	Bottom dead	one point eight	two point eight five	sixteen point one	one point five five	

	center	one eight	seven	zero four	eight	
6#	Top dead center	two point five nine seven	twelve point seven two seven	one point two nine nine	sixty	sixty point one seven three
	Bottom dead center	three point zero three	nine point zero nine one	one point eight one eight	zero point eight two three	

After 1500 hours, there are obvious friction marks on the top dead center position of the ordinary corrosion-resistant cast iron cylinder liner. The deepest friction mark on the main thrust side of the top dead center is 111.039 μ m. Corrosion resistant cast iron cannot meet the requirements for heavy-duty engine use.

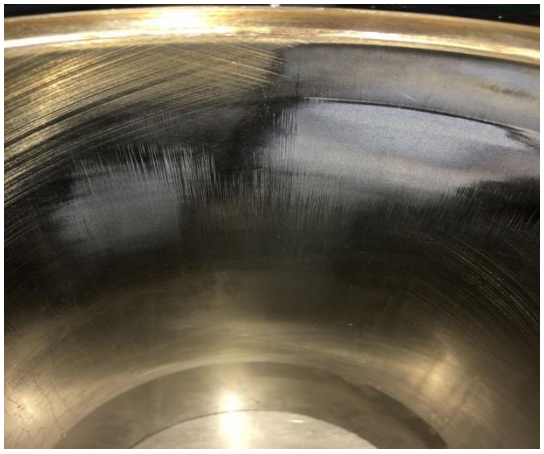

Figure 5.15 Bore morphology of corrosion-resistant gray cast iron cylinder liner after 1500 hours of operation

1300 hour durability test of 13L heavy-duty methanol engine

Compared with the 1500 hour test described in 3.3.3, the cylinder liner material of this test model has been replaced with high chromium cast iron, with the same size and technical requirements, and other components remain the same. After 1300 hours of durability test, the overall wear of the cylinder liner was relatively light, with no obvious corrosion and wear marks on the surface, and the wear amount was close to normal diesel engine test. The wear values are shown in Table 5.6, and the surface morphology is shown in Figure 5.16

Table 5.6 Wear amount of high chromium cast iron cylinder liner after 1300 hours of operation

Wear amount of cylinder liner after 1300h durability test of Hualing 6130 (G) （μ M)					
number	position	1 (front side)	2 (Auxiliary push side)	3 (rear side)	4 (Main push side)
1#	Top dead center	one point three eight	twelve point	zero point five one	ten point six four

		five	seven two seven	nine	nine
	Bottom dead center	one point three eight five	one point one two six	one point five five eight	zero point eight six six
2#	Top dead center	one point one two six	eleven point three four two	zero point nine five two	eleven point zero eight two
	Bottom dead center	one point five five eight	zero point seven seven nine	one point six four five	one point three eight five
3#	Top dead center	zero point six zero six	eight point three nine eight	zero point six zero six	ten point zero four three
	Bottom dead center	one point five five eight	one point one two six	one point zero three nine	two point seven seven one
4#	Top dead center	one point six four five	ten point nine zero nine	zero point six zero six	ten point two one six
	Bottom dead center	zero point nine zero nine	one point two nine nine	one point four seven two	one point one two six
	Top dead	one point	twelve	one point	nine point

5#	center	zero three nine	point four six eight	zero three nine	three five one
	Bottom dead center	one point three eight five	zero point nine five two	one point three eight five	one point three eight five
6#	Top dead center	one point five five eight	eight point two two five	zero point eight six six	five point five four one
	Bottom dead center	one point four seven two	one point one two six	one point five five eight	one point two one two

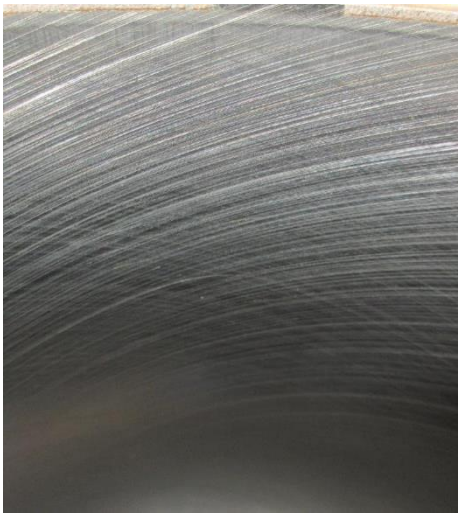

Figure 5.16 Inner hole morphology of high chromium gray cast iron cylinder liner after 1300 hours of operation

5.3.4 Detection of piston and piston ring after durability test of methanol engine

3500h durability test for an 11L (cylinder diameter 123mm) methanol engine. The engine adopts methanol engine specific lubricating oil, corrosion-resistant gray cast iron cylinder liner, 38MnVS6Ti material piston, and DLC coated piston rings (one ring DLC, two rings chrome plated, oil ring DLC). After the experiment, the clearance between the piston and cylinder liner, as well as the size of the piston ring, were inspected. The inspection data are shown in Tables 5.7, 5.8, and 5.9.

(1) Clearance between piston and cylinder liner

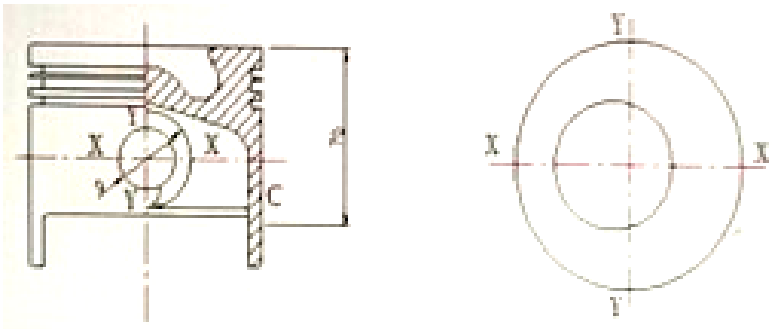

Figure 5.17 Detection position of clearance between piston and cylinder liner

Table 5.7 Fit clearance between piston and cylinder liner of methanol engine after 3500 hours of durability

Cylinder serial number	Measurement location	After durability		
		Cylinder liner	Piston skirt C	Cylinder clearance
		Y-Y	Y-Y	Y-Y
one	1B	zero point zero two five	-0.075	zero point one

	1C	zero point zero two six	-0.075	zero point one zero one
two	2B	zero point zero one	-0.076	zero point zero eight six
	2C	zero point zero two one	-0.076	zero point zero nine seven
three	3B	zero point zero one seven	-0.075	zero point zero nine two
	3C	zero point zero two five	-0.075	zero point one zero zero
four	4B	zero point zero one five	-0.079	zero point zero nine four
	4C	zero point zero two	-0.079	zero point zero nine nine
five	5B	zero point zero two	-0.08	zero point one zero zero
	5C	zero point zero two five	-0.08	zero point one zero five
six	6B	zero point zero zero	-0.075	zero point zero

		nine		eight four
	6C	zero point zero one five	-0.075	zero point zero nine zero
Maximum value		zero point zero two six	-0.075	zero point one zero one
minimum value		zero point zero zero nine	-0.08	zero point zero eight nine
technical requirement		0.000-0.025	-0.070~-0.050	0.050-0.095

From the results of cylinder liner inspection in Table 5.7, it can be seen that the size of the durability test for cylinders 1 to 6 in the Y-Y direction is 0.009-0.026mm (technical requirement: 0.000-0.025mm), and the local size of the cylinder liner has increased; From the piston inspection results, it can be seen that the durability test results at piston C from 1 to 6 are -0.08-0.075mm (technical requirement: -0.07-0.05mm), and the Dn value of the piston skirt is slightly reduced, indicating slight wear of the piston; After the durability of cylinders 1-6, the clearance between the cylinder liner and the C position of the piston group is between 0.084-0.105mm, with some gaps exceeding the technical requirements of 0.05-0.095mm. Overall, the clearance between the piston and cylinder liner can basically meet the requirements of engine use.

（2） Piston ring inspection

The test data shows that after the durability of cylinders 1 to 6, the dimensions of the first and second piston rings are all within the design requirements, indicating that using DLC

for the first ring and chrome plating for the second ring can meet the requirements of engine use.

Table 5.8 First Ring Detection Results

Number	Testing items	Test results after 3500 hours					
		one	two	three	four	five	six
one	Base circle height: 2.816 (-0.03--0.01)	two point seven nine one	two point seven nine two	two point seven nine two	two point seven nine one	two point seven nine four	two point seven nine four
two	Radial thickness 4.7 ± 0.15	four point seven two	four point seven three	four point seven two	four point seven three	four point seven four	four point seven three
three	Closed gap: 0.25-0.35	zero point two nine	zero point two nine	zero point two eight	zero point two eight	zero point three zero	zero point three zero

Table 5.9 Second Ring Detection Results

Number	Testing items	Test results after 3500 hours					
		one	two	three	four	five	six

one	Ring height: 2.5 (-0.03--0.01)	two point four eight five	two point four eight eight	two point four eight seven	two point four eight three	two point four eight eight	two point four eight eight
two	Radial thickness 4.7 ± 0.15	four point seven two	four point seven three	four point seven one	four point seven one	four point seven zero	four point seven zero
three	Closing gap: 0.50-0.70	zero point six seven	zero point six eight	zero point six seven	zero point six six	zero point six six	zero point six nine

5.4. Conclusion:

1. Methanol engines require the development of specialized lubricating oils, with a focus on improving stable alkali value and antioxidant properties.

2. The use of high chromium cast iron material cylinder liners can significantly improve the service life of cylinder liners in methanol engines.

3. The selection of steel pistons can basically meet the operating conditions of methanol engines.

4. The first and oil rings of the piston ring are coated with DLC, while the second ring is chrome plated, making it an ideal piston ring selection for methanol engines.

Reference:

【1】 Li Xianmin. Research on the Impact and Countermeasures of Methanol Gasoline as a Positive Ignition Fuel on Engine Materials, Ph.D. Dissertation, Chang'an University, April 2012.

【2】 Zeng Qunfeng, Xu Feiyan, Liu Peng, Peng Runling, Dong Guangneng. Research on the Corrosion Performance of M15 Methanol Gasoline and Its Combustion Products on Cast Iron, Petrochemical Corrosion and Protection, Volume 32, Issue 2, 2015, pp. 1-5.

【3】 Xu Hanli. Internal combustion engine lubricating oil products and applications [Xiu. Beijing: China Petrochemical Press, 2005: 130-138]

【4】 Wang Xiang, Guo Yongjun, Zhang Jianjun. Comparison of properties of methanol gasoline and methanol gasoline as internal combustion engine fuels [J]. Chemical Times, 2005, (3): 47-48

【5】 Yao Wenzhao, Li Guangtao, Wang Zhiwen, and Wang Binwen. Research on the Application of Special Lubricating Oil for Methanol Engine, Petroleum Business Technology, April 2020, Issue 2.

【6】 Chen Hailan, Lu Ruijun, Zhang Zhidong, Su Maohui, Cai Wenyuan. Research on Test Characteristics of Lubricating Oil for Commercial Methanol Engine, Small Internal Combustion Engine and Vehicle Technology, Issue 6, 2019

Chapter 6. Engine crank connecting rod mechanism.

6.1、 Regional contact characteristics and wear mechanism of connecting rod crankshaft bearing pair based on phase angle

6.1.1. Analysis of Regionalized Stress Distribution and Dynamic Characteristics in the Circumferential Direction of High Explosive Pressure crankshaft Journal

1.1 The force state of crankshafts with different phase angles and the principle of crankshaft follow-up grinding motion

The force situation of the internal combustion engine crankshaft during actual operation is relatively complex, mainly affected by the gas pressure in the cylinder and the inertial force generated by the movement of the crankshaft and connecting rod, as shown in Figure 6.1. The gas pressure inside the cylinder varies periodically with the rotation of the crankshaft. For a cylinder that is firing and doing work, the load on the connecting rod journal reaches its maximum value. The distribution of load in the axial direction (x-axis direction) of the connecting rod journal is a quadratic parabolic function distribution; The distribution of load in the radial (y-axis direction) direction of the connecting rod journal, along the cosine distribution within a 120 ° range, is shown in Figure 6.2.

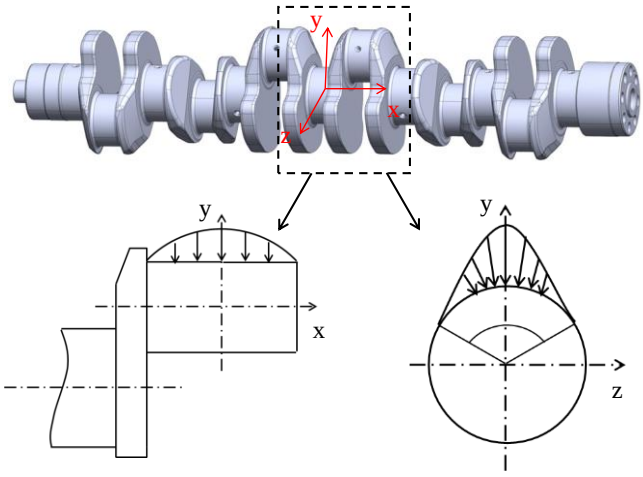

Figure 6.1 Schematic diagram of load distribution on connecting rod journal

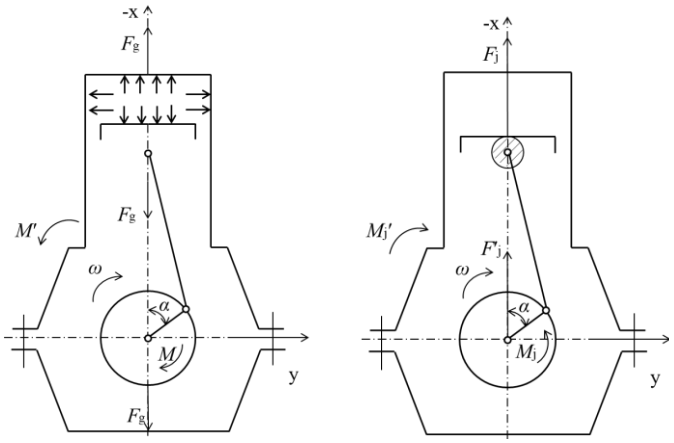

a) Schematic diagram of gas force b) Schematic diagram of reciprocating force

Figure 6.2 Schematic diagram of gas force and reciprocating inertia force

The follow-up grinding of the contour of the crankshaft connecting rod journal is formed by the reciprocating motion of the grinding wheel following the rotational motion of the crankshaft. During the grinding process, the grinding wheel always maintains tangency with the connecting rod journal. The crankshaft connecting rod neck has a standard circular contour, and the tangent point, which is the grinding point *G,* is located on the line connecting the center $_{Op}$ of the connecting rod neck and the center $_{Ogw}$ of the grinding wheel. The grinding motion principle is shown in Figure 6.3.

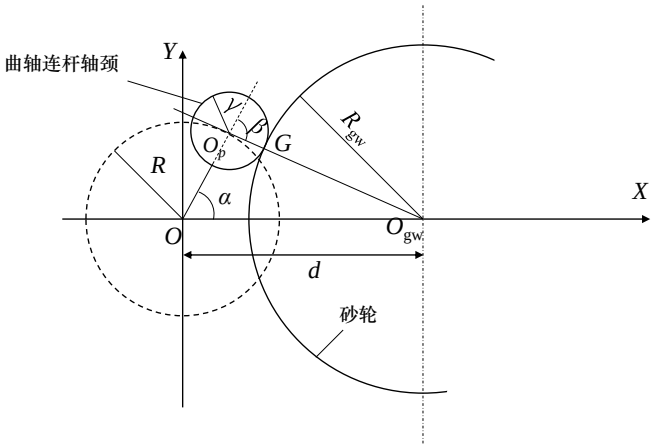

Figure 6.3 Principle diagram of crankshaft follow-up grinding motion under ideal conditions

This project obtains the **theoretical grinding motion control equation** based on the contour control equation, and generates an accurate model of the crankshaft's grinding contour with motion.

$$\alpha = \alpha(t) \quad (1)$$

$$d(t) = R\cos\alpha(t) + \sqrt{(r + R_{gw})^2 + (R\sin\alpha(t))^2} \quad (2)$$

6.1.2 Stress and strain distribution characteristics of the contact area of the connecting rod journal under maximum contact pressure.

Using the existing precise model of the crankshaft, combined with finite element analysis software, stress, strength, fatigue life, and modal analysis were conducted on a certain type of heavy-duty engine crankshaft; Add boundary conditions and loads to the crankshaft for finite element analysis, compare them with design requirements such as strength and avoiding resonance, and verify the rationality and reliability of the crankshaft design parameters and structure. The grid division result of the crankshaft structure is shown in Figure 6.4; The stress-strain cloud map is shown in Figure 6.5 and Figure 6.6.

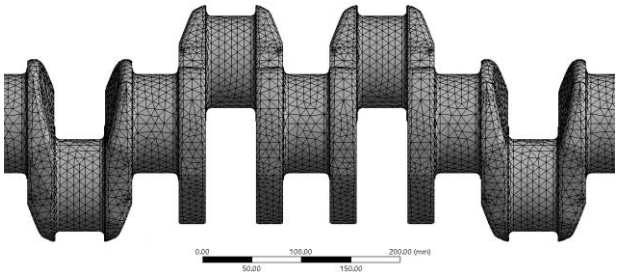

Figure 6.4 Grid division results of crankshaft structure

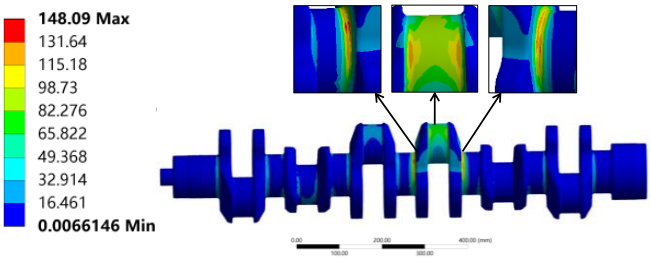

Figure 6.5 Cloud diagram of stress distribution at 130 ° angle of crankshaft

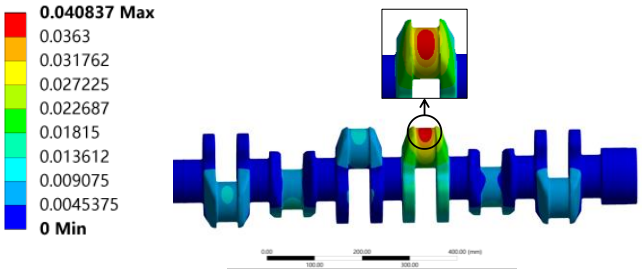

Figure 6.6 Cloud map of crankshaft 130 ° angle displacement distribution

Based on Hertz stress theory, derive the formula for calculating crankshaft stress, and compare it with finite element method to verify the rationality and reliability of crankshaft design parameters and structure.

$$\sigma_{H\max} = \frac{2F_n}{\pi bL}$$

$$\sigma_{H\max} = \sqrt{\frac{F_n}{\pi L} \times \frac{\frac{1}{R_1} + \frac{1}{R_2}}{\frac{1-u_1^2}{E_1} + \frac{1-u_1^2}{E_2}}}$$

6.2. Exploring the physical mechanism of contact stress fluctuations caused by dynamic changes in key structural parameters of crankshaft systems

6.2.1 The influence of key geometric structural parameters of the crankshaft on contact stress.

The above calculation shows that the transition fillet between the main journal and the crank arm, as well as the transition fillet between the connecting rod journal and the crank arm, are the most dangerous and weakest areas for fatigue cracks in the crankshaft. Using the response surface method to explore the influence of key parameters of the crankshaft on the maximum contact stress, finite element analysis is conducted by establishing approximate functions of design variables and output variables, and the accuracy of fitting the response surface is determined to determine the impact accuracy. Use the Box Behnken matrix method in response surface methodology for analysis. Select key parameters such as spindle neck radius $_{R1}$, spindle neck length $_{L1}$, crank pin radius $_{R2}$, and transition fillet radius *r* as design variables for analysis. The initial values and range of variation of design variables are shown in Table 6.1.

（1） Table 6.1 Initial values and range of variation of design variables

Parameter	Variable of design	Initial value/mm	Range of variation/mm
P_1	Transition fill radius	three	2.45-3.55
P_2	Radius of main journal	fifty-six	53.5-58.5
P_3	Length of main journal	forty-eight	46.5-49.5

P_4	Radius of connecting rod journal	forty-five	43.5-46.5
P_5	Length of connecting rod journal	fifty-six	52.5-59.5

The sensitivity analysis of this project uses the magnitude of sensitivity to reflect the degree of impact on evaluation indicators. Select the maximum stress load for calculation and obtain the stress and deformation sensitivity analysis diagram shown in Figure 6.7. Select the maximum stress load for response surface calculation, and use the multi-objective method based on response surface in Design Exploration to analyze the crankshaft. The method is screening, and the initial sample size is 1000. The response map shown in Figure 6.8 is obtained.

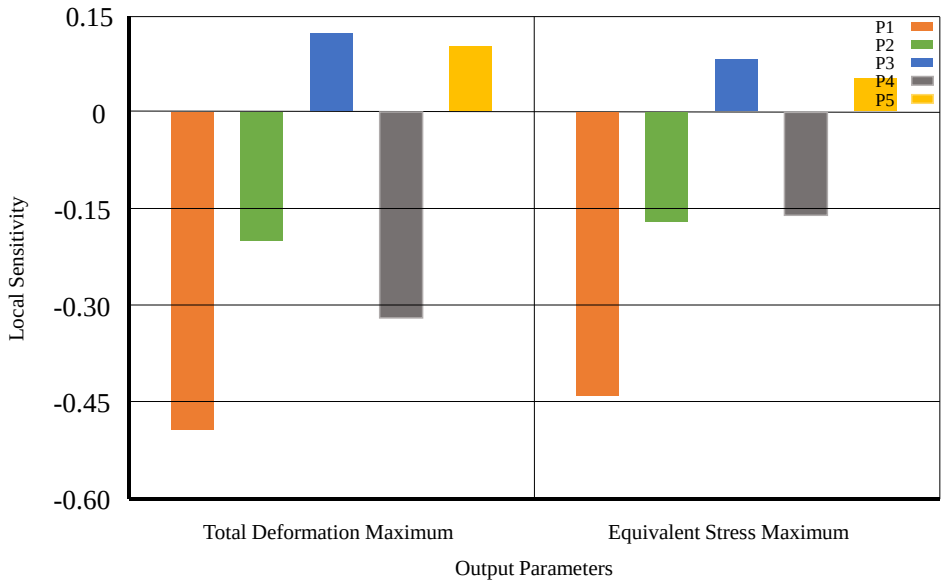

Figure 6.7 Cloud map of crankshaft 130 ° angle displacement distribution

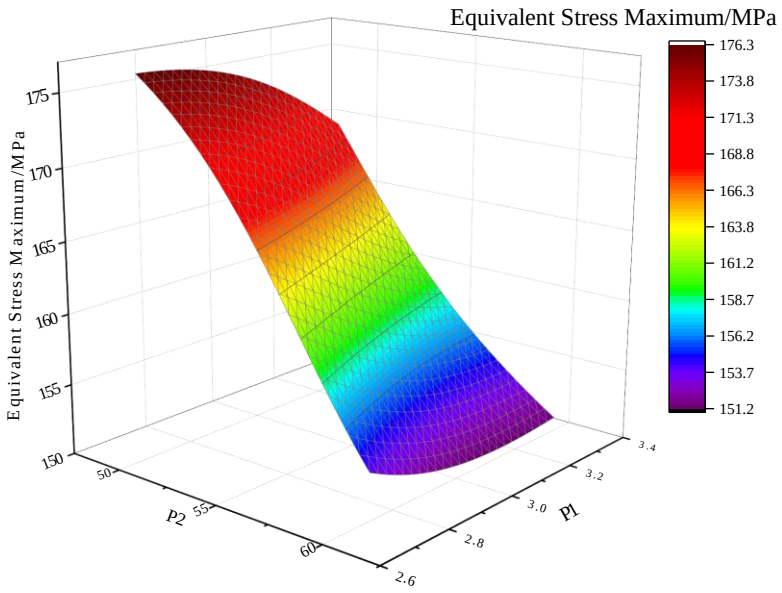

Figure 6.8 Cloud map of crankshaft 130 ° angle displacement distribution

6.2.2 The influence of different clearance sizes on the dynamic characteristics of internal combustion engine crankshaft connecting rod mechanisms.

The flowchart for constructing the ADAMS model of the crankshaft connecting rod mechanism is shown in Figure 6.9. A simulation model of a crankshaft connecting rod mechanism with clearance was constructed, and a three-dimensional model of the crankshaft connecting rod mechanism was established in Pro/E software. The mass and motion parameters of the model were set, and the clearance motion pair model and the setting of collision forces in ADAMS were analyzed. Comparative analysis of the dynamic characteristics of crankshaft connecting rod mechanisms under different wear faults and wear clearances.

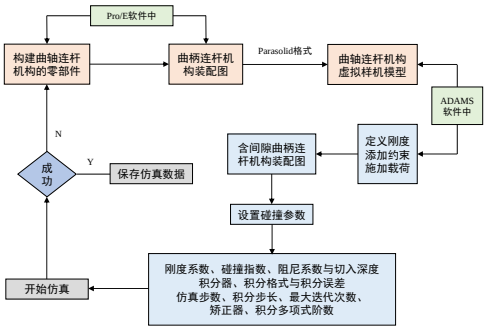

Figure 6.9 Construction of ADAMS model flow chart for crankshaft connecting rod mechanism

Establish a wear phase diagram of the connecting rod journal (Figure 6.10), express the linear wear amount using mathematical formulas, and study the uniform wear of the crankshaft journal in the circumferential direction and the uneven wear caused by centrifugal inertia force, as well as the phenomenon of eccentric wear of the crankshaft journal. In general, the amount of online wear is directly proportional to the positive pressure. Line wear can indicate

$$\delta = a + b\sin\frac{\alpha}{2}$$

Among them, uniform wear $a = kp_a$ and eccentric wear $b = \frac{15kF_n}{16\sqrt{2}r_0}$.

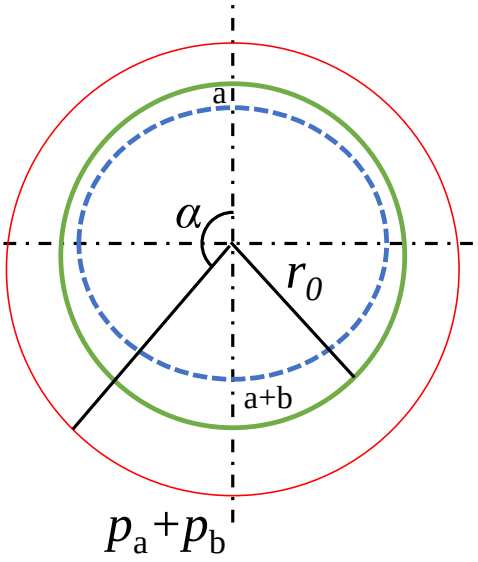

Figure 6.10 Wear phase diagram of connecting rod journal

6.3. Explore the mechanism of localized and severe wear of the connecting rod journal bearing friction pair under explosive pressure

6.3.1 The problem of zero kilometer brake failure of heavy-duty vehicles under different working conditions.

Analyze the 0 kilometer bearing of the engine crankshaft through methods such as macroscopic analysis, scanning electron microscopy, energy spectrum analysis, and ferrography Observation of the macroscopic morphology of the crankshaft: observe the direction and depth of the wear marks on the crankshaft connecting rod journal, whether there are any signs of tension on the surface of the journal, and whether the direction is consistent with the direction of the connecting rod movement; ② Perform matrix inclusion analysis and metallographic structure analysis, take longitudinal samples parallel to the fracture near the severely worn connecting rod journal, and observe the morphology and metallographic structure of inclusions in the crankshaft matrix after metallographic polishing. ③ Perform ferrographic analysis to deposit the abrasive particles generated during high-speed operation of the crankshaft. Observe the size and shape characteristics of the

abrasive particles generated on the crankshaft connecting rod journal through the microscope of a ferrograph.

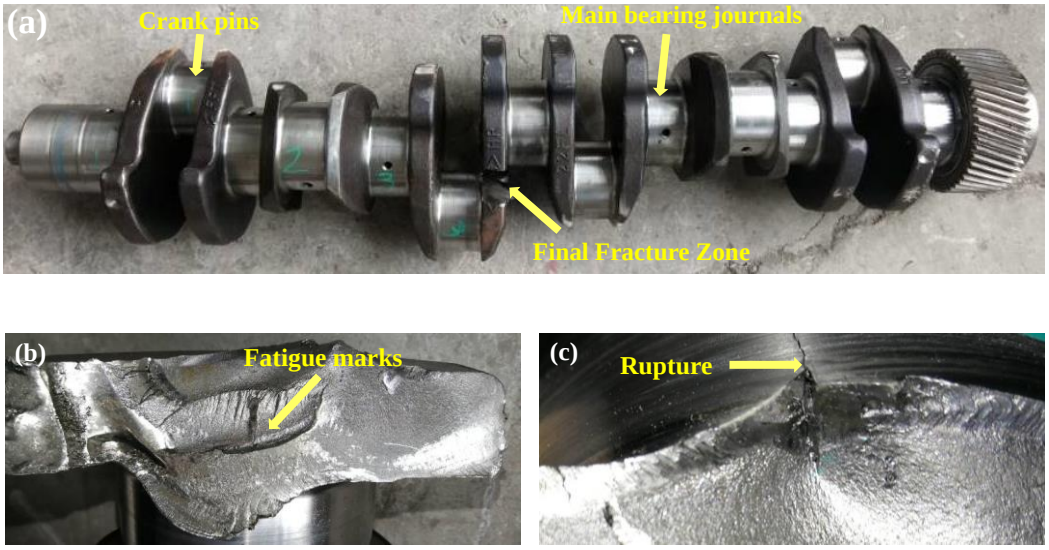

Figure 6.11 Macro observation of the 0-kilometer Lava crankshaft

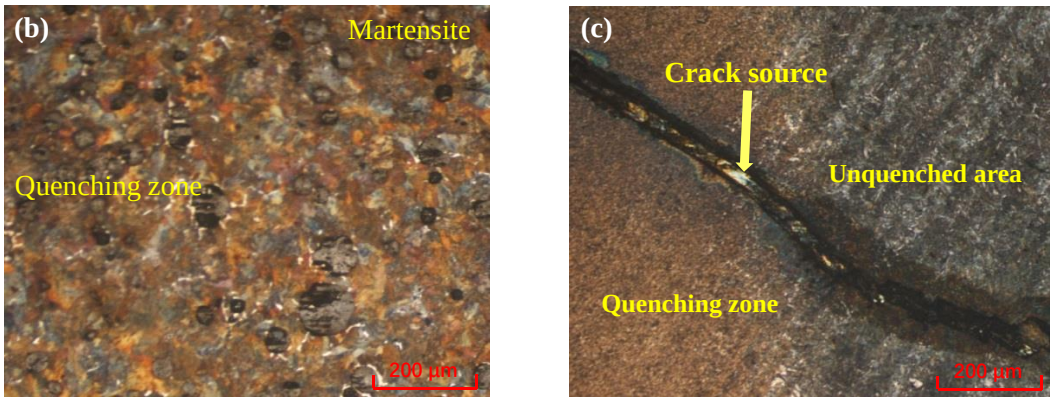

Figure 6.12 Metallographic organization diagram of the

Lava crankshaft

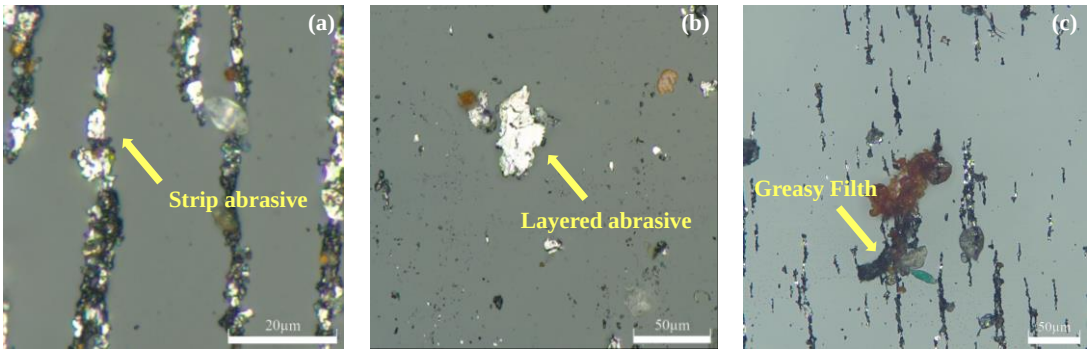

Figure 6.13 Iron spectrum particle image of worn crankshaft

6.3.2 Exploring the early wear mechanism of crankshafts based on engineering practice.

In engineering practice, based on the observed images of the early wear area of the crankshaft mentioned above, a comparative analysis is conducted on the impact of the connecting rod journal and the main journal on the severe localized wear of the bearing, and finite element technology is used to simulate the wear amount of the connecting rod journal and the main journal of the crankshaft system under actual working conditions.

This project is based on the wear failure analysis finite element model of the measured surface morphology of the connecting rod journal. A wear model is established in the grid motion constraint subroutine using FORTRAN programming language. The measured micro morphology of the connecting rod journal is imported into the finite element analysis software using PYTHON programming language. The evolution of the micro morphology in the cyclic contact of the connecting rod bearing is simulated. Using the damage evolution criteria in damage mechanics, the plastic deformation caused by wear on the surface of the connecting rod journal is calculated, and the influence of different roll slip ratios, vibration frequencies, amplitudes, surface roughness, surface hardness, and surface residual stress

on the accumulation of surface stress and strain, plastic strain, and wear state of the bearing is explored.

Chapter 7. Research on Bearing Wear of Methanol Fuel Engine.

After the combustion of methanol fuel in the cylinder, the gas pressure causes the crank connecting rod mechanism to move back and forth. The engine crankshaft connecting rod bearing not only supports the journal during the high-speed reciprocating operation of the crankshaft connecting rod mechanism, but more importantly, it carries the high explosive pressure and strong reciprocating inertia force transmitted by the cylinder through the piston connecting rod. For connecting rod bearings, the high-pressure gas generated in the cylinder after fuel combustion drives the piston downwards, and the force is transmitted to the connecting rod bearing through the piston pin and connecting rod. The force borne by the shaft is the combined tangential and radial force of this pressure and the centrifugal force of the connecting rod head rotation. For crankshaft bearings, the combined force of tangential and radial forces transmitted by the crankshaft journal, centrifugal forces of the connecting rod head and crankshaft at the center of the crankshaft pin, and centrifugal forces of the counterweight are shown in Figure 7.1.

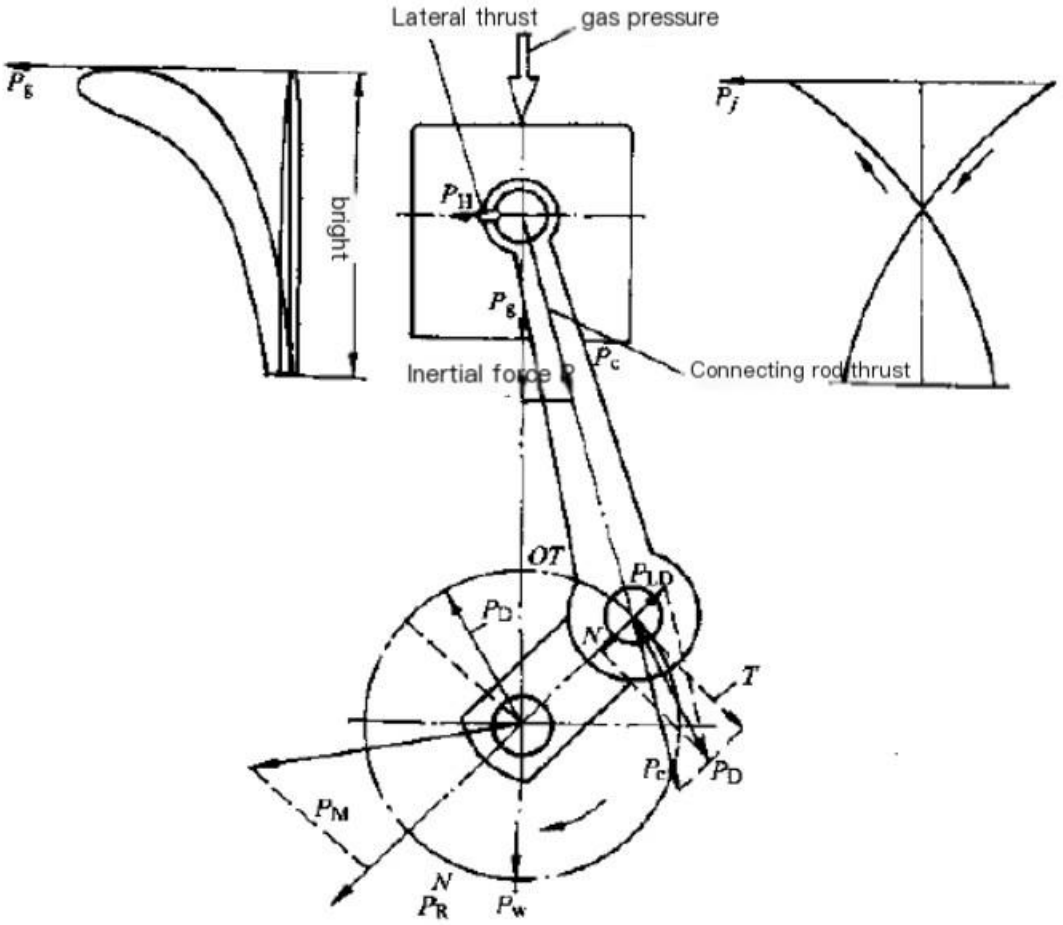

Figure 7.1 Force analysis of crankshaft and connecting rod shaft

Due to frequent changes in engine speed and load, the load borne by the bearings will change continuously with the operation of the engine. The actual contact between the bearings and the shaft occurs in the following three situations: when the lubricating oil between the bearings and the journal is sufficient and completely separated by an oil film, it is complete liquid friction; When the oil film becomes thinner and only one layer of oil film separates it, it becomes mixed friction; When the oil film ruptures and cannot separate the

bearing from the shaft, transient dry friction occurs. The damage of dry friction to bearings is very obvious, and the formation of oil film directly affects the wear life of bearings.

There are differences in the characteristics of methanol and gasoline fuels. The main components of methanol are carbon, hydrogen, and oxygen, which are relatively simple in composition. The calorific value is lower than gasoline, and the latent heat of vaporization is higher than gasoline. The theoretical air-fuel ratio is relatively lower than gasoline. The low boiling point of methanol helps to form a mixture, and the latent heat of vaporization is three times that of gasoline, which can reduce the intake temperature and improve inflation efficiency. Methanol has good anti knock properties, and the power performance of methanol engines is better than that of gasoline engines. By conducting durability tests on methanol fuel engine test benches, the reliability and wear of components (especially pistons, connecting rods, crankshafts, bearings, etc.) of the engine under continuously changing mechanical and dynamic loads are tested.

The experiment found that the engine has a good appearance and no liquid or air leakage on each joint surface; The cylinder pressure, valve clearance value, valve sinking, external characteristic data, lubricating oil consumption, piston leakage, and other data all meet the design requirements. However, both crankshaft bearings and connecting rod bearings exhibit varying degrees of alloy layer peeling. By analyzing the mechanism of the peeling off of the bearing alloy layer, it is determined that the factors causing the peeling off of the bearing alloy layer can be summarized as the following two points: methanol corrosion of the alloy layer material requires the selection of better lubricating oil; New bearings need to be designed so that the structure and materials can meet the requirements for direct combustion of methanol, improve fatigue resistance, and solve the impact of bearing oil film clearance.

7.1. Technical requirements for bearing materials.

The selection of bearing materials is crucial as it directly determines whether the bearing meets the wear resistance requirements. Bearing failure is often caused by improper material selection, resulting in abnormal wear, bite, and fatigue damage. The crankshaft

connecting rod bearings are subjected to periodic dynamic and static loads during operation, and the acidic substances in the lubricating oil can also corrode the bearing surface, causing bearing aging and bearing failure. The harsh working environment places high demands on materials. The bearing material meets the following characteristics to be suitable for various engine working conditions: 1) Strong fatigue wear resistance, less prone to surface dents or cracks under periodic loads; 2) Good friction compatibility, the bearing will not produce cold welding and bite during operation; 3) Good compliance, with slight deflection or misalignment of the shaft neck, continue to maintain normal operation; 4) Good embeddedness, when foreign particles are embedded, it reduces the surface wear of the alloy layer; 5) Strong corrosion resistance is required to prevent the oxidation of lubricating oil and additives in the oil at high temperatures, which can generate acidic substances and oxides to corrode the bearings and journals, forming pits and accelerating the fatigue wear of the bearing system; 6) The bearing capacity should be high, and the material can withstand high specific pressure without generating excessive friction, wear, and fatigue damage; 7) The melting point should be high, and it should not melt or soften at a high temperature of 200 ℃. The coefficient of linear expansion is small, and the change in bearing clearance is small.

7.2. Selection of lubricating oil grades.

In order to reduce friction, lubricating oil is used to separate the journal and bearings during operation. Good lubricating oil is selected to reduce friction between bearings and shafts, reduce wear, and facilitate the removal of excess heat to achieve cooling effect. More importantly, suitable oil film gaps are formed to ensure normal engine operation and reduce fuel consumption. The selection of lubricating oil requires attention to viscosity indicators. The higher the viscosity, the greater the friction force, and the lower the fluidity. The viscosity of lubricating oil will decrease with the increase of temperature. The viscosity of lubricating oil varies with temperature, as shown in Figure 7.2. When selecting lubricating oil, full consideration should be given to the operating speed of the shaft, the condition of the friction surface, the bearing capacity of the shaft, and the lubrication method. The formulas for calculating dynamic viscosity and kinematic viscosity are shown in equations (2-1) and (2-2).

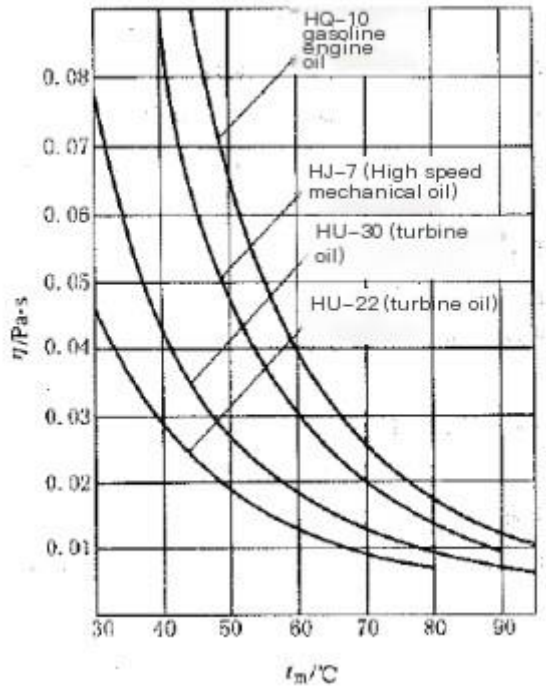

Figure 7.2 Temperature dependent curve of lubricating oil viscosity

$$\eta = \frac{\left(\frac{n}{60}\right)^{-\frac{1}{3}}}{1x106^{7}} \quad (2\text{-}1)$$

五、 $\frac{\eta}{P}$ (2-2)

In the formula, η— The dynamic viscosity of lubricating oil, $Pa\cdot s$; n - Journal speed, r/min; v— The kinematic viscosity of lubricating oil, cSt, 1cSt=1 × 10-6 m 2 s/; ρ— The density of lubricating oil, kgm 3.

7.3. Minimum oil film thickness of crankshaft connecting rod bearings in methanol engines

There is an oil film between the shaft and the bearing to ensure lubrication, and the thickness of the oil film varies during operation. Therefore, there is eccentricity when the center of the journal and the bearing do not coincide. The distribution of oil film pressure during the operation of radial sliding bearings is shown in Figure 7.3. The minimum oil film thickness hmn is calculated. Due to the limitations of the journal and bearing surface roughness and rigidity, in order to not damage the oil film, hmn is not less than the sum of the micro roughness of the journal and bearing surface. Firstly, calculate the oil film bearing capacity coefficient Cp, relative clearance ψ, and circumferential velocity of the journal separately ϑ、 Eccentricity ε Afterwards, perform the hmn calculation. The relative clearance is selected based on the load and the running speed of the shaft neck. The relationship between the load and the relative clearance is that the larger the load, the smaller the relative clearance, which improves the bearing capacity; The relationship between the running speed of the journal and the relative clearance is that the higher the speed, the larger the relative clearance, and the lower the heat generation.

By calculating the oil film bearing capacity coefficient, circumferential velocity of the journal, relative clearance, and eccentricity, the minimum oil film thickness between the crankshaft bearing and connecting rod bearing and the journal is obtained. The oil film thickness is used for verification to determine whether the crankshaft connecting rod bearing meets the requirements of fatigue strength and lubrication characteristics.

7.4. The clearance between the crankshaft connecting rod bearing and the journal of a methanol engine.

In order to confirm whether the clearance between the bearing and the journal meets the requirements for matching use, it is necessary to define the inner diameter tolerance of the bearing, calculate the maximum and minimum clearances between the bearing and the journal, as well as the diameter clearance Δ, Diameter gap Δ Calculate as equation (2-3). If the diameter gap Δ If it is between the maximum and minimum values, then the fit is applicable, otherwise it is not applicable, and thus the bearing structure and performance

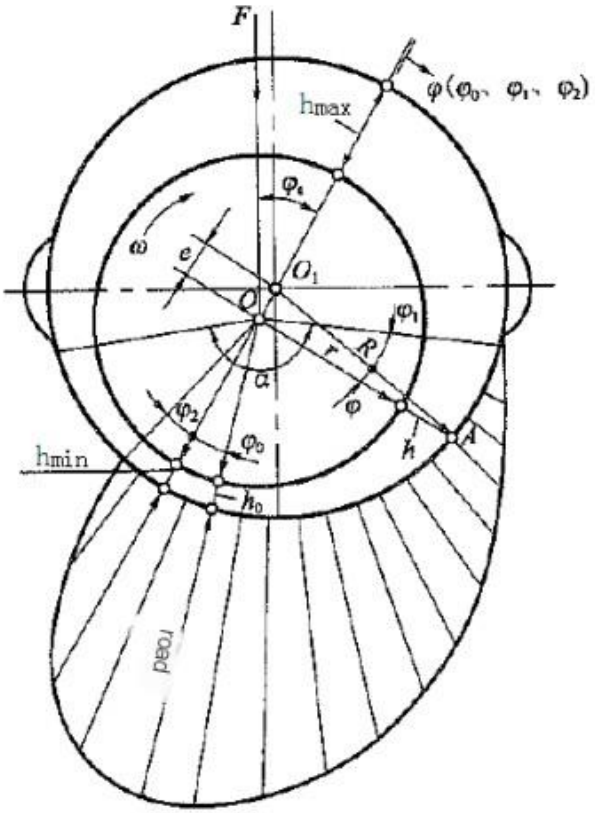

1、 Figure 7.3 Distribution of bearing oil film pressure

parameters are determined. The fit relationship between the journal and bearing is selected according to the national standards GB/T 1801-1999 "Selection of Limits and Fits, Tolerance Zones and Fits" and GB/T 1800.4-1999 "Limits and Fits, Standard Tolerance Grades and Limit Deviation Tables for Holes and Shafts".

$\Delta = \psi d$ (2-3)

Chapter 8. Engine as a Whole.

8.1. Background

Methanol fuel, as an alternative energy source for vehicles, has advantages such as high octane value, high latent heat of evaporation, and low emission pollution. It is also abundant in resources and has certain advantages in technology and cost. Therefore, it is considered an ideal clean energy source. However, methanol is a highly polar and corrosive solvent that can cause certain corrosion and swelling effects on certain metal, rubber, and plastic components. At present, most engines are made of metal and alloy materials, and some components and seals are made of rubber and plastic materials. These materials undergo certain corrosion, swelling, and aging phenomena during the operation and use of methanol engines, which affect their performance, reliability, and lifespan. The methanol supply system, including the methanol fuel tank, methanol pump, methanol filter, methanol injector, and supply pipeline directly in contact with methanol fuel, exhibits particularly prominent corrosion and swelling. At the same time, the basic components of a methanol engine directly come into contact with methanol fuel, such as the intake system, cylinder head intake duct, or parts that come into contact with combustion products such as unburned methanol and formaldehyde, such as cylinder liners, piston rings, catalytic converters, as well as unburned methanol seeping into the engine oil, causing wear on engine parts such as bearing shells and turbochargers.

8.2. Corrosion of main components of methanol engine.

8.2.1 Corrosion of Metal Components in the Supply System by Methanol

Methanol can cause corrosion and wear on the surface of engine metal components, mainly due to the high latent heat of evaporation of methanol itself. During the evaporation process, due to poor vaporization, liquid forms and flows into the cylinder wall, causing corrosion and wear of the lubricating oil film. At the same time, due to the reaction of additives in the lubricating oil, the lubricating oil loses its anti-corrosion effect, thereby intensifying the corrosion and wear of the piston and cylinder wall; In addition, during the combustion process, free radical reactions occur, and the generated combustion products contain

organic acids such as formic acid that cause corrosion to the metal surface; Secondly, methanol is prone to adsorbing moisture during use, and the presence of moisture can activate methanol's acid corrosion and electrochemical corrosion of metals. In general, when methanol does not contain water, its acidic corrosion is weak, mainly due to the corrosion of metal by active sulfides. However, when there is water in methanol, it will cause the decomposition and ionization of water, resulting in electrochemical corrosion and activating the corrosion behavior of methanol.

8.2.2 Corrosion of non-metallic components in the supply system by methanol

Methanol is an excellent organic solvent that has swelling, viscosity, brittleness, softening, hardening, and cracking effects on many non-metallic materials such as rubber and plastic stools in automotive engines, affecting their performance. Some components of additives used to improve the performance of methanol can also cause corrosion and deterioration of rubber and plastics. There are currently two main ways to solve this problem: one is to use fluororubber that is not corroded by methanol; The second is to add swelling inhibitors to methanol.

8. 2.3 ignition system

The spark plug electrode spark gap increases due to improper material and direct impact from methanol oil beam, resulting in misfire phenomenon. The electrode plug incandescent body part undergoes pitting and ablation, and the excessively long incandescent body deforms and bends. The end of the incandescent body is worn unevenly due to the presence of alcohol gas flow, and some electric heating plugs may experience ablation at the ceramic end after 250 hours of operation.

8.2.4 Pistons and cylinder liners

The piston ring is worn, the gap between the openings increases, and the upper part of the cylinder liner is more worn. When individual engine pistons experience knocking or abnormal combustion due to early ignition, the head is partially melted and small pieces fall off. But some methanol engine pistons wear normally after working for a long time, and the carbon deposits in the head and combustion chamber cavities are less than those in the original

diesel engine; The wear of cylinder liners is smaller than that of diesel engines, and even honing patterns can be seen. This may be due to the clean combustion of methanol and the small amount of soot particles. Lubricating oil is less contaminated, with very little particle wear and infiltration of methanol, water, etc.

8.2.5 Air valve group

On the basis of gasoline or diesel engines, when using M100, the wear between the sealing cone of the intake and exhaust valves and the valve seat, as well as between the valve guide, is relatively large. The wear of the parts that drive the valve, such as the cam, push rod, and rocker arm, is also greater than that of the original engine. Some diesel engine exhaust valves have a service life of up to 10000 hours, but after being changed to M100, they only last for 2000 hours. This is caused by two reasons: firstly, the lubricating oil contains a lot of methanol, water, and acidic substances, which mainly cause acidic corrosion; Another type is that there are fewer carbon soot particles in methanol fuel products, less lubricating oil between the gas valve and the sealing cone, and friction and wear between metals are the main factors.

8.2.6 Lubricating oil system

The main problem is that the filter is blocked, the sealing components lose function, and the lubricating oil pump experiences a decrease in supply pressure due to component wear.

8.2.7 Other components

The wear and failure of components that come into contact with alcohol fuel, combustion products, and lubricating oil, such as bearings of various moving parts, exhaust systems, and turbocharger components, may be positively or negatively affected. Positive effects refer to the solvent properties of alcohol fuel, which can remove dirt and deposits on the surface of some parts, and can also absorb some heat to reduce surface heat load; The negative impact is rust, corrosion, and malfunction. In some engines, when the catalytic converter in the exhaust system loses fire due to spark plug failure, more unburned alcohol fuel enters the exhaust pipe and converter, oxidizes and even burns locally, generating heat. The exhaust temperature can reach up to 1200 ℃, causing the catalytic converter to malfunction.

The solution is to monitor the catalytic converter temperature, and when the temperature reaches a certain value, bypass the exhaust without passing through the converter.

8.3. Corrosion and corrosion mechanism of 3-methanol engine

8.3.1 Adding methanol and water to lubricating oil

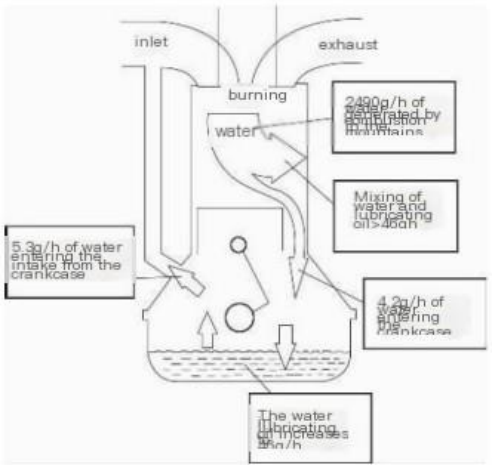

Figure 8.1 Path of methanol entering lubricating oil and its mixture

Methanol is an oxygen-containing fuel, and its combustion products contain more water vapor. When the engine is running at low load and the temperature is not high, the water vapor in the exhaust will condense into water, which seeps into the lubricating oil in the oil pan through the gap between the piston and cylinder liner and the pumping effect of the piston ring. The path of water entering the lubricating oil is shown in Figure 8.1. In addition, a portion of unburned methanol from the exhaust will also condense into a liquid at low temperatures and enter the lubricating oil, forming an emulsion like liquid.

The formic acid (HCOOH) in the exhaust and crankcase of methanol engines is 7.4 times that in gasoline engines, and aldehydes are twice that in gasoline engines. Like water, formic acid mainly enters the oil pan through the lubricating oil film on the cylinder wall and the

lubricating oil in the piston ring groove.

Due to the infiltration of more water, formic acid, and unburned methanol into the lubricating oil, as the usage time increases, the total alkali value in the lubrication decreases, while the acid value increases, resulting in a decrease in the viscosity and lubrication performance of the lubricating oil. These factors all promote an increase in rust and wear of alcohol engine components. There are two main measures to solve the problem of harmful emulsions formed by water infiltration in lubricating oil: first, try to shorten the operating time of the engine at low temperatures as much as possible, so that the temperature of cooling water and lubricating oil can reach 70-80 ℃ or above as soon as possible; Another is when lubricating oil forms an emulsion containing water and methanol, the lubricating oil is heated to above 90 ℃ to remove the water and methanol from it.

8.3.2 Methanol and lubricating oil

8.3.3 Corrosion and wear

The addition of methanol and water to lubricating oil can cause corrosion and wear on the surface of the parts. On the research surface, there are obvious phenomena of corrosion and rust on the surface of engine parts, as well as situations where methanol damages the lubricating oil film. The infiltration of liquid methanol into the lubricating oil film on the surface of the parts disrupts its lubricity, increases mechanical abrasive wear, and the acidic substances formed by alcohol fuel or its combustion products corrode the metal. The high conductivity of alcohols also promotes electrochemical corrosion.

Sampling analysis from the exhaust gas leaked from alcohol fuel engines shows that the exhaust gas contains formic acid, formaldehyde, acetaldehyde, methanol and methane. In addition, the chemical component H/C of alcohol fuel is relatively large, and the resulting products contain more water. When the temperature of the cylinder wall is below 70-80 ℃, condensate is formed on the cylinder wall, of which 60% is water, and the rest is methanol, trace amounts of acid, and formaldehyde. The pH value of the condensate is only 1.79-1.9. The acidity of the condensate is greater than when burning gasoline.

Methanol produces an intermediate product HCHO during combustion, which can be further oxidized to formic acid under certain conditions:

$$CHOHHCHOHCOOH$$

The formed formic acid reacts with cast iron to form formate low iron $Fe(HCOO)_3$, which is then rubbed off by the piston ring. On the other hand, the proportion of NO in the exhaust of alcohol fuel engines is relatively high in the nitrogen oxides emitted. NO forms nitric acid when it encounters water, and the condensate generated in the cooling zone promotes the generation of nitric acid, which has an erosive effect on the cylinder wall and other components.

Methanol combustion produces more water than gasoline combustion. The dew point temperature inside the cylinder of a methanol engine is high. However, methanol has a high latent heat of vaporization and a strong cooling effect on the working fluid in the cylinder, which increases the time required for the cylinder temperature to be higher than the dew point temperature after startup. This promotes the formation of condensates and acidic substances, leading to a higher wear rate of components in methanol internal combustion engines than in petroleum fuel engines.

8.3.4 Friction and abrasive wear

When no corresponding measures are taken, the components of alcohol fuel engines wear heavily due to friction and abrasives. The condensed water and methanol in the combustion chamber can wash and damage the lubricating oil film on the surface of the parts, reduce the viscosity of the lubricating oil, and deteriorate the lubrication performance, which will accelerate the friction and wear of the moving parts. The filtration accuracy of the lubricating oil filter is not high, and it is partially or severely blocked, resulting in a large amount of impurity particles in the lubricating oil. After aluminum parts come into contact with fuel and are corroded, small alumina particles form and infiltrate into the contact surface of moving parts, which exacerbates the abrasive wear of the parts.

Research on the Reliability of 4-Methanol Engine

The reliability, maintainability, and durability of the engine are the comprehensive top-level requirements for engine design, which directly determine the performance and overall life cycle cost of the engine. The reliability design of an engine must consider the safety, maintainability, and durability requirements of the engine, which involve a wide range of aspects such as performance, system, and structure.

Reliability is one of the key elements of product competitiveness, and commercial vehicle users are generally concerned about the power and economy of the vehicle, while also paying more attention to its reliability. At present, the market capacity of methanol commercial vehicles is relatively small, and users have a weak acceptance of methanol engines, making their reliability more important. This section provides examples to illustrate the characteristics of reliability development for methanol engines.

The basic engine used is a CNG engine, which is a four stroke, inline six cylinder, water-cooled, two valve, closed-loop single point hybrid gas engine, and uses electronic throttle control (ETC) and electronic accelerator pedal (PPS). The technical characteristics of methanol engines include multi-point sequential injection, single cylinder independent ignition, theoretical air-fuel ratio combustion and turbocharger control, emission technology routes, cooled EGR system, and three-way catalytic converter.

The polarity and high latent heat of vaporization of methanol fuel bring some problems to the engine, which are worthy of in-depth and continuous attention by engineering and technical personnel. The faults and causes of failure in the components of the heavy-duty methanol engine base are as follows:

① There are abnormal signs of wear inside the cylinder liner, particularly evident in the fourth cylinder. Analyze the reasons for the failure, including poor methanol evaporation, non repeated combustion in the cylinder, and unburned methanol adhering to the inner wall of the cylinder liner, resulting in poor oil lubrication, which is a key factor in cylinder liner wear (see Figure 8.2).

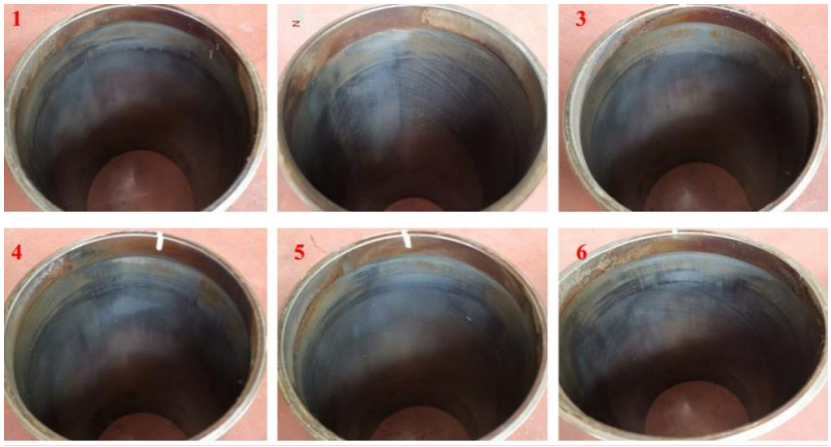

Figure 8.2 Reliability cylinder liner wear of heavy-duty methanol engines

② The first piston ring has excessive wear, and there are attachments in the piston ring groove/combination oil ring.

The reason for the failure of piston rings with excessive wear is poor methanol evaporation, non repeated combustion in the cylinder, and unburned methanol adhering to the inner wall of the cylinder liner, resulting in poor oil lubrication, which is a key factor in piston ring wear. The matching between the cylinder liner and the piston ring is unreasonable.

The main reason for the attachment of the piston ring groove/combination oil ring is that the ash content in the methanol engine oil additive has increased, and the content of elements such as Ca and P detected in the sediment is relatively high, similar to the composition of the engine oil additive; The products of thermal oxidation and normal combustion of methanol in the cylinder contain formic acid. formic acid reacts with methanol to produce high viscosity product esters, which are miscible with the lubricating oil on the cylinder wall, causing the lubricating oil on the cylinder wall to thicken and affecting the fluidity of the lubricating oil.

Figure 8.3 Reliability piston of heavy-duty methanol engine

③ There is a large amount of oil sludge inside the rocker arm cover, and there is a large amount of oil sludge in the non flowing part of the gear chamber. Fault analysis: The oil sludge detection results show that there are more elements of calcium, magnesium, phosphorus, and zinc, all of which are engine oil additives, and it is speculated that they are from the engine oil. At the same time, the combustion process of the methanol fuel engine leaks a small amount of methanol into the exhaust gas in the crankcase, as well as a mixture of water vapor and engine oil produced by combustion, resulting in a small amount of emulsion adhering to the cylinder head cover and gear chamber wall.

Figure 8.4: Oil sludge situation for reliability of heavy-duty methanol engines

④ At the end of the engine reliability test, emulsion was sprayed from the outlet of the oil and gas separator. The reason for the blockage is that the sludge generated by the reaction between methanol and engine oil additives blocks the return oil channel. At the same time, the metal corrosion caused by methanol oxidation product formic acid intensifies the blockage of the return oil channel, leading to emulsification of the engine oil, water, and

methanol inside the oil and gas separator. Multiple engine fires have also exacerbated the occurrence of sludge and emulsification. The solution is to adjust the return oil structure of the oil and gas separator and replace the metal materials inside the oil and gas separator to accelerate the return of oil sludge and avoid corrosion.

Figure 8.5 Corrosion of Oil Gas Seperator for Reliability of Heavy Duty Methanol Engine

Chapter 9. Summary, Conclusion and Suggestions.

This project chooses the application of methanol fuel in internal combustion engines. Based on the characteristics of methanol fuel (low-carbon), it explores and studies the impact of wear on various engine systems, analyzes wear phenomena and possibilities, selects anti wear technology solutions, and predicts the results after implementing effective measures. Sufficient research and demonstration have been conducted.

In terms of selecting the research object for this project, the research group specifically selected the friction pairs of the main components and parts that directly contact methanol fuel. Starting from the analysis of the friction and wear mechanism, the influencing factors of friction and wear were analyzed (including quantitative analysis and weight ratio), revealing the phenomenon of friction and wear, determining the impact of using methanol fuel on friction pair wear, analyzing the reasons, and proposing suggestions.

Due to the research objective of "engine wear using alternative fuels" in this project, it is defined as the study of methanol fuel engine wear during the project initiation and organization process. Therefore, after repeated consultations between the Chinese research group organizers and participants, it is believed that in the next longer development stage, renewable synthetic fuels will be the dominant fuel for the main driving force in the transportation field. For this reason, the research group chose methanol fuel as an alternative fuel and focused on engine wear as the research content. Various parts were selected as the research objects to carry out the above work and reached a consensus.

The Chinese research group of the International Energy Agency's Advanced Automotive Fuel Research Group on "Using Alternative Fuel for Engine Wear" specifically reminds readers that the synthesis of renewable methanol fuel (e-fuel) can be obtained through different technological routes in different regions, countries, and enterprises, but the properties of the fuel are generally the same, especially the carbon content is basically the same. In China, this fuel is collectively referred to as low-carbon (zero carbon) fuel in the transportation sector. Based on this, research team members remind that when referring to the content and results of this report, please pay special attention to the meaning of

synthesizing renewable energy to avoid unnecessary misunderstandings.

Thank you only for the trust of the International Energy Agency in the Chinese writing team!

Members of the Chinese writing team for this project:

Wei Anli,Yang Huizhong,Li Jianhua and Chen Peng from Expert Guidance Committee for the Promotion and Application of Methanol Vehicles by the MIIT

Wang Liang from Beijing Lanhe Qingneng Methanol Technology Research Institute Co., Ltd

Lu Ruijun ,Su Maohui ,Chen Chong and Zhang Zhidong from Geely New Energy Commercial Vehicle Group

Zhu Weibo and Wang Wenjun from Chongqing San'ai Hailing Industrial Co., Ltd

Zou Wuhui ,Hou Qifei and Wang Yong from Zhongyuan Internal Distribution Group Co., Ltd

Sun Jun and Ni Peixiang from Tianrun Industrial Technology Co., Ltd

Liu Hui from Liaoning Sante Petrochemical Co., Ltd

Huang Fenlian from Kunming University of Science and Technology

Li Chengxiao,Deng Fei,Long Meibiao and Wu Xinyi from Nanyue Electric Control (Hengyang) Industrial Technology Co., Ltd

Yuan Yafei and Yu Jing from Wuxi Yajia Deyin Technology Co., Ltd

Zhang Yongming form Wuxi Weishite Automotive Motor Co., Ltd

Wang Nan and Chen Wei from Suzhou Dafei Filter Technology Co., Ltd

Mu Yun form Shanghai Yixiang Power System Co., Ltd